

A Study on Experimental and Mathematical Analysis of Parabolic
Shaped Mixing Chamber for Abrasive Water Jet Machining to Improve
Performance



JIMMA UNIVERSITY
JIMMA INSTITUTE OF TECHNOLOGY
SCHOOL OF POSTGRADUATE STUDIES

A Thesis Submitted to the graduate studies of Jimma University in
Partial Fulfilment of the Requirement for the Degree of Master of
Science in Mechanical Engineering (Manufacturing System
Engineering)

By
Fentaw Hafiz

February, 2024
Jimma, Ethiopia

A Study on Experimental and Mathematical Analysis of Parabolic Shaped
Mixing Chamber for Abrasive Water Jet Machining to Improve Performance

Jimma University
Jimma Institute of Technology
School of Postgraduate Studies

A Thesis Submitted to the graduate studies of Jimma University in Partial
Fulfilment of the Requirement for the Degree of Master of Science in Mechanical
Engineering (Manufacturing System Engineering)

By
Fentaw Hafiz Mohammed

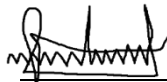
Advisor: Anil Kumar (Ph. D)
Co advisor: Hana Beyene (MSc.)

Declaration

I hereby declare that this thesis: “**A Study on Experimental and Mathematical Analysis of Parabolic Shaped Mixing Chamber for Abrasive Water Jet Machining to Improve Performance**” is my own work and this work has not been submitted elsewhere for the award of any other degree or diploma. It is being submitted for the degree of Master of Science in Mechanical Engineering (specialization in Manufacturing System engineering), and all sources of material used for this thesis have been dully acknowledged.

Fentaw Hafiz

Name of candidate



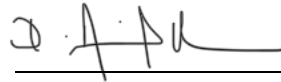
Signature

Date

This thesis has been submitted for examination with my approval as a University Supervisor.

Anil Kumar (Ph.D)

Name of Major Advisor



Signature

Date

Hana Beyene (MSc.)

Name of Co-Advisor



Signature

Date

Kuleni Diro (MSc.)

Name of Chairperson

Signature

Date

Ahmed Jemal (MSc.)

Name of Internal Examiner



Signature

Date

Besufekad Negash (Ph.D)

Name of External Examiner



Signature

Date

Acknowledgments

The author wants to say his deep appreciation to his main advisor Dr. Anil Kumar for his insightful advice, helpful criticism, and skilled oversight during the course of this effort.

The writer also wishes to express gratitude to his co advisor Mrs. Hana Beyene for her excellent support and guidance her Support was really helpful when things did not always go as planned.

The author wants to say thanks to Mr. Gebremariam Mamo who enthusiastically assisted the author while working on several facets of abrasive water jet cutting. A special thank you to the author's pals for their moral support and companionship. The author would not be able to complete the thesis and be here without these pals.

Finally, but just as importantly, the author would like to thank his brother and sister for their financial and spiritual assistance during this time. The author would especially want to thank his parents from the bottom of his heart. The author has been able to persevere through some trying times and finish this thesis thanks of their encouragement and emotional support. This thesis is narrated by the author to his cherished parents.

Abstract

The development of abrasive water jet (AWJ) as a type of high-density energy processing technology is widely recognized. Because of its heatless and noncontact processing capabilities, AWJ is used to quickly achieve cutting quality in a variety of materials, including metal, ceramics, glass, and composites. On the other hand, cutting parameters including pump pressure, cutting speed, orifice diameter, standoff distance, abrasive flow rate, and work piece affect surface roughness and dimension errors like round, burr, and taper.

Beyond changing the values of these input parameters, the shape of the mixing chamber plays a significant role in the quality and performance of abrasive water jet machining system. And therefore, in this thesis, there is a strong motivation and interest in analyzing and examining the impact of the mixing chamber's form on surface quality. A parametric mixing chamber is suggested, and using mathematical modeling and experimentation, the performance is analyzed and compared to that of a cylindrical mixing chamber. In addition, mathematical modeling of abrasive water jet machining system is included under this thesis. Here the effect of input parameters on velocity profile and thus the actual volumetric flow rate and the penetration depth has been analyzed numerically.

Experimental data was examined and analyzed using Minitab 17.1.0 software. Among this analysis are the normality test, and mean calculations as well as contour plots for both cylindrical and parabolic types of mixing chambers. Finally, by using a parabolic mixing chamber, the top and bottom surface roughness values were decreased from $4.9170\mu\text{m}$ to $4.7351\mu\text{m}$ and from $7.8673\mu\text{m}$ to $7.5754\mu\text{m}$ respectively. Furthermore, the taper angle was minimized from 0.8998° to 0.8098° .

Key words: *Abrasive water jet, Heatless, Non-contact, Parabolic mixing chamber.*

Dedication

For my mother.

Table of Contents

Declaration	ii
Acknowledgments	iii
Abstract	iv
Dedication	v
List of Figures	ix
List of Tables	xi
List of Abbreviations	xii
Nomenclature	xiii
Chapter One	1
1. Introduction	1
1.1. Theoretical background	1
1.2. Working principle	1
1.3. Research questions	5
1.4. Problem statement	5
1.5. Significance of the study	6
1.6. Research objectives	8
1.6.1. General objective	8
1.6.2. Specific objectives	8
1.7. Scope of the study	8
1.8. Structure of the thesis	12
Chapter Two	13
2. Review of Literatures	13
2.1. Categorization of literature review	13
2.1.1. Reviews of the literature on earlier research that lend support to this thesis	13
2.1.2. How parameters affect the characteristics of the kerf	21
2.1.3. Process parameters' effects on the rate of material removal	23
2.1.4. Elements influencing the workpieces' surface roughness	25
2.1.5. Important variables for adjusting the penetration or cut depth	27
2.1.6. Study of the effects of process parameters on overall process performance	30
2.2. Research gaps	35
Chapter Three	36
3. Materials and Methods	36

3.1. General Properties and Preparation of Bauxite Work piece	36
3.2. Data Acquisition	38
3.3. Experimental setup and design of experiment	39
3.4. Taguchi Experimental Design	45
3.5. Results and Data Measurement	47
Chapter Four	49
4. Parabolic Mixing Chamber-Based Modelling	49
4.1. Introduction	49
4.2. Design of mixing chamber	50
4.3. Modelling of abrasive water jet machining	51
4.4. Modified erosion model	51
4.5. Jet generation	55
4.6. Numerical simulation	55
4.7. Conclusions	58
Chapter Five	59
5. Cost of Machining	59
5.1. Background	59
5.2. Economic Comparison	60
5.3. Capital Costs	61
5.4. Running Costs	61
5.5. Cost Prediction	61
5.6. Conclusions	63
Chapter Six	65
6. Results and Discussions	65
6.1. Analysis of Experimental Data (Cylindrical Mixing Chamber)	65
6.2. Effect of selected input parameters on the taper angle (θ).	65
6.3. Effect of selected input parametrs on surface roughness.	66
6.4. Analysis of Experimental Data (Parabolic Mixing Chamber)	68
6.5. Effect of selected input parametrs on the taper angle (θ).	68
6.6. Effect of selected input parametrs on surface roughness .	70
6.7 . Discussions	72
Chapter Seven	73
7. Conclusions and Recommendations	73
7.1. Conclusions	73
7.2. Recommendations for Further Study	74

References	75
Appendices	85

List of Figures

Figure 1.1 Schematic diagram showing the operation of AWJM process	2
Figure 1.2 Schematic of a typical AWJ machine	3
Figure 1.3 Process parameters of AWJM	9
Figure 1.4 Schematic diagram of AWJM system.	11
Figure 3.1 The formation of an abrasive waterjet	36
Figure 3.2 Cross-sectional profiles of the hole	38
Figure 3.3 SEM image of bauxite work piece.	39
Figure 3.4 The different types of abrasive particles.	40
Figure 3.5 The schematic diagram of AWJ machining test rig	41
Figure 3.6 KMT abrasive water jet machine	42
Figure 3.7 Design of Experiment	43
Figure 4.1 Cross sectional view of the AWJ cutting head & vortex created inside the mixing chamber	51
Figure 4.2 Two types of mixing chamber geometry	51
Figure 4.3 Particle eroding a curve surface.	52
Figure 4.4 Effect of particle's attack angle on modelled surface generation.	54
Figure 4.5 Effect of particle striking a flat surface and a sinusoidal surface on modelled surface generation.	54
Figure 4.6 Advancement of the cutting front using the modified mode.	56
Figure 4.7 Effect of water pressure and abrasive mass flow rate on taper angle.	57
Figure 4.8 Effect of abrasive flow rate and cutting speed on taper angle	57
Figure 5.1 Cost breakdown for a 400 MPa AWJ	59
Figure 6.1 Effect of water pressure and abrasive mass flow rate on taper angle.	65
Figure 6.2 Effect of abrasive mass flow rate and cutting speed on taper angle	66
Figure 6.3 Effect of water pressure and abrasive mass flow rate on top roughness (3mm).	66
Figure 6.4 effect of abrasive mass flow rate and cutting speed on top roughness (3mm)	67

Figure 6.5 Effect of water pressure and abrasive mass flow rate on bottom surface roughness.	67
Figure 6.6 Effect of abrasive flow rate and cutting speed on bottom roughness	68
Figure 6.7 Effect of water pressure and abrasive mass flow rate on taper angle.	69
Figure 6.8 Effect of abrasive flow rate and cutting speed on taper angle.	69
Figure 6.9 Effect of water pressure and abrasive mass flow rate on top surface roughness.	70
Figure 6.10 Effect of abrasive mass flow rate and cutting speed on top surface roughness.	70
Figure 6.11 Effect of water pressure and abrasive mass flow rate on bottom surface roughness.	71
Figure 6.12 Effect of abrasive mass flow rate and cutting speed on bottom surface roughness.	71

List of Tables

Table 1.1 Typical AWJ machining conditions	3
Table 1.2 Typical materials and their mechanical properties	7
Table 3.1 Mechanical properties of the investigated refractory ceramics	39
Table 3.2 Chemical composition of garnet 80 mesh	40
Table 3.3 Values of constant parameters.	40
Table 3.4 Machine specification	41
Table 3.5 Actual experimental conditions	44
Table 3.6 Taguchi experimental design for three parameters with three levels each.	46
Table 3.7 Recorded experimental combinations of process parameters and corresponding values of responses/output parameters (cylindrical mixing chamber)	47
Table 3.8 Recorded experimental combinations of process parameters and corresponding values of responses/output parameters (parabolic mixing chamber)	47
Table 4.1 Process parameters employed to compare experimental and modelled results.	56
Table 5.1 AWJ production Costs	60
Table 5.2 . Capital cost for <i>CO2</i> Laser and AWJ cutting systems	61
Table 5.3 Running costs per hour for <i>CO2</i> laser and AWJ cutting systems.	61

List of Abbreviations

Notation	Description	Value (unit)
q_a	Density of abrasive particles	3.959×10^{-6} (kg/mm ³)
ν_a	Poisson ratio of abrasive particles	0.25
EY_a	Modulus of elasticity of abrasive particles	350,000 (MPa)
f_r	Roundness factor of abrasive particles	0.35
f_s	Sphericity factor of abrasive particles	0.78
g_a	Proportion of abrasive grains effectively participating in machining	0.70
m_w	Poisson ratio of work material	0.20
EY_w	Modulus of elasticity of work material	114,000 (MPa)
re_w	Elastic limit of work material	883 (MPa)
rf_w	Flow stress of work material	8,142 (MPa)
Cf_w	Drag friction coefficient of work material	0.002
n	Mixing efficiency between abrasive and water	0.8
P_{max}	Allowable power consumption value	56 (kW)
K_a	Constant	3

Nomenclature

C_c	Percentage of chemical additive concentration by mass	
C_p	Percentage of particle concentration by mass	
D_n	Nozzle diameter	(m)
D_p	Mean diameter of abrasive particle	(m)
E_m	Elastic modulus of target material	(pa)
H_m	Hardness of target material	(pa)
K_d	Discharge factor	
K_m	Fracture toughness of target material	(Pam ^{0.5})
R_e	Reynolds number	
v_p	Particle velocity	(m/s)
W_e	Weber number	
AFR	Mass flow rate of abrasive particle	(kg/s)
d, d_j	Jet diameter	(m)
DOC	Depth of cut	mm
h	Channel depth	(m)
JP	Water jet pressure	(MPa)
K	Consistency index	(N/m ²)(sn)
L	Jet compact (or stabilized) length	(m)
L/d	Characteristic length ratio	
MRR	Material removal rate	(m ³ /s)
n	Flow behavior index	
Ra	Surface roughness	μm
SOD	Nozzle standoff distance	(mm)
TR	Nozzle traverse rate	(m/s)
V	Removal volume of target material	(m ³)
v, V_j	Jet velocity	(m/s)
w	Channel width	(m)
θ	Taper angle	degree
κ	compressibility factor	

Greek letters

ϕ	Channel wall angle	(rad)
μ	Dynamic viscosity of slurry water jet momentum-transfer parameter	(Pa.s)
σ	Dynamic surface tension of slurry	(N/m)
ρ_s	Density of slurry	(kg/m ³)
ρ_p	Density of particle	(kg/m ³ s)
	Shear rate	

Chapter One

1. Introduction

1.1. Theoretical background

One of the newest non-traditional cutting techniques is (AWJ) machining. It cuts the target material by erosion using an abrasive slurry and a fine jet of ultrahigh pressure water [1,2]. In abrasive water jet during the cutting process, water is mostly used as an accelerating agent, with the abrasive particles handling the material removal task. Franz invented this cutting-edge technique for the first time in 1968 to cut laminated paper tubes [3] and was first introduced as a commercial system in 1983 [4] used in glass cutting. These days, this method is commonly utilized to mill materials that are challenging to machine, such ceramics, concrete, fiber-reinforced composites, laminates, and titanium alloys, for which conventional machining is frequently impractical from a technical or financial standpoint. It is perfect for automation because of its many unique advantages over other machining technologies, including its ability to cut complex shapes and even non-flat surfaces very effectively at close tolerances, its high speed and multidirectional cutting capability, its high cutting efficiency, and its low deformation stresses within the work material [5][6].

The main mineral that contains aluminum for the industrial manufacturing of aluminum metal is bauxite. After being processed from bauxite, alumina is melted to produce primary aluminum. Gibbsite, boehmite, and diasporite are the main aluminum-bearing minerals (also known as aluminum hydroxides or aluminum oxide hydroxides) that make up bauxite, a heterogeneous resource. In addition, different amounts of iron oxides, silica, and other contaminants are present (Hill and Sehnke, 2006). According to IAI (2009), the normal ranges for available aluminum oxide content are 31% to 52% and 16% to 27% for Al content. Gallium is a by-product that is mostly obtained from bauxite (Foley et al., 2017). The EU's list of Critical Raw Materials includes gallium.

1.2. Working principle

The primary principle of AWJM is the mixing of an abrasive particle with a narrow, focused water jet extreme pressure is used to spray this jet, creating extreme velocity that can cut through any material. Heat is almost completely eliminated and cutting forces are decreased by the waterjet. Erosion is the primary cutting mechanism.

The AWJ machine is made up of an abrasive feeding system, an intensifier pump that produces high pressure water, and a cutting head that injects abrasive material to create AWJ. A computer numerical control system governs the movement of the cutting head on the workpiece. The material that is eroded during machining is gathered in a catcher tank, where the wasted jet's residual energy is released.

Non-contact and wear-free, ideal for materials that are metallurgical or stressed enough to be unable to withstand the high temperatures used in other procedures. Fragile or brittle materials can be cut with surface finishes that rival those of conventional machining, with minimal force needed to cut, minimal temperature fluctuations, minimal scrape production, and no need for fixturing. Soft materials respond well to lower pressures. Higher pressures are needed for metals; by using tougher abrasives, the required jet pressure drops, and steel plates thicker than 3/32" can be cut. Can cut materials that are typically difficult to cut, like composites, ceramics, and glass, without the need for specialized tools.

Cut intricate patterns with ease; higher output, quick cutting, and superior parts; Amazing detail is possible with minimal kerf; savings on raw materials—less scrap; Minimal running costs – abrasive focusing nozzles and waterjet orifices need to be replaced periodically; cutting in all directions, even around tight corners; little lateral or vertical stresses and no requirement for a lot of part clamping; Depending on the thickness of the material, single-pass cutting; minimal or nonexistent hand finishing, net or near-net cutting; lighter, more flexible, and less expensive tools.

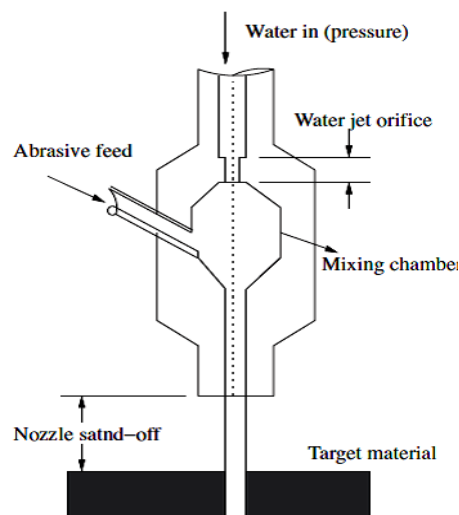


Figure 1.1 Schematic diagram showing the operation of AWJM process [7]

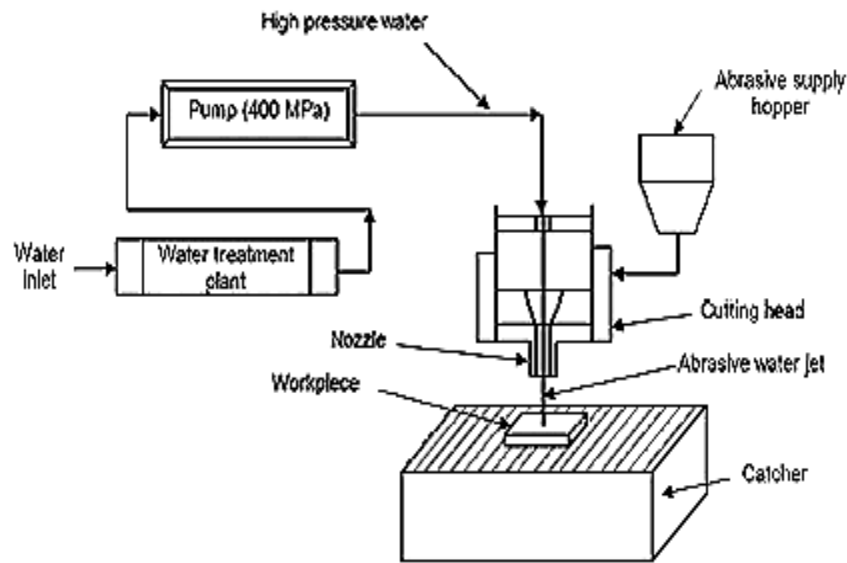


Figure 1.2 Schematic of a typical AWJ machine

A hydraulic pump moves water from the reservoir to the intensifier. Using an intensifier, water is pumped at an extremely high pressure of between 2000 and 4000 bar. A extremely high velocity jet of 1000 m/s is produced when water at such pressure is released through an aperture with a diameter of roughly 0.2 to 0.4 mm. This process transforms the potential energy of the water into kinetic energy. The materials are sliced to the proper size and shape by the high-velocity water jet that emerges from the nozzle.

Abrasives and water can be combined in two different ways to create AWJs: by direct pumping or by entrainment. Abrasives and water are combined in advance to create a slurry, which is pumped and released through a nozzle in a direct pumping system. Abrasives are entrained into the high-pressure waterjet created by the orifice in an entrainment system, where they combine with the waterjet to form AWJs.

Table 1.1 Typical AWJ machining conditions

Material	Thickness (in.)	Speed (ipm)
aluminum	0.5/1	5/2.5
stainless steel	0.5/1	2.5/1.5
mild steel	0.5/1	3/2
granite	0.5/1	4/2.5
glass	0.1/2	30/2
PVC	0.1/2	25/1

There are only a few minor variations between the pure and abrasive water jets. The material is eroded by the supersonic stream in a pure water jet. Abrasive particles are accelerated by the water jet stream in an abrasive water jet, and it is the particles—not the water—that erode the material. Compared to a pure Water jet, the abrasive Water jet has hundreds or even thousands of times more power. Each type of water jet—abrasive and water—has a specific use. Metals, stone, composites, and ceramics are among the hard materials that are cut by the abrasive water jet, while soft materials are cut by the pure water jet. Materials with hard nesses up to and slightly beyond aluminum oxide ceramic can be cut with abrasive water jets operating under standard parameters [8].

Cutting most textiles, foods, rubber insulation, car headliners and carpets, and plastics can all be done with water jet machining. Abrasive water jet machining (AWJM), which was initially created in 1974 to clean metal before it was surface treated, can be used to cut harder materials like glass, ceramics, concrete, and tough composites. Cutting speeds ranging from 51 to 460 mm/min were achieved by increasing the material removal rate of the water jet by adding abrasives. In general, AWJM can cut composite materials ten times faster than traditional machining techniques.

A large volume of a mixture of 30% abrasive and 70% water is accelerated by AWJM to a speed of 30 m/s at a low pressure of 4.2 bar. Abrasive materials commonly used are glass beads with a grain size of 10 to 150 μm , corundum, and silicon carbides [9].

The process becomes more complex when abrasive particles are added to the stream because there are now more variables to regulate. The other parameters include flow rate, grit size, and type of abrasive. The three most common abrasive materials are silicon dioxide, garnet (a silicate mineral), and aluminum oxide, with grit sizes varying from 60 to 120. Once the water has left the WJC nozzle, the abrasive particles are added to the stream at a rate of about 0.25 kg/min (0.5 lb/min).

The standoff distance, water pressure, and nozzle opening diameter are the remaining process parameters. Because nozzle orifice diameters are 0.25 to 0.63 mm (0.010 to 0.025 in) larger than in water jet cutting, more energy can be contained in the stream prior to abrasive injection, allowing for higher flow rates. The water pressure is comparable to that of WJC. In order to reduce the impact of the cutting fluid's dispersion—which now contains abrasive particles—standoff distances have been slightly reduced. Standoff distances typically range from 1/4 to 1/2 of those found in WJC[10].

1.3. Research questions

- ❖ How can the experimental design be structured to efficiently explore the relationships between these key variables?
- ❖ Which parameters significantly influence the performance of the abrasive water jet machining process?
- ❖ What are the dynamic aspects of abrasive water jet machining that need to be captured in the mathematical model?

1.4. Problem statement

One of the most important variables in precision abrasive waterjet cutting is the velocity distribution [11]. The mixing chamber, which facilitates the abrasive particles' mixing with water and air, is the most easily replaced component of a waterjet cutting head. Erosion happens as a result of high velocity and shear stress created on the focusing tube wall [12]. This leads to an increase in the mixing chamber's diameter and a loss in jet coherence, both of which are undesirable for precision cutting. Most importantly, the common type of cylindrical mixing chamber results in particle comminution in it and ineffective creation of a cohesive jet stream, which reduces the effectiveness of energy transmission [13]. Therefore, in order to increase efficiency, productivity and surface quality it is inevitably important to change the shape of the mixing chamber to parabolic one.

In the sense that they directly use alternative types of energy rather than traditional tools to remove metal, contemporary machining technologies are also known as non-traditional. To mold and cut the materials, these machining techniques make use of electrical, chemical, and optimum energy sources. Modern machining techniques may also be used to address issues with increased product accuracy and surface polish requirements, as well as challenges with complicated form and size. Since there is no cutting tool used in these procedures, a lot of input factors control the material removal mechanism. Precise control and adjustment of many input variables is crucial for removing the material quickly, at a cheap cost, and with a higher surface quality.

In addition, here kerf angle, and surface roughness are regarded as the benchmark for performance in several industrial applications [14]. These are the main constraints on the process applicability. In order to effectively control and optimize the AWJM process, predictive models for parabolic type of mixing chamber have not yet been developed for any of these materials such as bauxite, aluminum, stainless steel, brass, copper, titanium, mild steel etc. Here specifically predictive model has been developed for bauxite.

1.5. Significance of the study

Abrasive water jet Machining is a novel machining process capable of processing wide range of materials. Though its performance and quality enormously depend on the specified material characteristics and also the geometry of the different components. Fixing the shape of mixing chamber is one of those components that has paramount important in the generation of powerful stream of mixed abrasive and water flow. It is considered to be of parabolic in shape to get relatively smooth flow. Furthermore, during the cutting process, it significantly affects the work piece's surface quality. In order to dissolve the material, a hydrostatic energy is converted into a jet of sample kinetic energy, which provides the cutting power. By pressurizing water to extremely high pressure and concentrating high-speed water through a tiny aperture, an intense cutting stream is created, providing the energy needed to cut materials. The AWJM's use is predicated on the idea that jet impact erodes materials. Every one of the jet's two constituent parts the abrasive substance and the water has a distinct function. The abrasive material's main function in the jet stream is to supply the erosive.

It has several industrial uses and outperforms many other cutting processes when processing a wide range of materials. It is also an economical and ecologically beneficial method that may be used to treat many technical materials. very challenging materials to cut, like ceramics [15].

At up to 285 feet per second, or 1950 miles per hour, the stream's velocity is roughly 2.5 times that of sound. The cutting energy is directly related to the velocity's root. Transient spikes in the pressures up to three times the base cutting pressure are also possible. The energy in the beam can be expressed with Bernoulli's equation,

$$z_1 - z_2 + \frac{p_1 - p_2}{\rho} + \frac{v_1^2 - v_2^2}{2g} = 0 \quad (1.1)$$

$(z_1 - z_2)$ is negligible

Therefore,

$$\Delta p \propto \Delta v^2 \quad (1.2)$$

Surface quality deteriorates at the bottom side first, surfaces tend to have waves, likely from intensifiers, the jet flares from 0.1" to 1" and faster cutting speeds result in more flaring. A larger orifice yields a rougher surface finish, surface finish > 100 micro in. (Ra). Deeper cuts yield a rougher surface finish and cutting speeds < 1 ipm up to 5 ipm.

In general, feeds are quicker than wire EDM, slower than plasma cutters, and slower than lasers. Operating costs range from \$20 to \$40 per hour, mostly due to abrasives. However, hourly rates

can be somewhat high, flaring can grow, and the costly maintenance needs make it unsuitable for mass manufacturing.

For hard materials, the effective jet range is up to 8 inches. Typical cut width (Kerf loss) is 0.030" and higher. Typical orifice sizes are 0.007,9,13, and 15 in. The pressure decreases after one inch, and the jet will have a well-behaved center jet encircled by a thin mist. The pressure, diameter, standoff, abrasive feed rate, and material feed rate are typical process jet characteristics.

The more the energy supplied, the tougher the material, smoother the finish, and thicker the cut. Cutting in many passes' entails producing a cut that doesn't go through completely and doesn't chip edges. Although less energy is used, the quality of the surface will suffer.

Table 1.2 Typical materials and their mechanical properties

<i>Material</i>	<i>Ultimate compression (Kpsi)</i>
Titanium	50-135
Aluminum	19-110
Granite	19
Marble	12
Wood	5-9
brick	4

1.6. Research objectives

1.6.1. General objective

The purpose of this particular work is to study on experimental and mathematical analysis of parabolic shaped mixing chamber for abrasive water jet machining to improve performance.

1.6.2. Specific objectives

- Design a structured set of experiments to systematically explore the relationships between key variables
- Investigate the effects of varying parameters on the performance of abrasive water jet through rigorous experimental analysis.
- Develop a comprehensive mathematical model to represent the dynamic behavior of abrasive water jet machining

1.7. Scope of the study

In this section, a thorough literature review that covers recent, pertinent research and advancements in AWJ machining is used to emphasize the purpose and scope of the current project. The study makes clear that prior work has mostly concentrated on straight-slit cutting, and that further in-depth studies into the geometrical characteristics of the kerf and how they relate to process factors in AWJ contouring are required. The thesis also notes that the development of predictive mathematical models is necessary for the various cutting performance measurements, and that, at this time, empirical or semi-empirical modeling is likely to yield the best results rather than a strictly theoretical approach. It is also noted that a deeper comprehension of jet and particle properties is necessary.

AWJ cutting is a complex process with many factors that determine performances. Mechanism of erosion depends on the level of various process factors and is explained by multiple phenomena. AWJ cutting factors can be classified into six categories,

- ❖ Work piece characteristics (type of material, thickness, chemical composition, toughness, hardness, grain size, tolerances, and roughness).
 - ❖ Water system components (high pressure tubing, accumulator volume, water purity, flow rate, and pump pressure).
 - ❖ Abrasive system factors (kind of abrasive material, hardness, size, shape, and distribution of abrasive particles, as well as manner of abrasive input).
 - ❖ Cutting head factors, including orifice diameter, orifice material, focusing tube diameter, length, and material.
 - ❖ The motion system's components (working conditions, stiffness, accuracy, and precision).
-

- ❖ Process variables (impact angle, standoff distance, abrasive flow rate, traverse rate, and water pressure).

The five categories into which AWJ cutting performances may be divided are:

- Process performances, including temperature, vibration, noise, and orifice and focusing tube wear.
- Quality performances (form deviations, dimension deviations, cut quality: striations, burr, edge radius, jet impacted zone, surface roughness, kerf depth, kerf breadth, and perpendicularity deviation of the cut surfaces).
- Productivity metrics (productivity, machining time).
- Economic performances (cost of manufacture, electricity used, water used, and abrasive consumption).
- Ecological performances: recycling, pollution, and noise

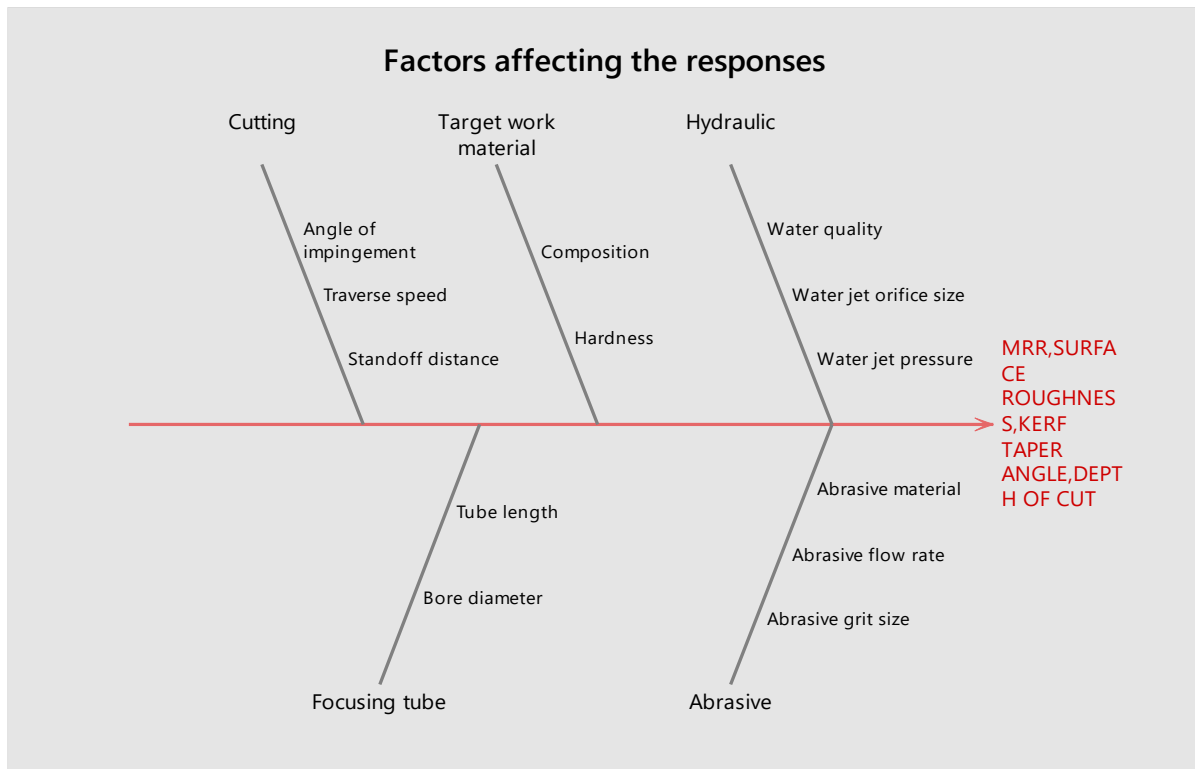


Figure 1.3 Process parameters of AWJM

Adding garnet or another abrasive particle to high pressure water allows abrasive waterjet cutting to cut through tough materials. When machining, garnet is used as an abrasive particle in around 90% of cases. Olivine can be used as an abrasive in place of garnet since it is softer and less likely to chip, break, or produce other surface imperfections. It also leaves a polished, smooth edge after cutting. The water in the nozzle of a waterjet cutting machine is mixed with the abrasive particle. The abrasive particle really performs the cutting action on the material in

this procedure. The water's function is to guide the abrasive particle and accelerate it to a speed appropriate for cutting.

The system is divided into four primary components. They are the jet former, the abrasive supply system, the pressure generation system, and the water preparation system. Abrasives and the waterjet are mixed in a mixing chamber using an abrasive waterjet entrainment system. The high-velocity water stream accelerates the abrasive particles, which subsequently exit the focusing tube (or nozzle) together with the stream. Harder materials including titanium alloys, composite materials, glass, stainless steel, and ceramics are cut using a high-velocity water and abrasive beam.

Water supply system is one of the abrasive water jets cutting machine's system components. The motion control system drives the AWJ cutting head device, which is connected to an intensification system, a high-pressure waterway system, an abrasive material supply system, and a reception device. In order to increase the cutting machine's precision and dependability, the machine body is built into the platform construction and the cutting head is driven by a gear-rack.

- ❖ Filters: increases water pressure using compressors and intensifiers, delivers intensified water through water delivery tubes and fittings, and filters the water to prolong system life. The abrasive hopper is used to provide the abrasive, the NC gantry is used to position the cutting head and catcher is used to stop the spent jet, and the orifice/mixing chamber/refocusing nozzle is used to combine the high-pressure water and abrasives.
- ❖ The water filter: use filters to get rid of tiny particles that may harm the orifice and other high-pressure components. The water is driven through 10-micron, 1 micron, and 0.5-micron filters using a conventional pump, and the average flow rate at standard tap pressure is one gallon per minute.
- ❖ Intensifiers: Essentially, a smaller hydraulic piston powers a larger hydraulic piston. As the hydraulic unit in the middle pumps in both directions, the opposing cylinder changes a huge differential volume for a large differential pressure, creating a high pressure in the water cylinders at either end. Check valves control the flow of water in and out as needed. By adjusting the hydraulic pressures and around 2Hz, one may regulate the pressures produced by the intensifier.
- ❖ Accumulator: serves as a pressurized reservoir for the water; a variable dimension delivery system is needed for the tubing and fittings that are located between the accumulator and the moveable head. Flexible rubber hoses would be utilized at lower pressures, but a coiled stainless-steel tube is frequently employed at these pressures. High pressure swivels are used to join the tube ends. To guard against damage in the case of a leak, a protective sheath

is positioned around the tubes. Moreover, flow valves are employed to lessen the possibility of harm.

- ❖ **Mixing head:** blends abrasive and water, combines nozzle, mixing chamber, refocusing, and orifice, and concentrates for cutting. Often, tungsten carbide or materials comparable to it are used to make mixing tubes.
- ❖ **The catcher:** The jet can be stopped once it has past the cutting surface, which lowers pressure, noise, and dust while increasing safety. A water filled tube can be utilized, and the jet should be distributed throughout the tube's length (up to 24"). For systems that employ a tank with a 2" steel plate at the bottom, shorter tubes must have strong materials at the far end.
- ❖ **Abrasives:** are common additives used to facilitate the cutting of hard materials, such as garnet and aluminum oxide. Because garnet is readily available, reasonably priced, effective, sharp-edged, and reasonably hard, it is commonly employed as an abrasive. Additionally, it performs better than other abrasives including glass beads, steel grit, silicon carbide, aluminum oxide, silica sand, and copper slag.

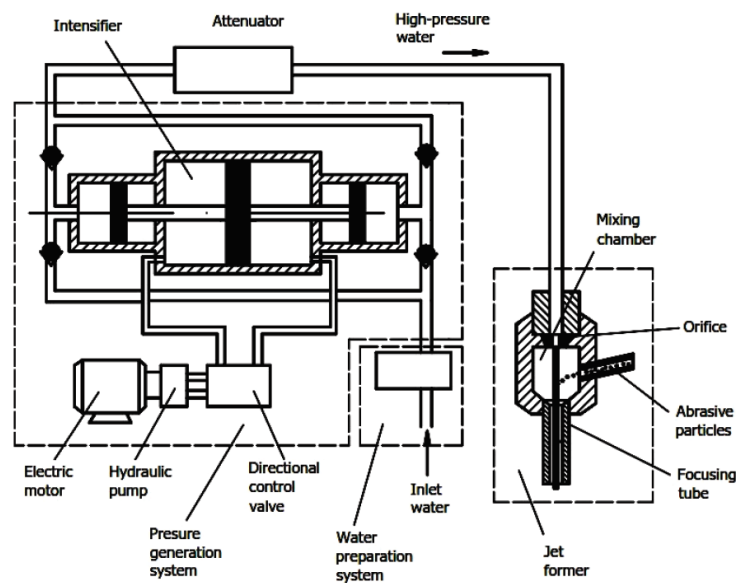


Figure 1.4 Schematic diagram of AWJM system.[7]

The first application of abrasive water jet machining was in 1974 to clean metal before it was surface treated [16]. The late 1980s saw the introduction of AWJM technology into the market, marking a significant advancement in the field of non-traditional processing methods. In the industrial sector, this technique has been widely used, especially for contouring or profile cutting challenging materials including ceramics, marbles, and multilayer composites [17].

Glass may be cut using abrasive waterjet cutting technology as it can create forms and curves that are not possible with other cutting tools at an affordable price. Applications for this

technique include replacement windows for vintage automobiles, intricate stained-glass patterns, mirrors, glass decorations, and more.

It is crucial that the initial holes be made at a lower pressure of 7,200 PSI/500 bar to 11,600 PSI/800 bar since glass has a propensity to break. The pressure then has to be raised to a cost-effective cutting speed. It is meant to progressively raise and decrease the cutting pressure for glass, ceramics, and other fragile materials using the intensifier pump's proportionate pressure control; otherwise, the material would be damaged. Almost no secondary finishing is needed when using water jet cutting since it does not induce vibrations in the glass, create heat-affected zones (HAZ), or leave rough edges behind.

In this study the comparison of two types of mixing chambers is considered with respect to same value of parametric qualities. It will investigate the effect of the physical shape of the two chambers on performance and quality characteristics such as surface roughness and taper angles.

1.8. Structure of the thesis

The seven chapters that follow make up this thesis. An outline of the study is provided in Chapter 1. This chapter also includes the study's background and rationale, problem statement, aim, scope, limitations, significances, and organizational structure. In Chapter 2, the problem is identified and past research studies by others are reviewed. The procedure is covered in Chapter 3. This chapter describes the approach taken and the development of the thesis work, including the design of the experiment, the selection of important input factors, and the final tabulation of the findings. Chapter 4 includes the basics of modeling of the output parameters and that of mixing chamber. Chapter 5 includes a general approach of estimation of machining cost. Chapter 6 presents brief discussion of results obtained. Finally, Chapter 7 outlines the major points to be considered as conclusion and recommendations. The references will be expressed.

Chapter Two

2. Review of Literatures

2.1. Categorization of literature review

This literature review may be broadly divided into five groups:

- Reviews of the literature on earlier research that lend support to this thesis
- How parameters affect the characteristics of the kerf
- Process parameters' effects on the rate of material removal
- Elements influencing the workpieces' surface roughness
- Important variables for adjusting the penetration or cut depth

2.1.1. Reviews of the literature on earlier research that lend support to this thesis

Alsoufi M.*et al.* A recent study examined the effects of two cutting-edge modern technologies on the surface roughness (Ra) and micro-hardness (μ -HV) of carbon steel material: abrasive water jet (AWJ) and laser beam cutting (LBC). According to experimental results, abrasive water jet cutting technology produced a better-quality final cutting surface for similar working environments in terms of surface roughness (Ra) and micro-hardness (μ -HV)[18].

Doreswamy D.*et al.* conducted experiments to determine how the feed rate and standoff distance affected the surface roughness, Ra, and (top/bottom) kerf width when machining D2 heat-treated steel using AWJC technology. The findings showed that in single pass machining, the bottom edge of the kerf width decreases by approximately 25% while the top edge increases by approximately 18% for every increase in standoff distance. The Ra value is increased by the feed rate and standoff distance parameters, which are equally significant[19].

Alberdi A.*et al.* carried out numerous tests using AWJ cutting technology to cut composite materials. An experimental method was used to determine the machinability index for a variety of composite materials with varying thicknesses. A study was conducted to determine how the parameters of the abrasive water jet cutting technology affected the surface roughness (Ra) and taper of the cut samples. In relation to absolute transverse feed rates, the kerf taper angle is greater than that of the corresponding separation[20].

Deng J. introduced the Gray Relational Analysis (GRA) method for determining the degree of correlation between experiment sequences with multiple output parameters. The orthogonal array in Taguchi's method provides a set of experiments that are well-balanced and a Signal-to-noise ratio (SN Ratio), which is a logarithmic function of the output and acts as an optimization objective function. With a few minimum experimental runs, it helps with the study of all the

parameters. A neater, less costly, and quicker partial factorial experiment takes the place of the full factorial experiments[21].

Nagdeve L.*et al.* conducted an experiment on AWJ to determine the ideal process parameter for cutting an aluminum sample and achieving the best possible material removal rate (MRR) and surface finish quality. To anticipate and optimize the best option for each process parameter, including standoff distance, traversal rate, abrasive flow rate, and water pressure, Taguchi's method and analysis of variance (ANOVA) were employed. The investigation shows that the surface roughness is influenced by the abrasive flow rate, whereas the standoff distance has a substantial impact on the metal removal rate (MRR). Using a L9 orthogonal array, tests are conducted by adjusting the pressure, standoff distance, traverse rate, and abrasive flow rate [22].

Reddy D.*et al.* investigated the optimization of the process parameters for surface roughness, Ra, and material removal rate (MRR) on AWJ using Taguchi's approach, variance analysis (ANOVA), and signal-to-noise ratio (SN Ratio) for Inconel 800H material. The outcomes demonstrated that the ideal AWJ cutting technology parameter combination satisfied the actual requirement for Inconel 800H material machining [23].

Raval M. and P. Patel conducted experiments on steel material utilizing Taguchi's orthogonal array L9 for the design of experiment (DoE) on AWJC technology parameter optimization. The technique of gray relation analysis (GRA) was also employed to determine the machine parameters at which the process is most effective and efficient. Pressure, tip distance, pole distance, and abrasive grain size were the controllable factors. The outcomes showed that magnetic abrasive in water jet machining is a workable substitute for conventional abrasives and aluminum oxide [24].

As stated by [25], genetic algorithm (GA) is of the most effective methods ever used. Several researchers have employed the GA approach to determine the ideal surface roughness for contemporary machining.

Zaina A.*et al.* focused on combining the two software computing approaches of genetic algorithms (GA) and simulated annealing (SA) to determine the best process parameters that result in the lowest possible machining performance value. The process parameters for assessing the surface roughness Ra were transverse speed, water jet pressure, and standoff distance. Using actual experimental data, the machining performance and process factors were taken into account in AWJ. When the output results were compared to real data results, the findings demonstrated that both suggested integration systems were able to predict the optimal AWJ process parameters, resulting in the lowest value of machining performance [26].

A. Murugarajan*et al.* examined the various methods for optimizing the abrasive water jet machining process parameters (AWJM). The AWJM process uses an impact erosion method to

remove work piece material through the use of a high-velocity water jet mixed with abrasive particles. The effectiveness of the AWJM process can be increased by utilizing a number of optimization approaches, including the Taguchi method, response surface methodology (RSM), fuzzy logic (FL), artificial neural networks (ANN), and genetic algorithm (GA). It was investigated how the operating factors are altered to produce various optimum outcomes using these optimization strategies [27].

C. Parmar et al. examined the use of an abrasive water jet machine for the commercial machining of three distinct materials: SS-316, fiber-reinforced plastic, and AL-6351. To determine how the process parameter for abrasive water jet machining (AWJM) affected surface roughness and MRR, experiments were carried out. The strategy was based on the AWJM process parameter optimization method developed by Taguchi for efficient machining. The stand-off distance from the work surface, work feed rate, and jet pressure were discovered to be the process parameters. Ultimately, the MRR and work surface roughness were assessed [28].

K. Prasad and G. Chaitanya made an attempt to review the AWJM-related research that has been done thus far. One of the unconventional machining techniques for brittle, hard, and thin materials that are challenging to cut is abrasive water jet machining (AWJM). The AWJM machining quality is primarily influenced by several process factors, including traverse speed, nozzle diameter, water pressure, stand-off distance, abrasive flow rate, and abrasive size.

This is a reasonably high material removal rate method that is both reasonably cheap and environmentally benign. Kerf Characteristics, Surface Roughness (SR), Material Removal Rate (MRR), Nozzle wear, and Depth of Cut are the quality criteria taken into account in AWJM. Process parameters are optimized using a variety of mathematical models and contemporary techniques, which enhances the performance characteristics [29].

S. Gurusamy et al. provided the ideal machining settings for aluminum alloy 5083 (AA5083) abrasive water jet machining (AWJM) using artificial neural network (ANN) modeling for a range of material thicknesses. Al 5083 alloy is used extensively in the construction of rail cars, vehicle bodies, ships, and cryogenic applications alone. Utilizing a Taguchi L18 orthogonal array, the experimental work examined the effects of process parameters on the material removal rate (MRR), surface roughness, and taper error over a range of thicknesses. These parameters included jet diameter, stand-off distance, and abrasive flow rate. A technological table was provided for the best way to machine AA5083 alloy in AWJM so that it is ready for industrial use [30].

K. Jai et al. AWJM process was modeled using fuzzy logic (FL), and a genetic algorithm (GA) was used to optimize the rule base, data base, and subsequent portion of the process. For this objective, a binary coded GA has been employed. Material removal rate (MRR) and

surface finish (Ra) are the output parameters that have been predicted while using FL modeling. These combinations of process parameters include water jet pressure at the nozzle exit, the diameter of the abrasive water jet nozzle, the traverse or feed rate of the nozzle mass flow rate of water and mass flow rate of abrasives between the nozzle and the work piece in addition to others [31].

T. Siddiqui *et al.* offered a comparison of the impact of three key process parameters, namely abrasive flow rate (AFR), quality level (QL), and water jet pressure (WJP), on two kerf quality characteristics (KQCs), namely kerf taper (Kt) and surface roughness (Ra), in AWJ cutting of three distinct grades (carbon, glass, and aramid) of bi-directional epoxy composite laminates made from prepregs. The Dornier transport aircraft program makes use of this grade of composite material. Using the Taguchi technique (TM), a robust parameter design for AWJ cutting of above FRCs is demonstrated. Using an L27 (33) Taguchi orthogonal array, three levels of process parameters were employed to investigate their impact on Ra and Kt and choose the best choice. It was discovered that reduced levels of QL and WJP and higher [32].

N. Yuvaraj and M. Kumar described an experimental study on the cutting process of an abrasive water jet (AWJ) on D2 steel, adjusting the impact of jet impingement angles using variable abrasive mesh sizes. The depth of penetration (DOP), material removal rate (MRR), surface roughness (Ra), and taper cut ratio (TCR) are the cutting performance parameters that are taken into consideration. In this work, the input process parameters and their levels were designed using the Taguchi experimental methodology. Studying the surface morphology of the AWJ kerf wall cut surfaces was done using a scanning electron microscope (SEM). Ultimately, the outcome shows that the cutting of D2 steel by AWJ is mostly influenced by jet impingement angles and abrasive mesh sizes. According to the current study, better cutting performance can be obtained in [33].

M. Azmir *et al.* investigated the impact of kerf taper ratio (TR) and surface roughness (Ra) of aramid fiber reinforced plastics (AFRP) composite on the parameters of the abrasive water jet machining (AWJM) process. The experimental strategy was based on Taguchi's experiment design. The traversal rate was determined to be the most important component in both the Ra and TR quality criteria by analysis of variance (ANOVA). Ra and TR decreased in tandem with hydraulic pressure increase, standoff distance, and traverse rate reduction. On Ra and TR, however, there was no discernible pattern for the mass flow rate of abrasive material. As a result, it was established that raising the water jet's kinetic energy may result in cuts of higher quality. Additionally, mathematical models were created utilizing several [34].

M. Todkar and J. Patkure examined the process parameter modeling and optimization for the abrasive water jet machining technology. The depth of cut for several process parameters, including water jet pressure, jet traverse rate, and abrasive flow rate at five levels each, have

been predicted using a set of experimental data to model the process of milling black granite material. In order to forecast the depth of cut that may be achieved with a given set of process parameters, a fuzzy model was constructed using the knowledge base created by means of experimental data. The process parameters were then optimized to maximize the material removal rate (MRR) by embedding the fuzzy model within a genetic algorithm [35].

A. Shaikh gathered information about the effects of various AWJ machining parameters on composite materials. The variables that were focused on for kerf taper angle, surface roughness, and depth of cut were hydraulic pressure, traverse speed, abrasive mass flow rate, standoff distance, types of abrasive materials, grit size, jet nozzle oscillation, and cutting orientation. The literature review revealed that surface roughness and the kerf taper angle decrease with increasing water pressure. Conversely, standoff distance and traverse speed exhibit opposite effects [36].

D. Johnbasha*et al.* AJM drilling was used to evaluate the process capabilities of Ti-6Al-4V with varying nozzle sizes, pressures, and SODs. AWJM uses a concentrated beam of abrasive-loaded gas to remove metal from the work piece. Because microparticles are driven by compressed air at high velocity, AJM can be used for drilling, polishing, cutting, etching, and cleaning. Additionally, the Taguchi technique for process parameter optimization of abrasive jet machining of Ti-6Al-4V was described. An analysis of variance (ANOVA) was performed on the values derived from the Taguchi study. L27 orthogonal array was used to conduct trials at different levels for both kerf width and MRR [37].

J. Aultrin and M. Dev examined the impact and parametric optimization of five process parameters using grey relation analysis (GRA) for aluminum 6061 alloy AWJM. Several sets of studies were carried out on this element using response surface methodology (RSM), changing five different factors on MRR and SR. To determine the important factors influencing the AWJM process's toughness, an ANOVA is run. There has been significant progress in the process, as evidenced by the results of the trials conducted to find the optimal setting. Converting the multiple response variable into a single response grade was the primary goal of GRA [38].

C. Narayanan*et al.* formulated a phenomenological representation of the three-phase flow within the cutting head of an abrasive water jet machine. The models that were previously provided have been enhanced in several ways. For example, the abrasive particle size distribution and the impact of particle breaking on the energy flux have been considered. A broad set of experimental data with wide changes in abrasive mass flow rates, operating pressure, and cutting-head shape was used to validate the model. For the whole range of studies, the cross-sectional averaged abrasive particle velocity at the focusing tube's exit has been predicted with good accuracy. Specifically, it is discovered that the model and experimental

findings have a Pearson correlation of greater than 95%, suggesting the usefulness of this model in design [39].

N. Yuvaraj and M. Pradeep Kumar formulated a phenomenological representation of the three-phase flow within the cutting head of an abrasive water jet machine. The models that were previously provided have been enhanced in several ways. For example, the abrasive particle size distribution and the impact of particle breaking on the energy flux have been considered. A broad set of experimental data with wide changes in abrasive mass flow rates, operating pressure, and cutting-head shape was used to validate the model. For the whole range of studies, the cross-sectional averaged abrasive particle velocity at the focusing tube's exit has been predicted with good accuracy. Specifically, it is discovered that the model and experimental findings have a Pearson correlation of greater than 95%, suggesting the usefulness of this model in design carried out in AWJ. The AWJ cut surfaces were examined using a scanning electron microscope (SEM) at the ideal level of process parameter settings. Utilizing energy dispersive X-ray spectroscopy, the quantity of silicon particles lodged in the sliced surfaces was verified. The experimental results show that the fuzzy TOPSIS method improves the quality of AWJ cutting by identifying more advantageous ideal input process parameters [40].

G. Kumar et al. examined how input process factors affected the outcome and optimized the process parameters to achieve optimum uses the AWJM method to simultaneously process responses including metal removal rate, surface roughness, and dimensional deviation while machining the duplex stainless steel 2205 alloy, which is based on austenite and ferrite. This material has been precipitation hardened and exhibits good creep-rupture strength. Even at elevated temperatures, its mechanical qualities remain strong. Submissions are For aerospace products, metal matrix composites, and ceramic matrix composites, intricate shapes are easily achieved [41].

G. Kumar and C. Sankar AWJM process was used to machine the nickel-chromium based super alloy Inconel 825. The impact of input process parameters was examined, and process parameters were optimized to achieve optimizing responses such as metal removal rate (MRR), surface roughness (Ra), and kerf width simultaneously. This material has been precipitation hardened and exhibits good creep-rupture strength. Even at elevated temperatures, its mechanical qualities remain strong. Applications: Aerospace items can readily attain intricate forms [42].

H. Orbanic and M. Junkar presented the unconventional technique of abrasive water jet (AWJ) machining, which accelerates extremely hard abrasive grains using a high-velocity water jet. The grains remove material as they come into contact with the work piece because of their high velocity and hardness. This kind of machining is a part of the erosion processes of solid particles. The abrasive grain type, eroded material type, impact angles, and kinetic energy

all affect the rate of material removal. On the basis of this supposition, the unit event model was introduced. The model analyzes the effect of every single abrasive grain (unit event) and provides the total effect of all the hits as machined surface topography. One can almost achieve satisfactory results with the unit event model, but the computation at the minuscule scale takes a lot of time [43].

P. Markopoulos *et al.* referred to the modeling and optimization of machining operations by the application of statistical and soft computing techniques. In particular, a detailed examination is conducted of the factorial design approach, Taguchi method, response surface methodology (RSM), analysis of variance, statistical regression methods, artificial neural networks (ANN), fuzzy logic, and genetic algorithms. The above-described methodologies and procedures have shown to be extremely effective and dependable when used as part of the design of experiments (DOE). Numerous studies have already been published highlighting the significance of these techniques, particularly in machining [44].

L. Nagdeveet *al.* using the Taguchi technique to determine the ideal Abrasive Water Jet Machining (AWJM) process parameters. In the unconventional machining technique known as "abrasive water jet machining," material is removed from a work piece by impact erosion of high pressure (1500–4000 bar), high water velocity, and entrained high velocity grit abrasives. The aim of this experimental study is to investigate the effects of machining parameters on the material recovery and shear rate of an Al 7075 work piece. The methodology employed involved the application of Taguchi's method, analysis of variance, and signal to noise ratio (SN Ratio) in order to predict the best option for each AWJM parameter, including traverse speed, abrasive flow rate, standoff distance, as well as coarse grit size. We employ a L9 orthogonal array and vary S, R, H, and D, respectively. We have three tests for each combination and use the Signal to Noise ratio to determine the best outcomes for AWJM. It was established that the ideal set of AWJM process parameters satisfied the actual need for Al 7075 machining in real-world applications [45].

J. Srinivas and A. Rao Shown is the process parameter optimization of Hastelloy C276 abrasive jet machining using the RSM methodology. An analysis of variance (ANOVA) was performed on the values derived from the RSM analysis. L15 orthogonal array is used to conduct experiments at different levels for both MRR and kerf [46].

K. Sasikumar *et al.* examined the optimization of abrasive water jet machining process settings for hybrid aluminum 7075 metal matrix composites with equal amounts of TiC and B4C reinforcement at 5%, 10%, and 15%. Water jet pressure, jet traverse speed, and standoff distance are the three abrasive water jet machining process parameters that were compared to the kerf characteristics, such as kerf top width, kerf angle, and surface roughness. Through

analysis of variance, the impact of these parameters on the replies was ascertained. We acquired regression models for the properties of kerf. It was discovered that traverse speed had a greater influence on top kerf width than other factors. Surface finish and kerf angle were more affected by water jet pressure. Using scanning electron microscopy, the microstructures of machined surfaces were also examined. The hybrid 7075 aluminum metal matrix composite's plastic deformation cutting was shown by scanning electron microscope research. The findings of the X-ray diffraction examination demonstrated that there were no abrasive particles trapped on the machined surface [47].

M. Uthayakumar *et al.* evaluated the abrasive waterjet cutting process parameters for the redmud reinforced banana/polyester hybrid composite. Using the compression molding technique, the composite was created with three different weight percentages of redmud: 10%, 20%, and 30%. Research has been done to determine how input parameters, such as material removal rate, top kerf width, bottom kerf width, and composite kerf angle, affect the output reactions. Using an L27 orthogonal array, experiments were conducted with different combinations of water pressure, traversal speed, and redmud percentage for the composite. To investigate the impact of each input parameter on the output answers, analysis of variance was also done. The research findings indicate that the water pressure was the most important factor on composite more chopping than others [48].

M. Singh *et al.* created a way to forecast the form of channels made with AWJM. Experiments were conducted to create channels by adjusting three process parameters: stand-off distance, pressure, and abrasive size. A simulation model based on non-uniform rational B-splines has been created and validated using experimental data to forecast the geometry of channels manufactured with AWJM [49].

S. Anwar *et al.* provided a broad summary of the abrasive waterjet machining research that has been published using bibliometric indicators. The primary characteristic of bibliometric indicators was their ability to provide an overall picture of research on abrasive water jets. According to the statistics, Wang J was the most prominent and active author in the subject of abrasive water jet research. Other notable figures in this domain included Hloch S, Kovacevic R, and Axinte D. In terms of abrasive water jet research, the United States of America was the most influential nation, followed by the Czech Republic. The two most prominent journals were the International Journal of Advanced Manufacturing Technology and the Journal of Materials Processing Technology [50].

J. Xu *et al.* The design, manufacture, and technological application of high-pressure water equipment can benefit from the experimental study done on a variety of common materials cut by water-jet cutting machines fitted with phased intensifiers. It effectively demonstrated the

system's ability to operate steadily, with water pressure fluctuations of no more than 2.0%, good cutting quality, and great production efficiency [51].

E. Averinet al. outlined a strategy for energy conservation and offered advice on how to destroy hard rock to the greatest extent possible. Rational ranges of values for the relationship between the abrasive flow rate and the water flow rate, standoff distance, and abrasive particle size are suggested. It was also given a parameter based on the temporary-structural method of fracture mechanics to determine the threshold conditions for the commencement of a material's destruction [17].

2.1.2. How parameters affect the characteristics of the kerf

A. Parthiban et al. has looked into the AWJC of 2mm thick stainless steel AISI 316L. The full factorial design method was used to implement the experiment's design. Associated with the aforementioned process parameters are the top and bottom kerf widths. To assess the connection between the top and bottom kerf widths and the process parameters, mathematical models were created. Additionally, the impacts of process factors on edge quality have been identified. Ultimately, the best AWJC conditions for achieving the finest edge quality, such as top and bottom kerf width, have been determined by numerical optimization [52].

D. Doreswamy et al. examined the impact of abrasive water jet (AWJ) machining parameters on the kerf width generated on graphite filled glass fiber reinforced epoxy composite, including jet operating pressure, feed rate, standoff distance (SOD), and abrasive concentration. Taguchi's L27 orthogonal arrays provided the basis for the experiments, and reduced kerf was achieved by optimizing the process parameters. Regression models were created to predict kerf width, and the main and interaction effects of the process parameters were examined using ANOVA. The top kerf width is found to be considerably influenced by the operating pressure, the SOD, and the feed rate, with corresponding contributions of 24.72%, 12.38%, and 52.16% to the kerf width. Scanning electron microscopy (SEM) is then used to do morphological analysis on the samples that were machined at optimal process settings. When process parameters were optimized, AWJ machined surfaces were found to be delamination-free [53].

A. Dhanawade et al. research on abrasive water jet machining of PZT ceramic material was given. The current study took into account three process parameters: traversal rate, water pressure, and stand-off distance. To plan the tests, the response surface methodology approach was employed. Analysis of variance was used to determine the relative importance of process parameters and how they affected the kerf characteristics. Water pressure and traversal rate were discovered to be the most important factors, with stand-off distance coming in second. Regression models were created based on experimental data to forecast the depth of cut and kerf taper. The quadratic terms, interaction, and significant parameters were taken into

consideration when developing the models. It was discovered that the model's predictions and the outcomes of the experiments agreed. Using the desirability technique, multi-response optimization of process parameters has also been carried out to increase depth of cut and reduce kerf taper. The machined surfaces' kerf wall characteristics were studied with the use of a scanning electron microscope [54].

C. Huang *et al.* Through a series of experiments using garnet abrasive and ultra-high pressure abrasive water jet numerical control machine tool, researchers investigated the effect of cutting parameters such as water pressure, nozzle traverse speed, and standoff distance on the granite cutting performance as characterized by kerf width, kerf taper, and striation drag angle. It was also investigated how system pressure and abrasive mass flow rate relate to one another. The findings of the study demonstrate that the abrasive mass flow rate was only related to water pressure, with no discernible impact from other cutting factors. It is discovered that a higher water pressure is linked to a wider kerf and a smaller kerf taper. The kerf taper increases significantly as the nozzle traverse speed increases, and the kerf breadth reduces as the speed increases. The kerf taper increases significantly from 3 to 4 mm at the standoff distance domain and then somewhat decreases from 4 to 5 mm at the standoff distance domain as a result of the kerf width growing with the standoff distance enhancement. As water pressure rises and nozzle traverse speed falls, the striation drag angle reduces [55].

I. Karakurt *et al.* carried out an experimental and statistical analysis on the kerf width, which is utilized in abrasive waterjet (AWJ) cutting in place of the cut width. Taguchi orthogonal arrays were utilized to design experiments that involved sampling pre-dimensioned granitic rocks. The rock parameters were associated with the kerf widths, and the impacts of the AWJ operating variables on the kerf width were examined. Furthermore, multivariable regression analysis was used to create predictive models for the kerf widths, and these models were validated using a number of statistical tests. The outcomes showed that the traverse speed and standoff distance had a major impact on the kerf widths. The findings also demonstrated a strong relationship between the kerf widths of the examined rocks and water absorption, unit weight, micro hardness, the maximum grain size of rock-forming minerals, and the mean grain size of the rock. Additionally, the modeling findings showed that the prediction models that were created based on the features of the rock can be effectively applied as a useful guide [56].

D. Shanmugam and S. Masood examined the kerf taper angle, a crucial metric for cutting performance, produced by the abrasive waterjet (AWJ) method for the machining of two different kinds of composites: glass epoxy and epoxy-impregnated graphite woven fabric. A thorough factorial design of trials was conducted with different standoff distances, water pressure, abrasive flowrate, and traversal speeds. A prediction model that links the kerf taper angle to the operational parameters has been created by utilizing the dimensional technique and

the energy conservation approach. The model's verification has been shown to agree with the experiments, making it suitable for use as a practical guideline [57].

V. Gupta *et al.* looked at the kerf properties of marble that is being machined using an abrasive water jet, a process that has several uses in residential, commercial, and industrial construction. For this investigation, three distinct process parameters—water pressure, nozzle transverse speed, and abrasive flow rate—were investigated. The trials were carried out in compliance with Taguchi's experimental design. The data were evaluated using analysis of variance (ANOVA) to identify the main significant process elements statistically influencing the kerf features. The findings showed that the most important factor influencing the top kerf width and the kerf taper angle was the nozzle transverse speed [16].

Gupta V. *et al.* explored utilizing Taguchi's method the minimizing of kerf width and kerf taper angle in AWJ of marble material. Abrasive flow rate, nozzle transverse speed, and water pressure were among the parameters taken into account. The most important factor influencing the top kerf width and the kerf taper angle was found to be the nozzle transverse speed [58].

2.1.3. Process parameters' effects on the rate of material removal

A. El-Domiaty *et al.* developed a model that can forecast, based on varying process parameters, the maximum depth of cut for various types of materials. The findings of the suggested model and the models published in the literature are compared, and the shortcomings of those models are also discussed [59].

M. Selvan and N. Raju evaluated the impact of process variables on cut depth, a crucial cutting performance metric in stainless steel abrasive waterjet cutting. The traversal speed, water pressure, standoff distance, and abrasive flow rate are among the process variables taken into account here. In order to cut stainless steel utilizing an abrasive waterjet cutting method, experiments were carried out with different parameter values. Regression analysis is used to create an empirical model for the prediction of cut depth in abrasive waterjet cutting of stainless steel, which is necessary to accurately choose the process parameters. The constructed model has been validated by the experimental results, which indicate that the model has a high applicability within the employed experimental range [60].

M.Selvan and Dr.N. Raju evaluated the impact of process variables on cut depth, a crucial cutting performance metric in mild steel abrasive waterjet cutting. Abrasive waterjet cutting was used to cut mild steel in experiments with different water pressure, nozzle traverse speed, abrasive mass flow rate, and standoff distance. Based on the outcomes of the experiment, the impacts of these parameters on the depth of cut have been investigated. Regression analysis is used to create an empirical model for the prediction of cut depth in mild steel abrasive waterjet cutting in order to accurately choose the process parameters. The constructed model has been

validated by the experimental results, which indicate that the model has a high applicability within the employed experimental range [61].

U. Aichet *al.* carried out tests using AWJM to cut borosilicate glass. Water pressure, abrasive flowrate, traverse speed, and standoff distance were the machine parameter settings that were used to measure the depth of cut. The model that was subsequently created on depth of cut provides insight into how various parameters affect the cutting of amorphous borosilicate glass by AWJM. Particle swarm optimization was also used to seek for the ideal conditions for setting control parameters (PSO). Additionally, qualitative information on the nature of the cut surface and the erosion behavior of amorphous material was partially revealed by scanning electron microscopy images [62].

M. El - hofy *et al.* carried out statistical analysis and an experimental investigation for cutting two lay-up configurations of multidirectional CFRP laminates. Using a comprehensive factorial design of tests, various AWJM settings, such as jet pressure, feed rate, and standoff distance, were tested. Analysis of variance (ANOVA) has been used to assess machining process responses, including top and bottom kerf width, kerf taper, machinability, and surface properties. For the AWJM, a process cost model was shown [7].

K. Aultrine *et al.* examined experimentally how five process variables affected the MRR and SR of the element copper iron alloy, which was cut using an abrasive waterjet cutting machine. Several sets of experiments were carried out on this element utilizing the response surface methodology, changing the standoff distance, focusing nozzle diameter, orifice diameter, water pressure, and abrasive flow rate. Based on the experimental results, all of the process parameters' effects on MRR and SR were examined. Helpful suggestions were made regarding the selection of appropriate process parameters for the abrasive waterjet cutting of copper iron alloy, and regression analysis was used to create a predictive model for MRR and SR for this particular copper iron alloy. The MRR and SR were shown to be significantly impacted by water pressure, abrasive flow rate, orifice diameter, nozzle diameter, standoff distance, and their interactions [63].

M. Rajyalakshmi made an attempt to review the AWJM-related research that has been done thus far. Additionally, to enhance the performance characteristics, a variety of statistical and contemporary techniques were used to optimize input process parameters including hydraulic pressure, traverse speed, stand-off distance, abrasive flow rate, and abrasive kinds [64].

S. Arun *et al.* Taguchi robust design analysis was used to discover the best possible combination of process parameters. The most important factor was also determined by using the Analysis of Variance (ANOVA). In order to determine how process variables including pressure, transverse speed, stand-of-distance, and abrasive flow rate affected the Inconel surface roughness (Ra) and

metal removal rate (MRR), these variables were tuned. The L9 orthogonal array was used to conduct the experiments. The results were given to validate this method, and after discussing the plausible tendencies of the output parameters in relation to the input parameters, suggestions for process control and optimization were suggested [65].

2.1.4. Elements influencing the workpieces' surface roughness

Preeti *et al.* carried out a number of experimental studies to examine the impact of process factors on the material removal rate (MRR) of Makrana white marble material used in machined components. Process variables such as standoff distance, abrasive flow rate, and water pressure were examined using ANOVA and the F-test. The findings showed that the material removal rate (MRR) is significantly influenced by the water pressure and abrasive flow rate [66].

Jain N. *et al.* worked with the water jet machine (WJM), abrasive water jet machine (AWJM), abrasive jet machine (AJW), and ultrasonic machine (USM) to optimize four parameters of the advanced manufacturing process using genetic algorithms (GA). It was determined that when power consumption increases, water pressure at the nozzle outlet increases and so does the maximum value of material removal rate (MRR) in AWJM. MRR rises with nozzle feed rate and abrasive water jet nozzle diameter increases. Additionally, it concurrently increases power consumption and MRR and the mass flow rate of water pressure [67].

R. Khanna *et al.* marble's material removal rate by abrasive water jet machining was determined. It has been studied how the three process variables—water pressure, abrasive flow rate, and standoff distance—affect the rate of material removal. The analysis of variance and the L16 orthogonal array were helpful in this inquiry in identifying the extremely significant, significant, and non-significant factors. When water pressure and abrasive flow rate rose, the rate of material removal increased as well [68].

S. Bhati *et al.* investigated the AJMM process parameters experimentally in order to obtain an optimal material removal rate (MRR). The level of experiments takes into account a few input elements for the aforementioned investigation, including pressure, nozzle tip distance (NTD), abrasive size (SOA), and nozzle diameter. Throughout the experimentation, these factors are changed. The process parameter's overall effect is investigated, and response surface methodology (RSM) is also used to create a mathematical model for MRR. Furthermore, in MATLAB, a genetic algorithm (GA) is used to optimize the MRR. By comparing the GA simulation result with the experimental result, error estimation is carried out, and it is found that there is no appreciable error in the simulation result estimation [69].

Ramprasad *et al.* used Taguchi's approach and ANOVA analysis to optimize the metal removal rate (MRR) of stainless steel 403 in AWJC technology. Three factors are used to optimize the MRR: standoff distance, abrasive flow rate, and water pressure. It was determined that the

standoff distance and abrasive flow rate were the next most important factors for stainless steel 403 work material, after water pressure [70].

F. Kolahan *et al.* focused on abrasive water jet machining technology modeling and process parameter optimization. A set of experimental data has been used to model the process and assess the effects of different parameter settings on the cutting of 6063-T6 aluminum alloy. The nozzle diameter, jet traverse rate, jet pressure, and abrasive flow rate are the process variables taken into consideration here. One of the most crucial output features, depth of cut, has been assessed using several parameter configurations. Regression modeling and the Taguchi technique are used to determine the relationships between the input and output parameters. With the use of the analysis of variance (ANOVA) approach, the model's suitability is assessed. A graphic was also used to illustrate the pairwise effects of process parameter settings on process response outputs. To optimize the process parameters, the suggested model was then incorporated into a simulated annealing technique. An optimization has been performed for any desired depth of cut value. The goal was to ascertain the appropriate process parameter levels to achieve a specific depth of cut [71].

S. M. Mullaikodi *et al.* created composite material combinations that had SiC Nanoparticles as secondary reinforcement and Kevlar 49 and S-glass fibers as main reinforcement, in varying amounts in epoxy resin at a ratio of 60% and 40%, respectively. A comparison was done between the laminates' tensile strength with and without SiC particles. When compared to the 272MPa tensile strength produced without SiC particles, there was a 35% and an 18% increase in tensile strength for 5% and 10% SiC, respectively. 5% SiC was added to the laminate to attain the maximum tensile strength of 368 MPa. Abrasive water jet machining was applied to the composites with high tensile strength. Surface finish, kerf width, and material removal rate were among the quality characteristics that were validated using a quadratic function, which was employed in the statistical model that was constructed using the RSM technique. The purpose of the morphological research was to correlate the filler material, matrix, and fiber bonding. The homogeneous dispersion of particles in the epoxy resin with reduced viscosity and air traps resulted in an increased strength [72].

M. Hasan *et al.* The article lists the main micro production techniques for composite materials, classifies their subclasses, and discusses recent advancements, emerging trends, and the impact of important variables on the cost, quality, and efficiency of composite material manufacture. A comparative analysis is provided that demonstrates the possibilities and adaptability of creating composite materials as well as potential uses in the future. In order to fulfill the increasing industrial demand, this review will be useful in advancing micro manufacturing technology for creating tiny items composed of composite materials [73].

Z. Zhang *et al.* examined and contrasted the most recent developments in high-precision material removal manufacturing technologies, with a focus on ultra-precision grinding, cutting, deterministic form correction polishing, and super smooth polishing. The evaluation included information on the concepts, processes, and uses of each technology. Future R&D should take into account these critical difficulties in extreme precision manufacturing, which are discussed below [74].

T. Nguyen *et al.* examined some of the research done at UNSW Sydney regarding the creation of an AWJ technology, with a focus on the system design that is currently being used to produce a micro abrasive jet and the erosion mechanisms related to the processing of a few common single- and two-phased brittle materials. Additionally, processing models derived from the results were showcased. The review finishes with a discussion of the technology's viability and the dominant development trend [75].

2.1.5. Important variables for adjusting the penetration or cut depth

M. Chithirai *et al.* demonstrated how process variables affect surface roughness (Ra), a crucial cutting performance metric in aluminum abrasive waterjet cutting. The purpose of carrying out Taguchi's experiment design was to gather surface roughness values. To cut aluminum utilizing an abrasive waterjet cutting method, experiments were carried out with different water pressures, nozzle traverse speeds, abrasive mass flow rates, and standoff distances. Based on the outcomes of the experiments, the impacts of these parameters on surface roughness have been investigated [76].

D. Hajdarevica *et al.* examined the impact of traverse speed, abrasive mass flow rate, and material thickness on surface roughness during aluminum abrasive water jet cutting. 80 mesh GMT garnet was utilized as an abrasive material. The depth of cut was used to measure the surface roughness. The experimental findings demonstrate that traverse speed significantly influences the surface roughness at the cut's bottom. The relationship between surface roughness and other variables related to abrasive water jet cutting was also studied. The trials were used to determine the ideal process parameters for each thickness of material [77].

D. Ashanira *et al.* Determine the lowest possible surface roughness value using end milling and abrasive water jet (AWJ) machining, two non-conventional methods. As a result, SVM model advancements tend to provide the greatest machining performance solution by obtaining the lowest possible surface roughness value. Nonetheless, by utilizing SVM's augmentation, the machining process's performances that have been modeled can be enhanced. To increase the accuracy of prediction models, the current SVM model building procedure is being modified to include the Grey Relational Analysis (GRA) approach for calculating the minimum surface roughness values of end milling and AWJ machining processes. In the suggested model

hybrid grey relational – support vector machine (GR-SVM), GRA serves as a feature selection approach in the SVM preprocessing process and has determined the factors of process parameters that have an influence on the surface roughness value. The accuracy of the hybrid GR-SVM model is then determined by comparing its output with that of the traditional SVM model [78].

G. Yadav and B. Singh examined how to handle scheduling the exams for abrasive water jet cutting using the box-Behnken outline method, with the overall objective of optimizing the process to provide higher-quality surfaces. An experiment was conducted to evaluate how process parameters affected the aluminum's surface roughness (Ra). The response surface approach (BOX BEHNKEN) and analysis of variance (ANOVA) were the main tools used by the philosophy to improve the process plan parameter for appropriate machining and to forecast the best option for each of the following: pressure, standoff distance, and traverse rate. With the aid of ANOVA, the combination produced in the box-Behnken technique by the design of expert software (DOE) test directed is discovered to have an impact on surface harshness (SR), a machining quality. The study concludes that surface roughness (SR) is significantly influenced by pressure and traverse speed, although standoff distance has very little overall effect. Respondent surface method has been implemented using Design of Experiment software (DX10) [79].

D. Bejic et al. examined the impact of traverse speed, abrasive mass flow rate, and material thickness on surface roughness during aluminum abrasive water jet cutting. 80 mesh GMT garnet was utilized as an abrasive material. The depth of cut was used to measure the surface roughness. The experimental findings demonstrate that traverse speed significantly influences the surface roughness at the cut's bottom. The relationship between surface roughness and other abrasive waterjet cutting parameters was also explored. The trials were used to determine the ideal process parameters for each thickness of material [77].

N. Yuvaraj and M. Kumar By adjusting the water jet pressure and jet impact angle, the abrasive water jet (AWJ) cutting of AISI D2 steel kerf wall cut surfaces examined the 3D surface topography, 2D roughness profiles, and micrographs. Roughness characteristics in 3D surface topography, including Sq, Ssk, Sp, Sv, Sku, Sz, and Sa, were enhanced by varying jet impact angles and water jet pressures. On the other hand, the water jet pressure and jet impact angle have a significant influence on the roughness metrics Ssk and Sku. The kerf wall cut profile structures verify this. 2D roughness profiles clearly show that the AWJ cut surfaces have fine imperfections of peaks and valleys. By employing a jet impact angle of 70° and a water jet pressure of 200 MPa, the SEM micrographs verify the creation of an upper zone that is not severely damaged and a bottom zone that is devoid of striations. Ultimately, the findings show that a jet impact angle of 70° preserves D2 steel's surface integrity more effectively than a jet

impact angle of 90°. The findings hold value in mating scenarios when wear and friction are present.

The AWJ machined D2 steel components now operate better as a result of this [80].

N. Tosun et al. carried out tests using various traverse speeds and waterjet pressures. It has been discovered that when cutting materials with superior mechanical qualities, the surface roughness obtained is superior to that of cutting materials with inferior mechanical properties [81].

C. Selvan et al. evaluated the impact of process variables on surface roughness (Ra), a crucial cutting performance metric in cast iron abrasive waterjet cutting. The purpose of carrying out Taguchi's experiment design was to gather surface roughness values. To cut cast iron with an abrasive waterjet cutting technique, experiments were carried out with different water pressures, nozzle traverse speeds, abrasive mass flow rates, and standoff distances. Based on the outcomes of the experiments, the impacts of these parameters on surface roughness have been investigated [82].

Li R. et al. Utilizing cutting-edge abrasive water jet cutting recombinant bamboo material, researchers examined the effects of pressure, feed rate, and abrasive mass flow rate on the surface roughness, Ra. Cuts were made in both the longitudinal and transverse directions at varying thicknesses. The average value of Ra increased with each increase in the federate and abrasive mass flow rate values, but it decreased with each increase in water pressure, according to the data. When cutting recombinant bamboo longitudinally as opposed to transversely, the Ra average value was lower [83].

Monkova K. et al. examined the elements of AWJ cutting that influence the titanium (22Ti) material's surface roughness, Ra. The Ra was assessed using the following parameters: depth of cut, angle of attack, transverse speed, and abrasive mass flow rate. Various engineering material thicknesses were subjected to a full factorial design of experiments (DoE). The findings indicated that the Ra morphology with relation to micro cutting quality is influenced by varied independent factors. Additionally, they demonstrated that raising the transverse speed results in a higher value of Ra [84].

Mutavgjic V. et al. conducted an experimental investigation on the surface roughness, Ra, of aluminum and stainless-steel samples that were cut using an AWJ technique. Water pressure, transverse rate, standoff distance, and abrasive flow rate were taken into account. The results showed that the mean value of the Ra significantly improved as the abrasive flow rate and water pressure rose. Furthermore, a direct proportionality between the Ra value and the transverse speed was noted [85].

Shanmughasundaram demonstrated how three separate random locations, such as traversal speed, water pressure, and standoff distance, might affect the surface roughness (Ra) of

materials made of Al-graphite composites. The L9 Taguchi methodology was employed for experimental analysis, and squeeze casting was employed as the production method. It was discovered that standoff distance and traverse speed were not as significant to Ra as the effect of water pressure was. Unfortunately, it was established that Ra of composite materials may be predicted by mathematical modeling [86].

Begic-Hajdarevic D.*et al.* used AWJC technology to conduct several experiments on the impact of different process parameters on the aluminum plate's surface roughness, or Ra. The experimental findings show that the Ra at the lower border of the kerf width is significantly influenced by traversal speed. Additionally, since raising the abrasive mass flow rate somewhat changes the Ra values, the abrasive mass flow rate may be lowered to the manufacturer's recommended value in order to save total manufacturing costs [87].

Rao M.*et al.* explored the effects of AWJC technology for mild steel material on surface roughness, Ra, by examining the effects of process parameters like traverse speed, water pressure, and standoff distance. Taguchi's method, variance analysis (ANOVA), signal-to-noise ratio (SN Ratio), and F-test were used to optimize the chosen AWJ process parameters. After using the L9 orthogonal array and Taguchi's design of experimentation (DoE), it was determined that standoff distance is a less significant parameter and that transverse speed and water pressure were the most critical ones [88].

2.1.6. Study of the effects of process parameters on overall process performance

Chauhan D. and K. Chauhan conducted several tests on titanium alloy material to determine the maximum lifetime that a physical vapor deposition coated cemented carbide tool on a milling machine could achieve. The signal-to-noise ratio (SN Ratio) and Taguchi's approach were applied. The maximum tool lifetime might be determined by factors like cutting speed, feed rate, depth of cut, and coolant flow rate, according to the results [89].

M. Korat*et al.* examined the studies that have been conducted during the last ten years, starting from the creation of AWJM. It provides information about AWJM research on process optimization, process control and monitoring, and performance measure improvement. There are numerous, varied reports of AWJM industrial uses for various material categories. It also covered the direction of upcoming studies in the same field [90].

R.Varun and T. Nanjundeswaraswamy provided a summary of earlier studies conducted on the abrasive jet and abrasive water jet machining process parameters. It was discovered that the machining process's accuracy was significantly impacted by the following process parameters: nozzle design and stand-off distance (SOD); fluid and flow properties; particle type, size, shape, and hardness; velocity and jet angle; traverse speed; and surface profile and geometry [91].

S. Chakraborty and A. Mitra utilized the grey wolf optimizer (GWO), a novel evolutionary algorithm based on the hunting habits of grey wolves, to determine the ideal parametric

combinations for AWJM processes. This algorithm's primary benefit is that it doesn't accumulate towards any local optima, and the social hierarchy facilitates the storage of the finest solutions found thus far. When comparing the resulting findings with GWO to the earlier attempts at parametric optimization of AWJM processes with other methods, there is a noticeable improvement in the response values [92].

M. Dittrich *et al.* discussed how an analysis based on the Design of Experiments (DoE) method is being used to carry out a process design with regard to productivity and machining precision. It becomes clear which factors, like water pressure, abrasive flow rate, or path offset, have the greatest influence. The parameters enable a particular process dimensioning concerning taper angle, surface roughness, and material removal rate. Additionally, the studies demonstrated that, with the right process settings, the results were highly reproducible. The study demonstrated how surface patterns can be precisely and effectively inserted into ceramic materials by using a water abrasive injector fine jet [93].

P. Milano *et al.* examined thin-sheet machining using a DOE approach at Tecnia R&I in partnership with Politecnico di Milano, with the goal of optimizing the FAWJ cutting parameters and testing its viability as a concrete high-precision technology to machine ceramic materials, including lead titanate zirconate (PZT) piezoelectric material. Lastly, a case study demonstrating the use of PZT as the foundation for micro positional actuators was given [94].

M. Murugan *et al.* examined, utilizing a low-cost, in-house designed waterjet equipment, the effectiveness of the abrasive water jet machining technique at low cutting pressure. Its goal is to investigate whether different materials can be machined at low pressure, which will help in the future creation of an efficient, reasonably priced water jet machine. Three distinct materials were machined at 34 MPa, which is a low pressure. Mild steel, aluminum alloy 6061, and Delrin plastics make up the ingredients. Additionally, a traverse rate ranging from 1 to 3 mm/min was used. Surface roughness, kerf taper ratio, and depth penetration were the three parameters used in the research of cutting performance at low pressure for various materials. It was discovered that all samples may be machined with varying quality at low cutting pressure. Additionally, when the traverse rate increases, the taper angle decreases. Concurrently, as the traverse rate increases, so do the surface roughness and the kerf taper ratio. We find that some materials with acceptable characteristics can be successfully machined by a low-cost waterjet machine operating at a significantly lower water pressure rate [95].

S. Lohar and P. Kubade examined the studies that were conducted in the last few years, starting from the creation of AWJM. It provides an overview of the AWJM research on process variable optimization, monitoring and control, and performance measure improvement. There

are many different reported AWJM industrial uses for a wide range of materials. The study also covered the direction of AWJM research going forward [96].

D. Patel & P. Tandon Overview of the use of abrasive water slurry jet machining (AWSJM) to enhance the standard abrasive water jet machine's machining capabilities. This study suggested a novel method for AWSJM in which a programmable control valve is used to regulate the flow rates of the polymer solution and abrasive (AFR) using a traditional abrasive water jet machine (AWJM) outfitted with a liquid (gelatin) injection system. AWSJM with gelatin enabled has improved machining performance, as shown by parametric research. Abrasive flow velocity, abrasive size, water jet pressure, and gelatin concentration have all been varied in experimental studies. The current study determines the ideal range of response parameters—material removal rate, kerf width, and depth of cut—for AWSJM using natural gelatin as the binder. When compared to AWJ, gelatin generates a coherent, three-phase, four-content beam with a higher kinetic energy, increasing the rate of material removal and the depth of cut while reducing the kerf breadth [97].

A. Momber and R. Kovacevic calculated energy absorption capacity of materials using an energy balance within the work piece during abrasive water jet machining. To characterize and compute the energy absorption capabilities, a parameter $x(h)$ is defined. A parabolic striation model serves as the foundation for the development of a method for estimating these parameters. Using a second order equation, it was demonstrated that the energy absorption is dependent on the depth of incision. The relationship between the stainless steel critical point of abrasive water jet energy absorption and the relative depth of cut (h/h_{max}) is found at a depth of cut of $h = 0.25 h_{max}$, which is equivalent to a striation angle of roughly 75° [98].

M. Babu and O. Chetty discovered the impact of replenishing regional garnet abrasives (southern India of origin) during the abrasive water jet machining process for cutting aluminum. Studies are conducted to determine how the American Foundry Men's Society fineness number, depth of cut, top and bottom kerf width, kerf taper, and surface roughness are affected by the specially designed optimized abrasive test sample, pressure, traverse rate, and abrasive flowrate. The test sample's performance was contrasted with that of an abrasive of commercial grade with an 80-mesh size. Furthermore, investigations on recharging are conducted following the removal of particles smaller than $90 \mu\text{m}$. These tests assist in determining the ideal amount of recharging needed [99].

D. Patel & P. Tandon outlined the process of abrasive water slurry jet machining (AWSJM) in order to enhance the standard abrasive water jet machine's machining capabilities. This work presents a novel approach to AWSJM, in which a programmable control valve is used to regulate the flow rates of both the polymer solution and the abrasive (AFR) using a traditional abrasive water jet machine (AWJM) outfitted with a liquid (gelatin) injection system. AWSJM

with gelatin enabled has improved machining performance, as shown by parametric research. Abrasive flow velocity, abrasive size, water jet pressure, and gelatin concentration have all been varied in experimental studies. The current study determines the ideal range of response parameters—material removal rate, kerf width, and depth of cut—for AWSJM using natural gelatin as the binder. When compared to AWJ, gelatin generates a coherent, three-phase, four-content beam with a higher kinetic energy, increasing the rate of material removal and the depth of cut while reducing the kerf breadth [97].

V. Sharma *et al.* The optimal process parameters for raising coal mine productivity have been identified using the Taguchi-fuzzy decision approach. The internationally recognized Taguchi method of experimental design is a process that yields low-cost, high-quality goods. Fuzzy rule-based reasoning was combined with the Taguchi loss function in order to lessen the level of uncertainty during the decision-making process, as it is usual for complex processes to optimize several solutions [100].

M. Radovanovic *et al.* used predetermined formulas to determine the cutting parameters, such as cutting rate and specific power consumption, for abrasive water jet cutting of various sets of materials [101].

P. Vundavilli *et al.* created an expert system for the process of abrasive water jet machining (AWJM). Fuzzy logic (FL) has been used in the development of the expert system. It should be noted that a number of process variables, including the focusing nozzle diameter, water pressure, abrasive mass flow rate, and jet traverse speed, affect how well AWJM performs in terms of depth of cut. Using the FL system, three methods have been devised to forecast the depth of cut in AWJM. The first approach focuses on building a fuzzy logic system based on Mamdani. It is significant to remember that the FL's knowledge base determines how well it performs. Approach 2 optimizes the FL-system's data base and rule base, while Approach 3 automatically evolves the FL-system as a whole. For this goal, a genetic algorithm with binary coding has been employed. By using the created expert system, choosing the most influential AWJM parameters on the depth of cut may be done without requiring a lot of trial labor. With the aid of test cases, the generated FL-systems' performances have been evaluated in order to forecast the depth of cut in the AWJM process. It is discovered that Approach 3, or the automatic FL-system, has a higher prediction accuracy than the other two ways [102].

J. Wang *et al.* investigated cutting performance in abrasive waterjet (AWJ) machining through experimentation. The research employs jet forward impact angles and multipass operations as separate and simultaneous cutting procedures for alumina ceramics and polymer matrix composites. First, a quick report on the impact of the jet impact angle in single pass cutting is given, demonstrating that the ideal jet impact angle is roughly 80° for both ceramics and polymer matrix composites. It has been discovered that the multiphase cutting technology can

expand the application scope and cutting capability of AWJ cutting. When compared to single pass cutting in the same overall cutting time, it can also enhance important cutting performance like the depth of cut. When cutting alumina ceramics at a jet forward angle of 80°, the advantages of multipass cutting operations are amplified [103].

M. Yunus *et al.* Grey relation analysis (GRA) based on the hybrid Taguchi design technique was utilized to optimize the control parameters, such as coating thickness, type, bond coating, and exposure temperature. For analysis based on the bigger the better signal-to-noise (S/N) ratio, the relevant experiments were conducted using the Taguchi L16 factorial design of experiments. GRA accomplished the multi-response/output optimization and control factor grading satisfactorily. We looked into each factor's importance in relation to TD and TFC. The results of the ANOVA demonstrated the most significant parameters at a 95% confidence level, and these findings were confirmed by a confirmation test employing the best process factors. It demonstrates an improvement in thermal barrier coatings' TC [104].

G. Sonawane and R. Bachhav examined data on the features, benefits, restrictions, uses, properties, and observations of AWJM that were set up correctly and equipped in a specific way [105].

T. Min Oh *et al.* conducted experiments on rock cutting using five distinct coarse (40 mesh) garnets to investigate how the abrasive feed rate, physical characteristics, and particle size distribution affect the performance of the rock cutting process. Furthermore, the abrasive waterjet was used to study the disintegration of garnet particles using garnet properties.

The test findings show that the most crucial factors influencing the effectiveness of rock cutting are the hardness, specific gravity, garnet purity, and particle size distribution. Based on garnet properties, this study provides a deeper knowledge of coarse garnet performance and efficiency. This ought to help with the garnet choosing process so that hard rock cutting can function as intended [106].

V. Pi and T. Hung investigated the repurposing and replenishing of IMC garnet, also known as ultimate garnet, in abrasive waterjet machining. The reusability of recharged and recycled garnet was investigated in this work. Additionally, an investigation was conducted on the cutting quality and performance of the recharged and recycled abrasive. Ultimately, the ideal particle size for recycling and replenishment was identified [107].

M. Ravalet *et al.* investigated the exact processing phenomenon and the circumstances surrounding the abrasive machining of material using magnetic abrasive, high-velocity water, and other abrasive materials with hardness and grain size comparable to magnetic abrasive. Additionally, the outcome of the last experiment compared how well water and abrasive mixture affected the AISI 52100 steel materials' surface finish [108].

P.Sreekesh *et al.* talked about water jet cutting. A few benefits include the possibility for omnidirectional cutting and low mechanical and thermal loading. The effectiveness of abrasive water jet machining is determined by a number of factors. Crucial process variables that primarily impact cutting quality include traverse speed, hydraulic pressure, standoff distance, abrasive type, and work material. Important AWJM quality characteristics are material removal rate (MRR), surface roughness (Ra), taper of cut, and width of cut [109].

2.2. Research gaps

Performance and efficiency of abrasive water jet machining is affected by many factors such as shape and geometry of individual components in addition to that of the value of input parameters. Not many investigations have been conducted on analysis of the effect of components of some abrasive water jet machining system. There are some studies conducted on nozzle performance as well as wearing effect. However, the impact of mixing chamber geometry on overall performance has not yet been studied. Especially no study has been conducted on this area with great intention and effort by both experimental and mathematical techniques.

Chapter Three

3. Materials and Methods

This section explains the varied materials and the methodology that were utilized to successfully accomplish the study's specific objectives through the use of diverse materials and techniques. The material used as a work piece is bauxite. And the abrasive material is garnet. Surface roughness and taper angle are measured with a profilometer and a scanning electron microscope, respectively. MT machine is the main working equipment where the machining operation is made. The work piece is prepared, the surface roughness is measured, and the taper angle is measured.

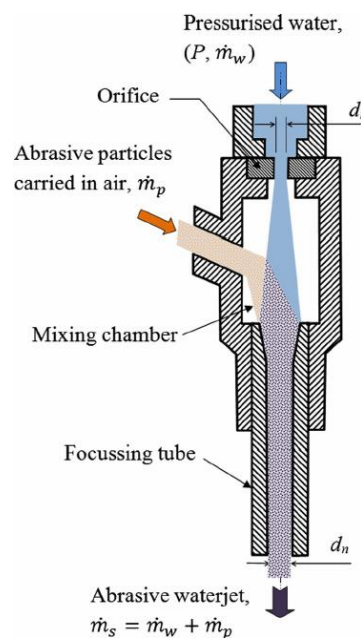


Figure 3.1 The formation of an abrasive waterjet

3.1. General Properties and Preparation of Bauxite Work piece

The United States Geological Survey estimates that there are between 55 and 75 billion tons of bauxite deposits in the world, of which 32% are in Africa, 23% are in Oceania, 21% are in South America and the Caribbean, 18% are in Asia, and 6% are elsewhere in the world. 30 billion tons are thought to be the world's known reserves of bauxite (USGS, 2020). Tropical and subtropical areas contain 90% of the world's bauxite reserves. Guinea has the highest reserves of bauxite in the world (24%), followed by Australia (20%). According to USGS (2020), three other nations possess notable reserves of bauxite, including Vietnam (12%), Brazil (9%), and Jamaica (7%). With an estimated 250 million tons of ore reserves, Greece has the

largest exploitable bauxite deposits in the EU, according to the United Geological Survey (USGS, 2018). France, Hungary, Romania, and Italy are other countries with bauxite resources (Minerals4EU, 2015).

The majority of bauxite extracted globally comes from opencast mining methods; underground mines produce a far smaller amount. A JRC investigation indicates that 2% of the world's bauxite mine capacity is underground, and 3% is of mixed type (both underground and open-pit); the remainder capacity is used only for open-pit exploitations (20). Because of its relatively high grade, the mined ore does not require complex processing (IAI, 2020b).

The world's bauxite output increased significantly between 2009 and 2018, with a compound annual growth rate of 5.3%. In 2018, the global bauxite production was approximately 335 million tons. With 29% of the total, Australia is the top producing nation, followed by Guinea (18%) and China (21%). In 2018, the EU produced about 1.7 million tons of bauxite, or 0.5% of the world's total. Greece contributed 95% of the EU's total, with the remaining 5% coming from France, Croatia, and Hungary.

Primarily a metallic material, bauxite has specific industrial use. It's the only material that can be used to produce large quantities of aluminum. Despite making up roughly 8% of all metallic elements in the crust of Earth, aluminum is most commonly found in non-extractable clays, soils, and rocks. Aluminum is a commonly used metal that is mostly derived from sedimentary rock called bauxite.

The residual deposit known as bauxite is created when atmospheric factors react with rocks that contain aluminum. It has minor levels of silica, iron and titanium oxides, and hydrated alumina in tropical circumstances. High alumina cement is made of limestone and bauxite as its primary ingredients. Al, lime, and iron oxides each make up 40% of the content of HA Cement.

The only material utilized for the same purpose is bauxite, which is the ideal material for manufacturing aluminum.

The extraction of aluminum from bauxite involves a number of procedures, including the Bayer and Hall Heroult processes. After mining, aluminum and alloys containing aluminum are utilized extensively in tools, automobiles, building, and electronics. A variety of industrial sectors employ bauxite. These industries include those in cement, steel, abrasives, chemical, and refractory materials. In chemicals: Aluminum compounds are made from bauxite and alumina.

In refractory: A variety of products are made using bauxite as a raw material.

The primary raw material used in the manufacturing of electric, mechanical, and civil tools is bauxite. It's also applied as an adsorbent, a desiccating agent, a catalyst in a variety of processes, and in the production of dental cement.

In the manufacture of road aggregates and building materials: Lateritic bauxite is frequently utilized in place of other materials in construction projects. In order to reduce accidents, construction companies employ calcined bauxite as an anti-skid road aggregate in specific locations. Bauxite is widely used in the production of paper, water purification, and petroleum refining, although its uses are limited. Additionally, bauxite is used in other sectors like the cosmetic industry. It is also used in the paint industry, rubber, and plastic industries and so on.

3.2. Data Acquisition

Two equipment's are used to collect data regarding surface roughness and taper angle. These are the scanning electron microscope and the Keyence respectively. Hitachi High-Tech Scanning electron microscope with the following specifications is used to measure surface roughness

From the cross-section graphs produced by the profilometer, hole dimensions such as hole diameter, maximum hole depth, hole center depth, and hole wall inclination angle were determined. Two cross-sectional profiles were made for each hole, intersecting at the center of the hole at a 90-degree angle.

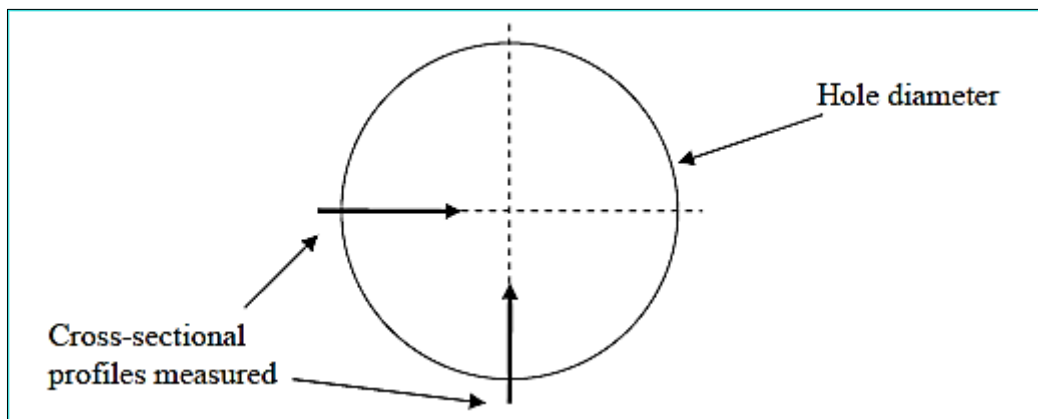


Figure 3.2 Cross-sectional profiles of the hole

For analysis, the geometrical features of the holes were measured on average. The number of pits on the hole surface was manually counted, and the surface quality of the holes was assessed by visually examining them under a digital microscope.

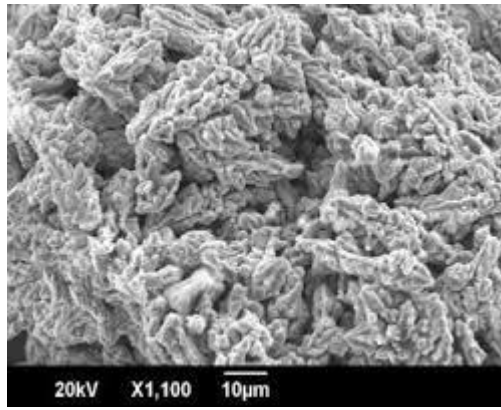


Figure 3.3 SEM image of bauxite work piece.

3.3. Experimental setup and design of experiment

Bauxite work piece material was used in experimental work. Typically, bauxite has a Mohs hardness of 1 to 3, making it a soft material. Its color ranges from white to reddish-brown, and its specific gravity is between 2.0 and 2.5. It also has an earthy shine and a pisolitic structure. These characteristics help distinguish bauxite, although they have no bearing on its worth or uses. This is due to the fact that bauxite is nearly always treated to create a substance that is not physically similar to bauxite.

The steel industry frequently uses bauxite bricks. The substance is mostly composed of 25%–35% mullite and 50%–70% corundum. Bauxite has a moderately good compressive strength and an average Young's modulus. In general, there is little resistance to temperature. Commercial refractory ceramic (Bauxite) mechanical properties are listed in Table 3.1

Table 3.1 Mechanical properties of the investigated refractory ceramics

Material	Density (gcm^{-3})	Porosity (%)	Cold compressive strength (MPa)	Cold bending tensile strength (MPa)	Young's modulus (MPa)
Bauxite	2.89	15	126	19	5900

The work item that is being measured is a plate that has the following dimensions: 100 x 50 x 2 mm; its density is 0.779 gm/cc. The plate is cut four times during the experiment.



Figure 3.4 The different types of abrasive particles.

Table 3.2 Chemical composition of garnet 80 mesh

Element	SiO ₂	Al ₂ O ₃	F _e O	M _g O	T _i O ₂	M _n O	C _a O	C _r ₂ O ₃	P ₂ O
Percentage	31	21.6	37	7.4	0.55	0.53	1.84	0.05	0.05

Table 3.3 Values of constant parameters.

Parameters	unit	value
Water orifice diameter, d_o	mm	0.3
Mixing tube length, l_f	mm	76
Abrasive material	Garnet	

At Gafat Engineering in Addis Abeba, the experimental work was carried out on an abrasive water jet machine, KMT model. An abrasive of garnet 80 mesh (0.180 mm) was employed. A pre-sized silicate sample measuring 300 x 300 x 14 mm was cut using the chosen equipment with consideration for its use in artistic and architectural applications. A picture of the used machine can be found in Figure 9.

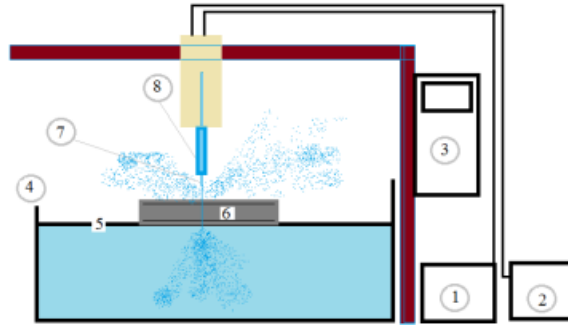


Figure 3.5 The schematic diagram of AWJ machining test rig [19]

In the Delhi material testing facility in India, materials are examined before being utilized in studies. The obtained chemical composition matches Table 3.2. Machine specification is shown in

Table 3.4.

Table 3.4 Machine specification

Maximum traverse speed	4572mm/min
Jet impingement angle	90°
Orifice diameter	0.33mm
Mixing tube diameter	0.762mm
Mixing tube length	101.6 mm
Maximum working pressure	450 Mpa
Voltage	415 V
Frequency	50 Hz
Phases	3
Power	3kW
Current	5.8A
Table Size	1600 x 2600 mm

$$MRR = H_t W D_i$$

H_t = depth of penetration

$$H_t = 16.5 \text{ mm}$$

V_f = Traverse speed of the abrasive water jet

V_f = varies at three different levels

W = width of the kerf

W = varies depending on the kerf value

A Vernier caliper is used to calculate the kerf width. A roughness testing equipment is used to determine the samples' surface roughness.

The trials made use of an abrasive water jet equipment from KMT. Industries with machine pressures of up to 450 Mpa utilize the Jet-Line JL-50 ultra-high-pressure pump. The machine has a 3000 x 3000 mm work piece table, an abrasive feeder system, a pneumatic control valve, and an abrasive hopper that is fed by gravity. aperture used to change the high-pressure water jet into a collimated jet with the use of a carbide nozzle. The nozzle was regularly inspected during the trials and replaced if it became worn out. Compressed air is used to transport the abrasive to the mixing chamber.

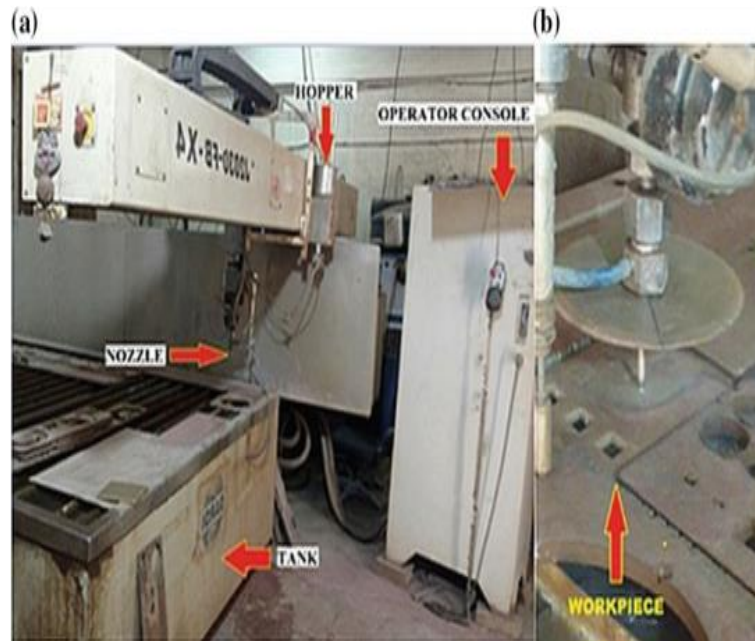


Figure 3.6 KMT abrasive water jet machine

Abrasive and material debris were gathered in the catcher tank. An abrasive water jet machine can quickly cut through a variety of hard materials; bauxite was utilized as a test material in this instance. Abrasive water jet cutting machines use a variety of abrasive minerals, including silicon carbide, garnet, silica, and aluminum oxides. Here, the abrasive is garnet. The outcome will be looked into. For the experiment, standard 80 mesh grit size has been chosen.

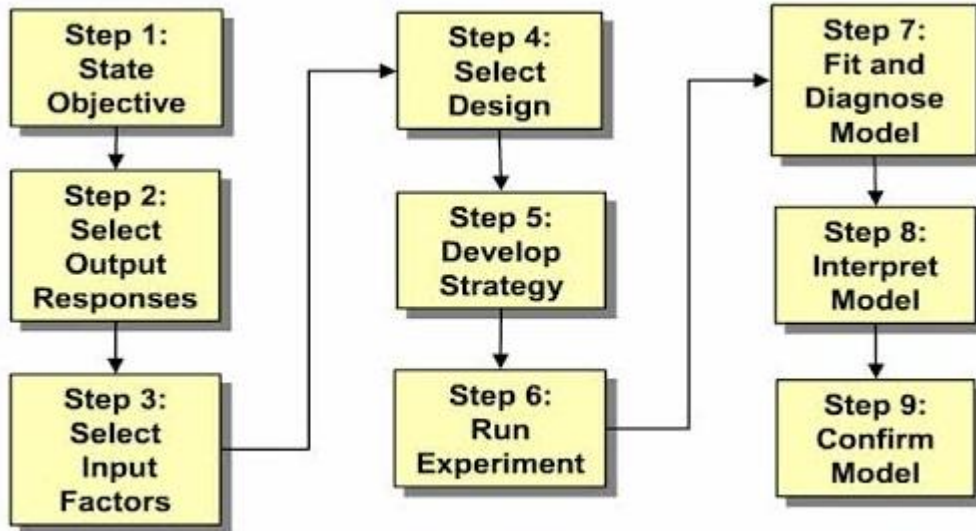


Figure 3.7 Design of Experiment

The purpose of the experimental study is to determine how surface quality is impacted by the form of the mixing chamber. Everybody tried out three levels.

Table 3.5 and to plan trials, the Response Surface Method (BBD) is applied. An abrasive substance with an 80-micron mesh size is employed in the experiments. The AWJM machine is configured with a voltage of 300 V, current of 20 A, and nozzle angle impingent angle of 90° for the duration of the trials. The AWJM machine is used in the experiment to create square holes that measure 20 mm by 20 mm.

Using a Vernier Caliper, the depth of cut is measured at the sample's jet entrance surface with an accuracy of 0.02 mm. After that, the response values are taken into account for model construction and optimization.

Surface roughness (SR) and taper angle (TA) were measured three times for each experiment, and the average values are used in the study. The following formulae are used to evaluate the output parameter (surface roughness, μ), and taper angle, TA) during experimentation:

Where W_a and W_b are initial and final weight, respectively; t is the cutting time; t_w is the thickness of workpiece, K_t and K_b are the top and bottom kerf width, respectively.

$$\text{Kerf taper} = \frac{w_t - w_b}{2t} \quad (3.1)$$

To assess the experimental results objectively, kerf properties such top kerf width and kerf taper angle were measured. Before separating the specimens to measure the smooth depth of cut, the kerf taper, top kerf width, and depth of cut were measured from the end of the kerf. It was predicted that the jet tail back effect would cause the two kerf walls in AWJ contouring to be asymmetrical. On each of the kerf walls, the kerf taper and smooth depth of cut were thus

obtained. By calculating the kerf wall inclination (w_t-w_b) from the top kerf edge, the kerf taper was determined. The following relation is used to calculate the taper angle.

Where w_t is the top kerf width, w_b is the bottom kerf width and 't' is the thickness of the work piece.

Table 3.5 Actual experimental conditions

Parameters	Conditions
Cutting pressure	3,700 3,800 3900bar
Abrasive flow rate	230, 330, 430g/min
Abrasive material	Garnet (#80)
Cutting speed (Traverse rate)	771,996,1387mm/min
Standoff distance	1.5mm
Orifice diameter	0.33mm
Workpiece material	Bauxite (refractory ceramic)
Workpiece thickness	12 mm
Nozzle diameter	1.01mm
Nozzle length	76.2mm
Mixing chamber type	Cylindrical, Parabolic

When selecting input parameters for an abrasive water jet machining operation with water pressure, abrasive mass flow rate, and cutting speed, it's essential to consider various factors. Here are seven justifications for choosing specific values:

❖ **Material Hardness and Thickness:**

A higher water pressure (e.g., 3,900 Bar) may be suitable for machining hard or thick materials, as it enhances the cutting force. This is crucial when dealing with challenging materials that require a more substantial force to achieve efficient cutting.

❖ **Precision Requirements:**

Lower cutting speeds (e.g., 771 mm/min) can be beneficial when precision is crucial. If the operation demands intricate designs or fine details, a slower cutting speed allows for more control over the machining process.

❖ **Productivity and Throughput:**

Higher cutting speeds (e.g., 1387 mm/min) can be chosen to maximize productivity and throughput, making it suitable for applications where speed is a priority, and the precision requirement is not extremely high.

❖ **Material Removal Rate:**

A higher abrasive mass flow rate (e.g., 430 g/min) contributes to a higher material removal rate. This is advantageous when the primary goal is to remove material quickly, which is especially important for applications where efficiency and speed are critical.

❖ **Surface Finish Requirements:**

Lower abrasive mass flow rates (e.g., 230 g/min) can be chosen when a smoother surface finish is required. This is beneficial for applications where the final product's aesthetic appearance or surface quality is a significant consideration.

❖ **Cost Efficiency:**

Opting for a moderate water pressure (e.g., 3,800 Bar) along with an optimized abrasive mass flow rate (e.g., 330 g/min) and cutting speed (e.g., 996 mm/min) may strike a balance between efficiency and cost-effectiveness. This combination aims to achieve reasonable productivity without excessive wear on equipment.

❖ **Nozzle Wear and Maintenance:**

Careful consideration should be given to the abrasive mass flow rate to prevent excessive wear on the machining nozzle. A balance must be struck to achieve efficient material removal without causing rapid nozzle deterioration, leading to increased maintenance frequency.

These justifications demonstrate the need to tailor the abrasive water jet machining parameters based on the specific requirements of the operation, considering factors such as material properties, precision, productivity, and cost efficiency.

3.4. Taguchi Experimental Design

The goal of the Taguchi approach is to minimize process variation by using a strong experimental design. The method's main goal is to provide high-quality goods at a price that is affordable for the producer. Genichi Taguchi is credited with creating the Taguchi technique. He created an approach to plan trials that looks into how various factors impact the mean and variance of a process performance characteristic, which indicates how well the process is operating.

In Taguchi's proposed experimental design, the process parameters and the levels at which they should be modified are arranged using orthogonal arrays. The Taguchi approach tests pairs of possibilities as opposed to needing to test every possible combination, as in the case of the factorial design. This saves time and money by enabling the gathering of the data required to identify the variables that most influence the quality of the product with the least amount of experimentation. When there are only a few major factors, minimal interactions between variables, and an intermediate number of variables (between three and fifty), and the Taguchi technique works best.

Traditional experimental design techniques are difficult to employ and excessively complex. When the number of process parameters rises, a lot more experiments must be conducted. The Taguchi technique employs a unique orthogonal array design to examine the whole parameter space with a minimal number of experiments in order to address this challenge. Three characteristics of abrasive water jet machining are thought to be governing factors. These are the abrasive mass flow rate, traverse rate (cutting speed), and jet pressure. The initial trial on a variety of different characteristics served as the basis for selecting the parameters. There are three levels for each parameter: low, medium, and high, represented by the numbers 1, 2, and 3, respectively. The Taguchi method states that an L9 orthogonal array should be used for the experiment if there are four parameters and three levels for each parameter.

Table 3.5 shows the abrasive water jet machining parameters and their levels considered for the experimentation.

Three process characteristics were taken into account when assessing the machining process's performance. Surface roughness (Ra) and taper angle are the responses that are taken into account for assessment. The Taguchi methodology's recommended order for conducting experiments was followed, and the results were computed using the formula below and documented in *Table 3.6.*

Table 3.6 Taguchi experimental design for three parameters with three levels each.

A	B	C
1	1	1
1	2	2
1	3	3
2	1	2
2	2	3
2	3	1
3	1	3
3	2	1
3	3	2

3.5. Results and Data Measurement

.Nine runs, each tripled, were performed in a total of twenty-seven experiments before the average value for each of the three output responses was determined. The values that are obtained after that are used as input data for additional ANOVA and graphical analysis.

Table 3.7 Recorded experimental combinations of process parameters and corresponding values of responses/output parameters (cylindrical mixing chamber)

S/N	CP (bar)	AFR (gm/min)	CS (mm/min)	Taper Angle (θ) (Degree)	Surface Roughness (Ra)	
					(μm)	
					Top (3mm)	Bottom (3mm)
1	3,700	230	771	0.7779	4.3713	6.9941
2	3,700	330	996	0.7954	3.2486	5.1978
3	3,700	430	1,387	0.8881	4.39	7.024
4	3,800	230	996	0.9167	4.2353	6.7765
5	3,800	330	1,387	0.9360	6.199	9.9184
6	3,800	430	771	0.9898	5.3146	8.5034
7	3,900	230	1,387	0.8753	6.7356	10.7770
8	3,900	330	771	0.9683	4.5263	7.2421
9	3,900	430	996	0.9512	5.233	8.3728

Table 3.8 Recorded experimental combinations of process parameters and corresponding values of responses/output parameters (parabolic mixing chamber)

S/N	CP (bar)	AFR (gm/min)	CS (mm/min)	Taper Angle (θ) (Degree)	Surface Roughness (Ra)	
					(μm)	
					Top (3mm)	Bottom (3mm)
1	3,700	230	771	0.7001	4.2095	6.7353
2	3,700	330	996	0.7158	3.1284	5.0055
3	3,700	430	1,387	0.7993	4.2275	6.1909
4	3,800	230	996	0.8250	4.0786	6.5258
5	3,800	330	1,387	0.8424	5.9696	9.5514
6	3,800	430	771	0.8908	5.1180	8.7548
7	3,900	230	1,387	0.7877	6.4864	10.3783
8	3,900	330	771	0.8715	4.3588	6.9741
9	3,900	430	996	0.85611	5.0393	8.0630

The measurements for the two different styles of mixing chambers are displayed in . Nine runs, each tripled, were performed in a total of twenty-seven experiments before the average value for each of the three output responses was determined. The values that are obtained after that are used as input data for additional ANOVA and graphical analysis.

Table 3.7, and Table 3.8. This means that given the same material, cutting speed, abrasive flow rate, and applied pressure.

Abrasive flow rate variation was displayed against the taper angle data for each condition for various mixing chambers. The trend that has been plotted indicates that when the abrasive flow rate increases, the taper angle values decrease. The surface roughness variation corresponding to the abrasive flow rate for altering the mixing chamber design is depicted in the figure. The variation in abrasive flow rate causes a variation in surface roughness. When the abrasive flow rate increases, surface roughness decreases while maintaining the same cutting speed and mixing chamber. Surface roughness achieved with a parabolic mixing chamber is minimal for any abrasive flow rate. Thus, it can be inferred from the appearance that the parabolic mixing chamber is preferable when it comes to mixing in an abrasive water jet cutting head. Overall analysis shows that the parabolic mixing chamber is more effective in combining abrasive, water, and air. Two separate research approaches were used to examine the mixing quality for various forms of mixing chamber.

Chapter Four

4. Parabolic Mixing Chamber-Based Modelling

4.1. Introduction

Materials with excellent quality and properties are always desired in any engineering applications [110]. One of the many types of material deterioration that are typically categorized as wear is the erosion of materials brought on by the impact of hard particles. Bitter gave a definition of erosion [111] described as "material damage caused by the attack of particles entrained in a fluid system impacting the surface at high speed" , according to Hutchings [112] The dictionary defined erosion as "an abrasive wear process in which the repeated impact of small particles entrained in a moving fluid against a surface results in the removal of material from that surface" . In gas turbines, rocket nozzles, cyclone separators, valves, pumps, and boiler tubes, solid particle erosion poses a major concern. Nonetheless, production procedures like abrasive waterjet cutting can benefit from the use of solid particle erosion.

Through the processes of brittle fracture and/or micro-plastic deformation, material is removed during erosion. The impact of hard particles on ductile materials, including pure metals and alloys, results in significant localized plastic strain at the surface's impact sites. In brittle materials like ceramic and intermetallic compounds, localized surface cracking is caused by the impact force of particles. These fractures spread and eventually connect with one another during more impact events, causing material to separate from the surface [113].

Models of the AWJ machining process have been created using both analytical and empirical techniques [114]. Researchers have also used techniques involving finite elements [115], fuzzy logic algorithms [116] and reaction kinetics [117], to model this highly complex manufacturing technique, which is fundamentally based on an ultra-high speed erosion process. A recent approach based on using a coherent set of models was presented by Hoogstrate et al. [118]. Examining the published models for the AWJ cutting reveals that every analytical model currently in use necessitates process-dependent, experimentally derived constants. Heuristic methods and empirical models both require a great deal of experimentation, which is a significant disadvantage because it takes time and has restricted application.

A review of the basic erosion models can be found in [119]. The published erosion models take two distinct techniques to solving, depending on the methodology used: (1) solving the equation of motion of individual particles, or (2) calculating an energy equation. Finnie [12] and Hashish [120] employed the former method whereas Bitter's model employed the energy

equation [2]. Currently, the existing erosion models for ductile material do not account for the simulation of multiple particle erosion.

This chapter introduces a novel method for simulating the abrasive waterjet machining procedure. This new method is based on an altered version of the erosion models that Finnie and Hashish created initially. This change makes it possible to mimic the erosion setup with numerous particles. The AWJ machining process is then modeled using the updated erosion model, which includes surface regeneration capabilities. In this process, a new surface is created following the erosion of each individual particle, and a new particle begins eroding the regenerated surface. Until the particle leaves the cut or its velocity changes, the numerical solution will keep running. This method makes it possible to model the AWJ machining process with thousands of particles, and even with a Pentium-based CPU, the calculation time will be reasonable.

4.2. Design of mixing chamber

A cross-sectional view of the AWJ cutting head is shown in (a). The focusing tube, orifice, mixing chamber, water channel, air and abrasive channel, and cutting head body are the components that make up an AWJ cutting head. The mixing chamber, where a high-speed water jet combines with air and abrasive, is formed by combining the water and abrasive channels. The focusing tube directs the water jet to the cutting spot and aids in the mixing of the abrasive particles with water and the transmission of kinetic energy to them.

Md. G. Mostofa demonstrated how the CFD simulation produced the vortex inside the mixing chamber. When the air inside the mixing chamber comes into touch with a high-speed water jet, it exhibits extremely high turbulence. Since air transports the abrasive, air streamlines are crucial because experimental research by M. Hashish revealed that turbulence inside the air is what causes the abrasive particle to entrain inside the high-speed water jet. The vortex phenomenon yields the first mechanism of abrasive entrainment from the consequence of the air stream line.

Figure 15 (b) depicts the vortex that is formed inside the mixing chamber by the abrasive, water, and air. In order to enhance abrasive entrainment and regulate the stream line, a parabolic-shaped mixing chamber was created and utilized for cutting. There will be a difference in the cutting performance if the prognosis is accurate. The cylindrical and parabolic mixing chambers are displayed in figure 15.

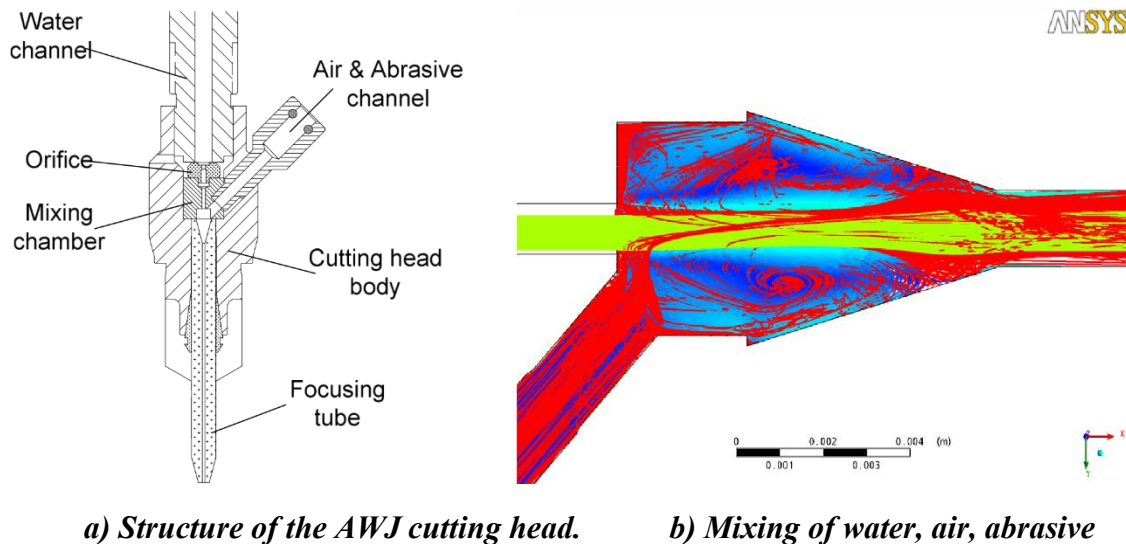


Figure 4.1 Cross sectional view of the AWJ cutting head & vortex created inside the mixing chamber

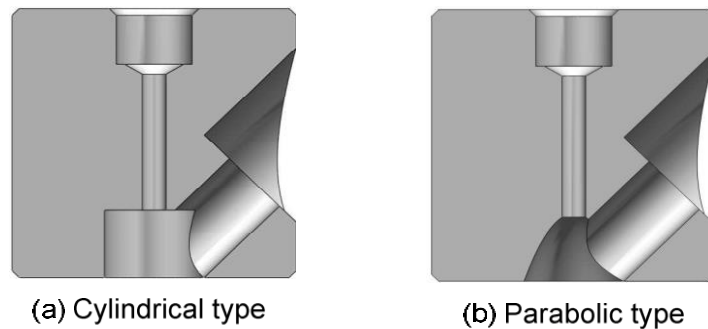


Figure 4.2 Two types of mixing chamber geometry

4.3. Modelling of abrasive water jet machining

The modeling of the AWJ process is essentially based on a surface generation technique, in which a different particle begins eroding the regenerated surface continuously after each individual particle has eroded, creating a new surface. Thousands of particles can be simulated with this technique in a reasonable amount of time utilizing standard computer resources. The model does not require any calibration constants or empirically obtained parameters; it just depends on the qualities of the work piece material.

4.4. Modified erosion model

The particle equation of motion serves as the foundation for the updated erosion model, which can also handle curved surfaces in addition to flat ones. Furthermore, the impacts of numerous particle impact can be simulated using this modeling technique. The microscale behavior is assumed by the model to be insensitive to temperature and strain rate, and to resemble the

behavior observed at the mesoscale level. The forces created during erosion were computed using an orthogonal cutting model. The direction of particle velocity determines the depth of incision. Figure 4.3 shows a particle with a striking velocity of $v(u)$ degrading a curve surface. This particle can freely spin in the x - y plane and move in the x , y coordinate. The particle's impact on the surface produces the cutting forces F_v and F_{vn} . Forces acting perpendicular to the cutting direction are denoted by F_{vn} and parallel to it by F_v . Equations can be utilized to compute F_v and F_{vn} by utilizing the streamlined version of the orthogonal cutting force model (4.1) and (4.2) respectively, where K_S is the specific cutting resistance of the workpiece material, t is the depth of cut perpendicular to the cutting velocity v , b is the width of cut, and C is a constant. Equation (4.1) is valid only when F_v is parallel to v as shown in Figure 18.

$$F_v = K_S b t \quad (4.1)$$

$$F_{vn} = C F_v \quad (4.2)$$

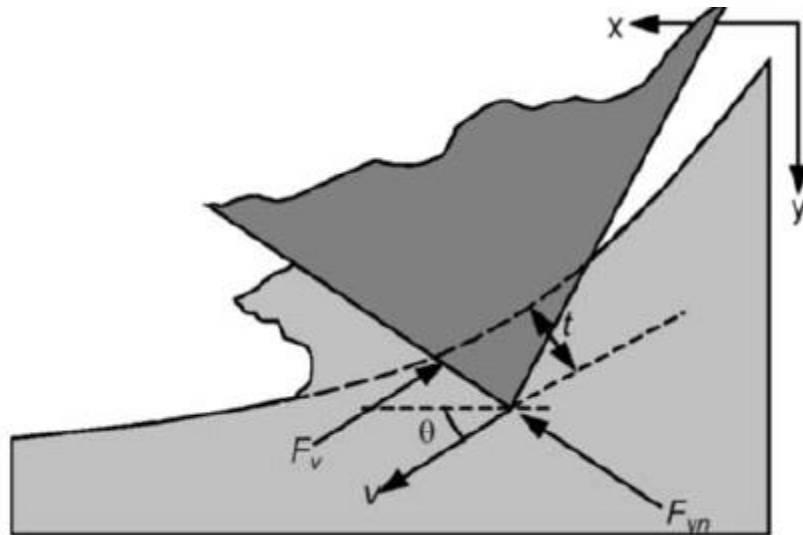


Figure 4.3 Particle eroding a curve surface.

The cutting forces F_v and F_{vn} can be discrete into x and y direction as shown in Equations (4.3) and (4.4) respectively, where θ can be determined with Equation (4.5).

$$F_x = F_v \cos(\theta) + F_{vn} \sin(\theta) \quad (4.3)$$

$$F_y = F_v \sin(\theta) + F_{vn} \cos(\theta) \quad (4.4)$$

$$\theta = \arctan(v_x/v_y) \quad (4.5)$$

Furthermore, it is assumed that damping is equal to zero and that the stiffness effect is mixed with the cutting forces. Equations displays the particle's equations of motion in the x and y directions (4.6) and (4.7) respectively, while the rotation motion is given in Equation (4.8), where r is the rotational radius and i , y , and are the accelerations at the center of gravity. Equations can be used to determine the particle tip's coordinates k and I (4.9) and (4.10)

respectively. Unfortunately, Equations (4.6) to (4.10) cannot be solved in a closed form, but the answers can be found using numerical techniques.

$$m\ddot{x} = K_s bt[\cos(\theta)+c\sin(\theta)] \quad (4.6)$$

$$m\ddot{y} = K_s bt[\sin(\theta)+ccos(\theta)] \quad (4.7)$$

$$I\ddot{\phi} = K_s btr[\cos(\theta) + c\sin(\theta)] \quad (4.8)$$

$$k = x + r\phi \quad (4.9)$$

$$l = y + r\phi \quad (4.10)$$

The central difference algorithm shown in Equation (4.11) was used to solve the single particle erosion problem.

$$M\ddot{U} = [F] \quad (4.11)$$

Initializing the particle's displacement, velocity, and acceleration is the first step in the numerical solution. A mathematical loop was utilized to calculate the components related to direction and velocity between using a unique search technique, a spot on the current surface that meets the requirement that the angle formed between the particle's tip and the velocity direction be around 90 degrees is located. The depth of cut and the vector direction from the particle tip to the surface point can be calculated once this requirement is satisfied. Next, Equations are updated to include the anticipated depth of cut and the impacting particle's direction (4.1) to (4.4) in order to compute the cutting forces. The particle's acceleration, velocity, and displacement are then modeled using equations in the following stage (4.12), (4.13) and (4.14) respectively. Next, in a subsequent iteration, the new surface location and the new particle tip position are computed. When the particle leaves the cut or when its velocity changes, this loop is terminated.

$$A_t = -[M][F]_t \quad (4.12)$$

$$V_t = V_{t-1} + dtA_t \quad (4.13)$$

$$U_t = U_{t-1} + (dtV_t) \quad (4.14)$$

Figure 4.4 demonstrates how the predicted surface creation is affected by the particle's assault angle. Prior to collision, the surface was initially bent. We modelled four distinct attack angles. The surface shape following a single particle hit at each of the four orientations is displayed in the simulated findings. The erosion depth in the Y-direction was less at the attack angle of 15 degrees than it was at the 45-degree angle. This was due to the fact that the taper angle was lower at a lower attack angle (15 deg), where the particle momentum before reaching the surface in the y direction was lower than the momentum in the x direction. This illustrates how the

altered erosion model may forecast material removal for surfaces that are not flat. Nevertheless, there are no models or data accessible in the academic literature to compare the model's output.

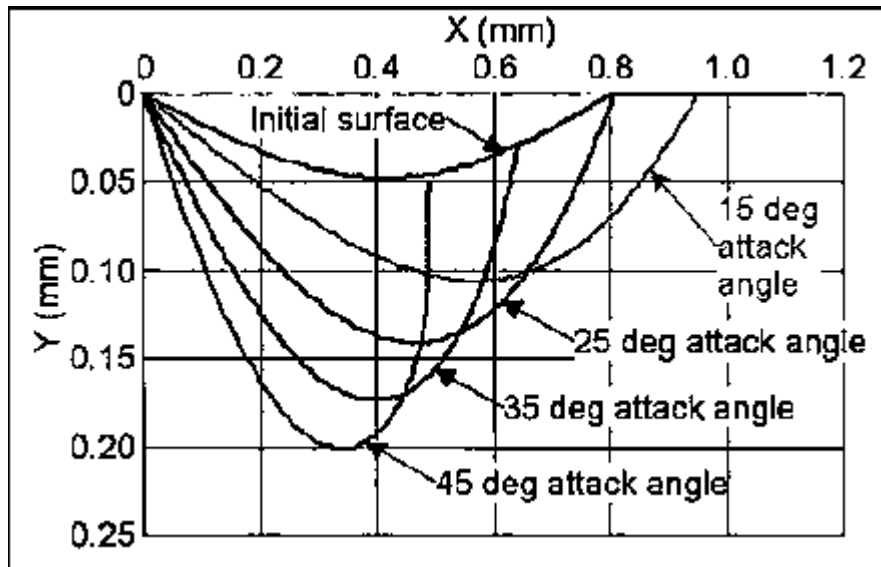


Figure 4.4 Effect of particle's attack angle on modelled surface generation.

Figure 4.5 describes two distinct modeling scenarios: the particle is hitting a completely flat surface in the first scenario, while a sinusoidal surface is being modeled in the second. In comparison to the particle striking the flat surface, the one striking the sinusoidal surface exhibits a deeper taper angle. This was probably because the initial Y-direction depth was already lower on the initial sinusoidal surface than it was on the flat surface.

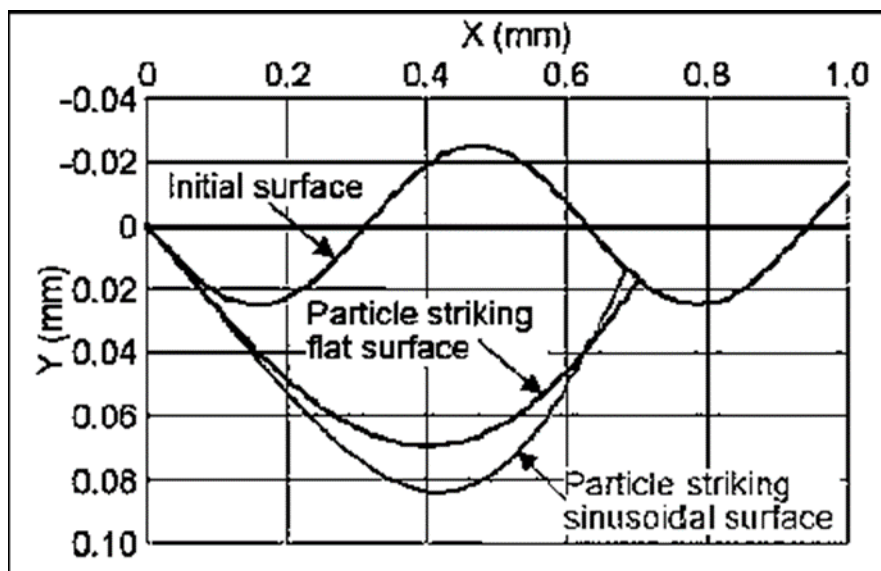


Figure 4.5 Effect of particle striking a flat surface and a sinusoidal surface on modelled surface generation.

4.5.

Jet generation

Equation describes how v_p , the abrasive particle velocity, must depend on water pressure P , the abrasive mass flow rate, and the water mass flow rate law in order to represent the jet formation process (4.15). Other factors that must be considered are the size of the abrasive particle and the geometry of the nozzle. The nozzle orifice, focus geometry, abrasive particle characterization, pump pressure, and other process variables all affect the constant. η_t values vary from 0.73 to 0.94. [121].

$$V_p = \eta_t \frac{V_0}{1 + \frac{\dot{m}_A}{\dot{m}_W}} \quad (4.15)$$

By employing Bernoulli's law, V_0 can be determined from Equation (4.16), whereby the real velocity of the high-pressure water is measured to yield coefficients and y , which are then compared with those obtained theoretically. The typical range of values for C_v and y is 0.83 to 0.93 [121].

$$V_0 = C_v y \sqrt{2P/\rho} \quad (4.16)$$

The actual volumetric flow rate of the water, Q_a can be determined using Equation (4.17), where C_d is a non-dimensional value that accounts for the decrease in jet velocity brought on by friction between the water and the orifice wall, as well as the reduction in the water mass flow rate, \dot{m}_w , as a result of the abrupt shift in fluid mechanic conditions on the orifice outlet. The actual observed flow rate is divided by the theoretical flow rate, which is often between 0.6 and 0.8, to determine the C_d [121].

$$Q_a = c_d \times A_n \sqrt{2P/\rho_0} \quad (4.17)$$

4.6.

Numerical simulation

The updated erosion model and the numerical solution of the single particle erosion problem serve as the foundation for the suggested method for simulating the AWJ process. Multiple particles' cumulative effects can be simulated by incorporating the modified erosion model. The computational code must reduce computing time in order to produce the simulation results in an acceptable amount of time. Currently, a Pentium 4, 1.8 GHz clock speed CPU can execute a simulation with 10,000 particles imparted on the surface in 60 minutes. The simulation operates under the following assumptions: (a) that the particle sizes and velocities are constant; (b) that the directions of the particles as they exit the nozzle are aligned with the nozzle.

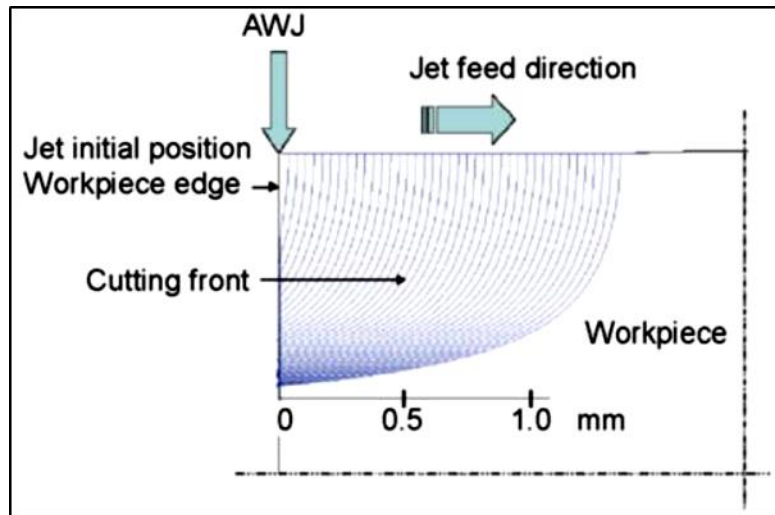


Figure 4.6 Advancement of the cutting front using the modified mode.

Figure 4.6 shows the results of the advancement of the cutting front, using the modified model Results and discussion

Figure 4.7 compare the effects of water delivery pressure on taper angle using data acquired from Hashish's analytical model [120], experimental results [121], and the newly developed modelling method, at nozzle velocities of 1,387 mm/min and 771 mm/min respectively. The workpiece material modelled was Bauxite. The KS value employed was 50 Joules per cubic mm, which is similar to that used for grinding process [122]. This KS value is 30 to 40 times higher when compared to metal cutting. Hashish first introduced his model for AWJ cutting, based on Finnie's erosion model, in 1984 [123]. He later modified the erosion model to simulate the AWJ cutting process [120]. The taper angle can be determined using Hashish's model, as detailed in Equation (4.18).

$$\frac{h}{d_j} = 0.282c \sqrt{\frac{\frac{\varepsilon}{\sigma}}{\frac{\pi \varepsilon d_j^2 u_t}{2 \dot{m} a v_p^2}} + \frac{(1 - \frac{v_{cr}}{v})^2}{\left(\frac{\pi \varepsilon d_j^2 u_t}{2 \dot{m} a v_p^2}\right) + C_f \left(1 - \frac{v_{cr}}{v}\right)}} \quad (4.18)$$

The process parameters employed by the experimental analysis, Hashish's model and the newly developed model are listed in Table 4.1.

Table 4.1 Process parameters employed to compare experimental and modelled results.

	p (Bar)		
CS (mm/min)	771	207	241
1387	0.75	0.83	1.11
771	1.74	2.32	3.00

When employing Hashish's model, the constants and c are acquired by assuming that C_f and v_{cr} are equal to zero (as suggested by Hashish). When the cutting speed modelled was 1,387 mm/min, both Hashish's and the newly developed model showed that with larger water delivery pressure, the taper angle increases, which agreed well with the experimental results, as shown in Figure 25.

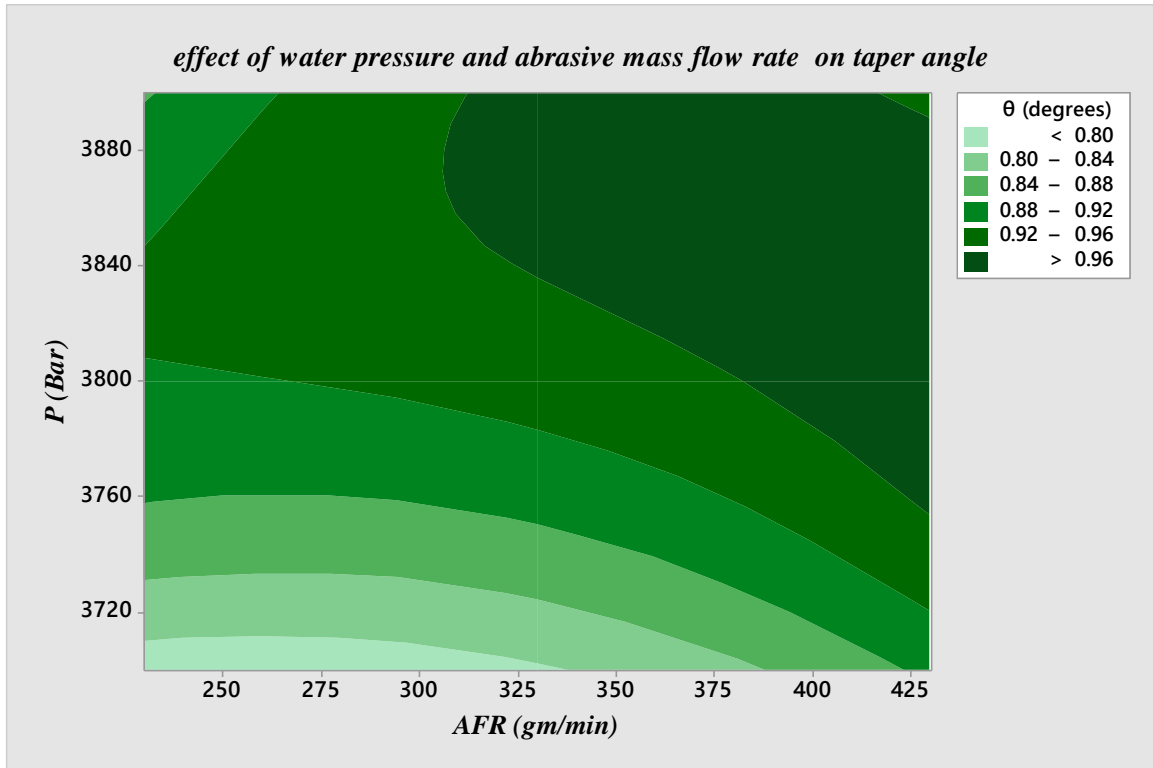


Figure 4.7 Effect of water pressure and abrasive mass flow rate on taper angle.

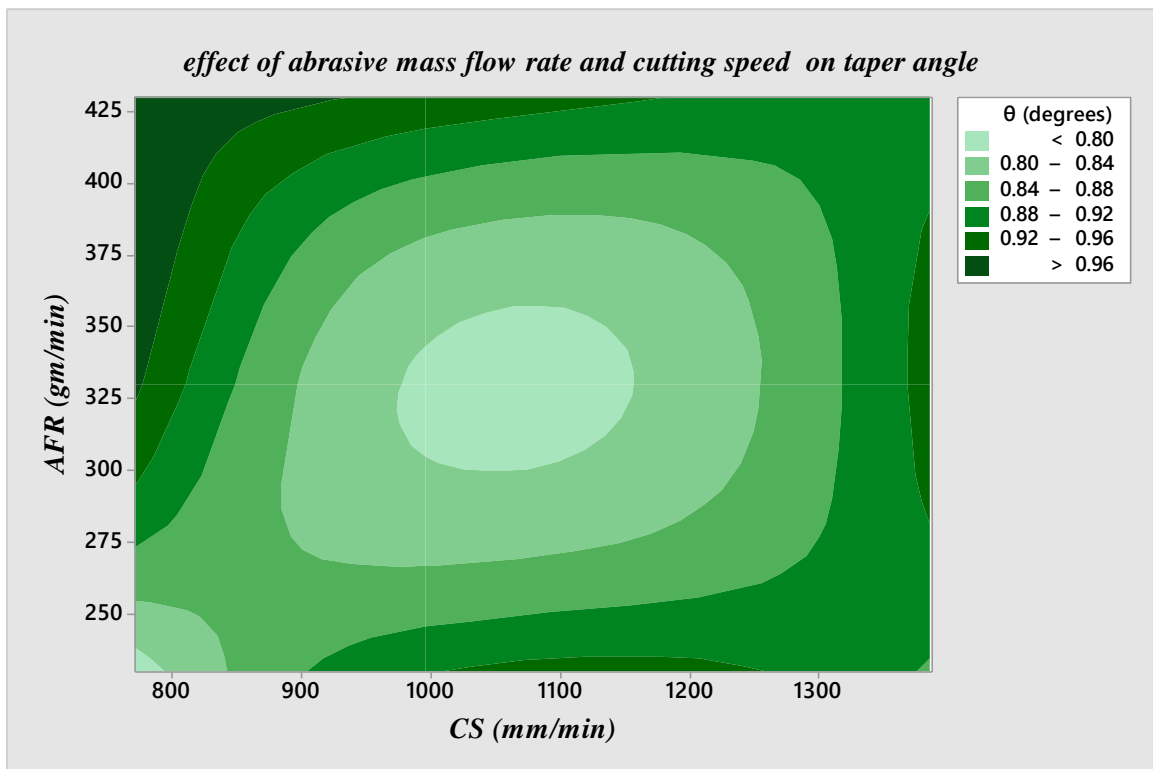


Figure 4.8 Effect of abrasive flow rate and cutting speed on taper angle

The taper angle predicted by the newly created model coincided with testing data better than Hashish's model when the transverse speed was reduced to 771 mm/min. Recalculating the calibration constants used in Hashish's model will increase its accuracy; yet, obtaining the calibration constants will require a great deal of experimental work. This is one of the primary drawbacks of using such modeling techniques; in contrast, the recently established method does not require a calibration constant when the nozzle transverse speed changes.

4.7. Conclusions

A novel method is showcased for modeling the parabolic AWJ machining mixing chamber. This method is essentially based on mathematical erosion model, which has been adapted by other researchers. It is changed to allow for the simulation of erosion caused by multiple particle impacts. Additionally, the model can forecast the rates of volumetric material removal and the creation of new surfaces as a result of many particles colliding with curved surfaces. Furthermore, the recently created erosion model is effectively used to simulate the extremely complex AWJ machining procedure while accounting for the abrasive particle flow properties. The primary advantage of using this method is that it does not require process-specific experimental constants, so the model remains independent of operating parameters even if it is dependent on the mechanical properties of the work piece material. Similar trends are seen in the new model as in Hashish's model [113,115], and agrees even better with the experimental results.

Chapter Five

5. Cost of Machining

5.1. Background

The water jet containing abrasive particles is the cutting tool in AWJ. According to the pie chart in the article, the abrasive cost is the main expense component of operating an AWJ system Figure 5.1. Although almost any material may be sliced by adding abrasives, minimizing abrasive use is necessary for the best economic outcome. Larger abrasive feeding amounts may also be linked to clogging and process disruptions, thereby increasing costs.

Additionally, there is a chance that the mixing tube's wear rate would quicken, increasing operating expenses. Therefore, lowering the amount of abrasive used will often improve the AWJ process's performance, dependability, and costs. But when calculating expenditures, other expenses like electricity, machine and pump maintenance, and basic consumables must also be considered. The traverse rate used to trim a length of CFRP material can be used to determine the process cost, which also takes into account the costs of abrasive, water, consumables (such as the cutting head and intensifier pump), power, and machine maintenance. Labor costs and machine depreciation are not included in this assessment. The precise expenses and formulas utilized to calculate cost/m are listed in Figure 5.1.

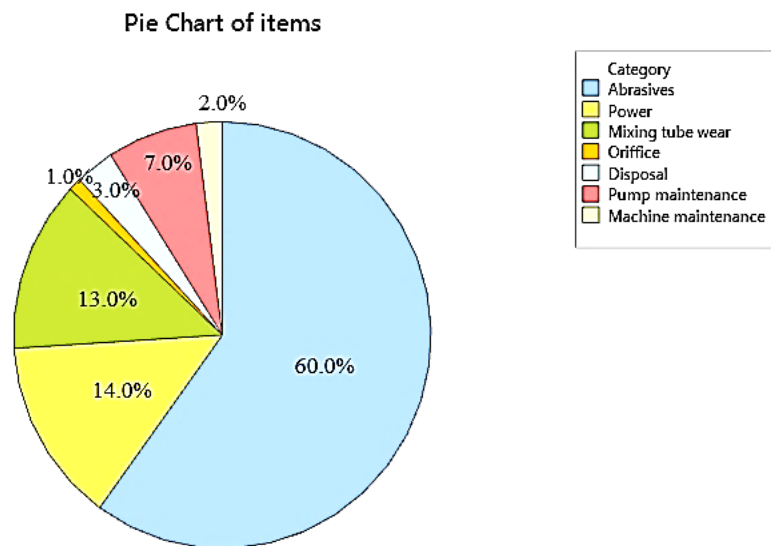


Figure 5.1 Cost breakdown for a 400 MPa AWJ [7]

Table 5.1 AWJ production Costs

Item	Abrasive Ca	Water Cw	Consumables Cr	Power Ce	Maintenance Cm
Specific cost	0.195 £/kg	0.0015 £/l	1.628 £/h	0.09 £/kwh	1,000£/year 2,000 h/year 5£/h
Cost per unit length, Cl	Ca. Ma/v	Cw.Vw/v	60Crv	60Ce.Pev	60Cm/v

The total cost per meter can be found by the summation of the terms in equation (5.1); where v is the traverse rate which varies with thickness. Added time should be considered for cornering and piercing.

$$Cl = \frac{1}{v} [(C_a \cdot m_a) + (C_w \cdot V_w)] + \frac{60}{v} [C_r + (C_e \cdot P_e) + C_m] \quad (5.1)[7]$$

The machine maker estimates that the cost of operating an AWJ machine is about £20 per hour. At a cutting speed of 150 mm/min, the cost per meter would be approximately £2. A 12 mm end mill for slot milling will cost approximately £60 for an uncoated burr carbide and approximately £300 for a poly-crystalline diamond PCD. Assuming a tool life requirement of 30 meters, regardless of tool condition—a typical cut length target in the aerospace sector—the cost would be between £2 and £10 per meter. High cutting pressures, temperature-induced damage, and dangerous dust are all produced during milling, especially in dry environments where hydrophilic composites are ideal and subsequent cleaning procedures are prevented. When the same laminates were trimmed with a laser, they suffered significant thermal damage, and utilizing wire EDM was much slower and wire snapped.

5.2. Economic Comparison

In this section an economic comparison is made between laser and AWJ cutting. Examples of "typical" capital and running costs for the two methods are given. It is important to remember that running costs vary depending on the type of profiling being carried out. If there are high demands on the quality of the profiled product it may be necessary for example, to use higher gas pressure, in the case of laser cutting, or higher abrasive feed rate if the AWJ is the chosen method.

The choice between both the laser and AWJ technique for profiling a component is not entirely based on the actual cutting cost. When choosing the method, it is very important to take in

account subsequent manufacturing operations on the component. By a correct cutting choice further operation might be reduced or even excluded.

5.3. Capital Costs

The capital cost is naturally dependent on the size and capacity of the cutting system. In Table 5.2 the capital cost for what can be considered to be a normal cutting system is presented.

Table 5.2. Capital cost for CO₂ Laser and AWJ cutting systems

CO ₂ Laser	AWJ
<ul style="list-style-type: none"> ○ CO₂ Laser 1200 W ○ X-Y table 2.5 x 1.25 m 	<ul style="list-style-type: none"> ○ High pressure pump (9 l/min) ○ X-Y table 3 x 3 m
<u>Capital cost (5 years. 10%)</u> 527 600 SEK/year 2000 h/year ⇒ 264 SEK/h	<u>Capital cost (5 years. 10%)</u> 580 360 SEK/year 2000 h/year ⇒ 290 SEK/h

5.4. Running Costs

Running costs are, as mentioned earlier, dependent on the type of product being profiled. In some extreme cases the running cost can be substantially higher than the figures presented in Table 5.3. However, the values in **Error! Reference source not found.** represents what can be taken as normal running costs for the two methods and can be used as guide-line figures.

Table 5.3 Running costs per hour for CO₂ laser and AWJ cutting systems.

CO ₂ Laser	AWJ
<ul style="list-style-type: none"> ○ Energy & water 35 ○ Lenses 10 ○ Cutting gas 30 ○ <u>Maintenance 35</u> <p>TOTAL 110 SEK/h</p>	<ul style="list-style-type: none"> ○ Energy & water 15 ○ Nozzles 35 ○ Abrasives 45 ○ <u>Maintenance 30</u> <p>TOTAL 125 SEK/h</p>

5.5. Cost Prediction

Cost effectiveness of AWJ cutting operations is always the key factor in determining its viability. Although some examples of cost analysis have been given by Hashish (1991, Houston), a more thorough evaluation method is still in need.

Actual cost composition of an abrasive waterjet cutting operation could fairly complicated. This study does not attempt to cover every aspect of AWJ cutting cost. Cost factors such as depreciation, income tax, risk, and many more are not included. The focus of analysis is placed on the major cost factors. The approach used here is to determine the hourly cost for operating

an abrasive waterjet system. Based on the parameter prediction as discussed in the previous section, cost for cutting a specific work piece can be evaluated.

To determine the hourly cost for operating an abrasive waterjet system, the following cost components are considered:

❖ Machine Hourly Cost (C_{mh})

It is assumed that capital investment in an abrasive waterjet cutting system is C_m U.S. dollars (\$), the service life of such a system is n years with h_y work hours per year, the salvage value by the end of n years is zero, the rate of return is i (%). Using the uniform annual cost method (Groover, 1980), the annual machine cost (C_{my}) can be calculated by:

$$C_{my} = \frac{i(1+i)^n C_m}{(1+i)^n - 1} \quad (\$ \text{ per year}) \quad (5.2)$$

Then the machine hourly cost can be determined by:

$$C_{mh} = \frac{C_{my}}{h_y} = \frac{i(1+i)^n C_m}{[(1+i)^n - 1] h_y} \quad (\$ \text{ per hour}) \quad (5.3)$$

❖ Labour Hourly Cost (C_{lh})

This component of cost analysis includes the wages paid to operate the abrasive waterjet cutting system, fringe benefits and supervision. Assuming the annual salary of the operator to be O_y (\$), the fringe benefit equivalent to be F_y (\$) and the supervision equivalent is S_y (\$), the labor hourly cost can be determined as:

$$C_{lh} = \frac{O_y + F_y + S_y}{h_y} \quad (\$ \text{ per hour}) \quad (5.4)$$

❖ Material Hourly Cost (C_{th})

Considering abrasive costs C_a (\$/kg), an abrasive flow rate of m (g/s) will generate hourly cost of $3.6mC_a$. Similarly, water hourly cost is $60m_w C_w$, where C_w is the cost of water (\$/litre) and is the water flow rate of (lpm). Assuming that an abrasive waterjet nozzle costs C_n (\$) and its service life is (L_n hr), the hourly cost of nozzle is C_n/L_n . Similarly, the hourly cost of the waterjet orifice is C_d/L_o , where C_o stands for the cost of an orifice (\$) and L_o stands for its service life (hr). Considering a downtime rate of T_d (%), the hourly cost of materials is calculated by:

$$C_{th} = (3.6mC_a + 60m_w C_w + \frac{C_n}{L_n} + \frac{C_o}{L_o})(1 - T_d) \quad (\$ \text{ per hour}) \quad (5.5)$$

❖ Power Hourly Cost (C_{ph})

If the electric power costs C_p (\$/kwh), an abrasive waterjet system of P (kw) will cost PC_p per hour. Considering the downtime rate, the hourly cost of power is:

$$C_{ph} = PC_p(1 - T_d) \quad (\$ \text{ per hour}) \quad (5.6)$$

❖ Hourly Cost of Maintenance and Disposal (C_{dh})

It is assumed that the maintenance costs C_{mt} dollars for every h_{mt} machine hours and disposal work costs C_{dp} dollars for every h_{dp} machine hours. Therefore, the hourly cost of maintenance and disposal is calculated by:

$$C_{dh} = \frac{C_{mt}}{h_{mt}} + \frac{C_{dp}}{h_{dp}} \quad (\$ \text{ per hour}) \quad (5.7)$$

By combining all of these cost components, the total hourly cost (C_h) for operating an abrasive waterjet cutting system is:

$$C_h = C_{mh} + C_{lh} + C_{th} + C_{ph} + C_{dh} \quad (\$ \text{ per hour}) \quad (5.8)$$

The cost for cutting unit length of workpiece (C_1) can be determined by:

$$C_1 = \frac{C_h}{u} = C_h \left(\frac{C_{qh} D^{0.618}}{N_m P_w^{1.25} m_w^{0.687} m^{0.343}} \right)^{1.15} \quad (\$ \text{ per unit length}) \quad (5.9)$$

5.6. Conclusions

From the analysis made above the following sort of conclusions can be drawn regarding the advantage and disadvantages of the two commonly used manufacturing methods.

The advantages of abrasive water jet cutting over co2 laser cutting

- The maximum thickness of material which can be cut is an order of magnitude or more than is possible by CO2 laser. Steel cutting in thicknesses up to 100 mm is common. Most materials can be cut in sections of several tens of millimeters.
- ❖ All materials can be cut irrespective of such physical properties as melting point and thermal conductivity. Materials which are impractical to laser cut by thermal methods such as marble or concrete are cut with great effectiveness.
- ❖ As the process is non-thermal there is no heat affected zone (HAZ) associated with the cut edge. This feature is particularly attractive when susceptible materials such as titanium alloys are being profiled.
- ❖ For some metals the cut edge quality can be superior. Dross is not a problem.
- ❖ Once an AWJ cutting machine has been installed it is easy to increase production capacity by adding a number of extra cutting heads at relatively low extra cost. (This is only possible if the water pump has sufficient capacity.)

The advantages of co2 laser cutting over abrasive water jet

- ❖ Kerf widths are substantially smaller if CO2 lasers are used (i.e., 0.2 mm rather than 2.0 mm). This means that finer details can be cut.
- ❖ CO2 laser cutting is generally much faster for cutting metals in the range of thicknesses where the two compete (i.e., up to -16 mm Mild Steel).

- ❖ The capital and running costs of the two processes are of the same order of magnitude but the cost per unit length of cut will be smaller for CO2 lasers as a result of the higher cutting speeds.
- ❖ Laser cutting is generally quieter and cleaner than AWJ cutting.

Both processes have demonstrated that they are extremely versatile and of great commercial as well as technical interest. The processes can be considered to be more complementary than competitive although there are areas where they could share the same workload. Although they compete directly when cutting, for example, polymers, the AWJ technique is often used for metals in sections greater than 10 mm whereas the laser technique carries out the majority of its work at thinner sections. Bearing in mind the advantages of these energy beam cutting methods for batch production, it is clear that they both have an extremely promising future.

Chapter Six

6. Results and Discussions

6.1. Analysis of Experimental Data (Cylindrical Mixing Chamber)

All experimental data has been analyzed using Minitab 17.1.0 software. The analysis includes normality test of taper angle, 3mm from both top and bottom surface roughness values. Accordingly, these tests proof that the data set taken from the experiment fall inside the normal category. And these are the resulting findings with the help of contour plot.

6.2. Effect of selected input parameters on the taper angle (θ).

The four parameters studied and considered here are water pressure, abrasive mass flow rate and cutting speed. All of these parameters play significant role in determining the shape and quality of the kerf characteristics such as kerf taper angle and roughness. The following contour plots show the relationship between two output variables; taper angle and surface roughness with three input parameters already mentioned above.

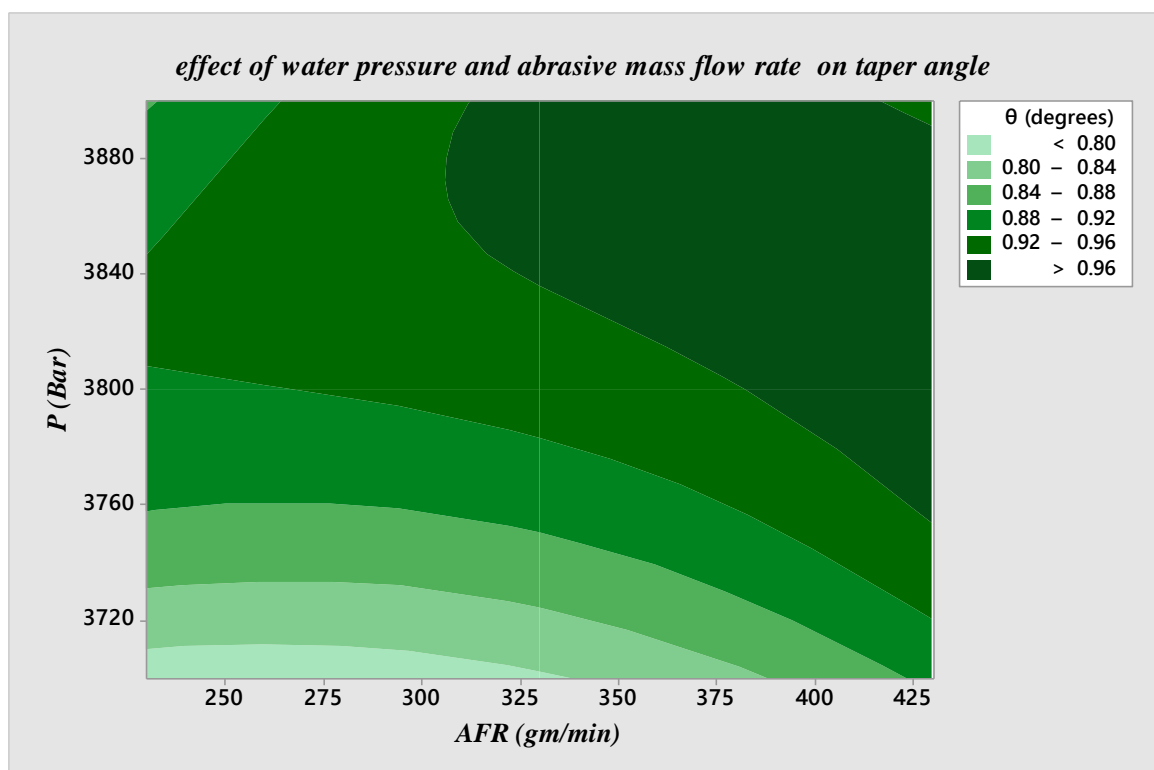


Figure 6.1 Effect of water pressure and abrasive mass flow rate on taper angle.

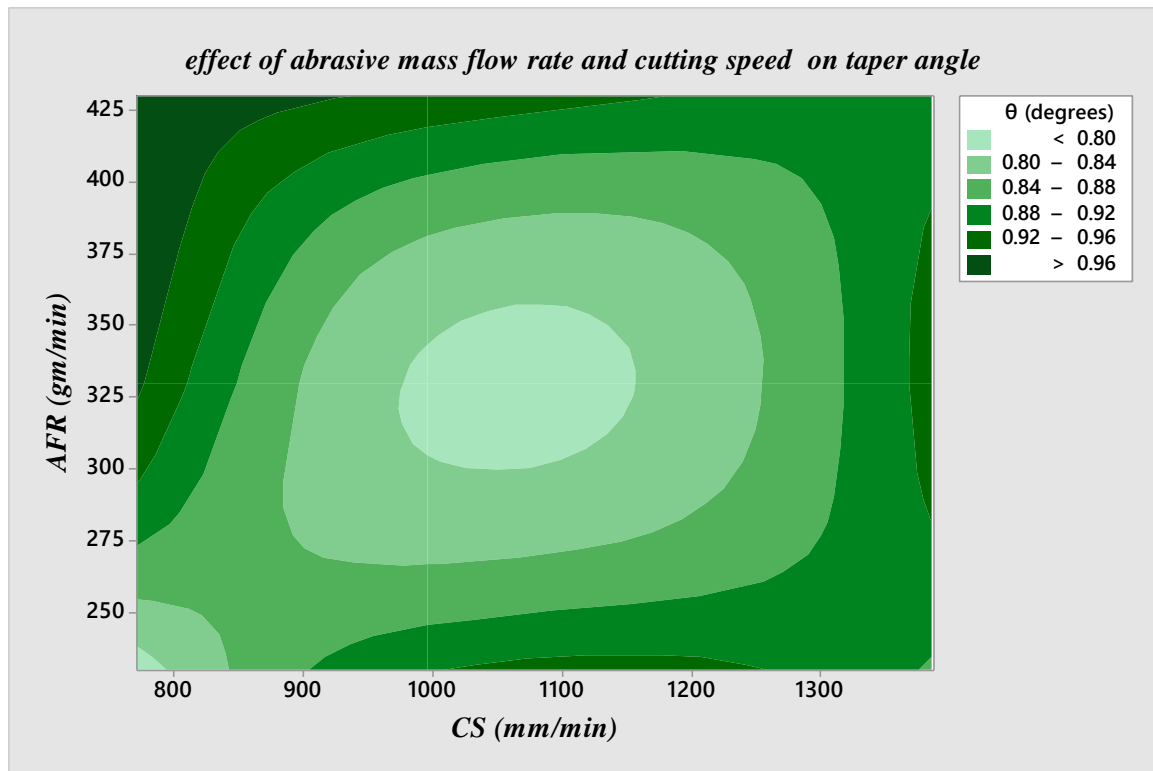


Figure 6.2 Effect of abrasive mass flow rate and cutting speed on taper angle

6.3. Effect of selected input parameters on surface roughness.

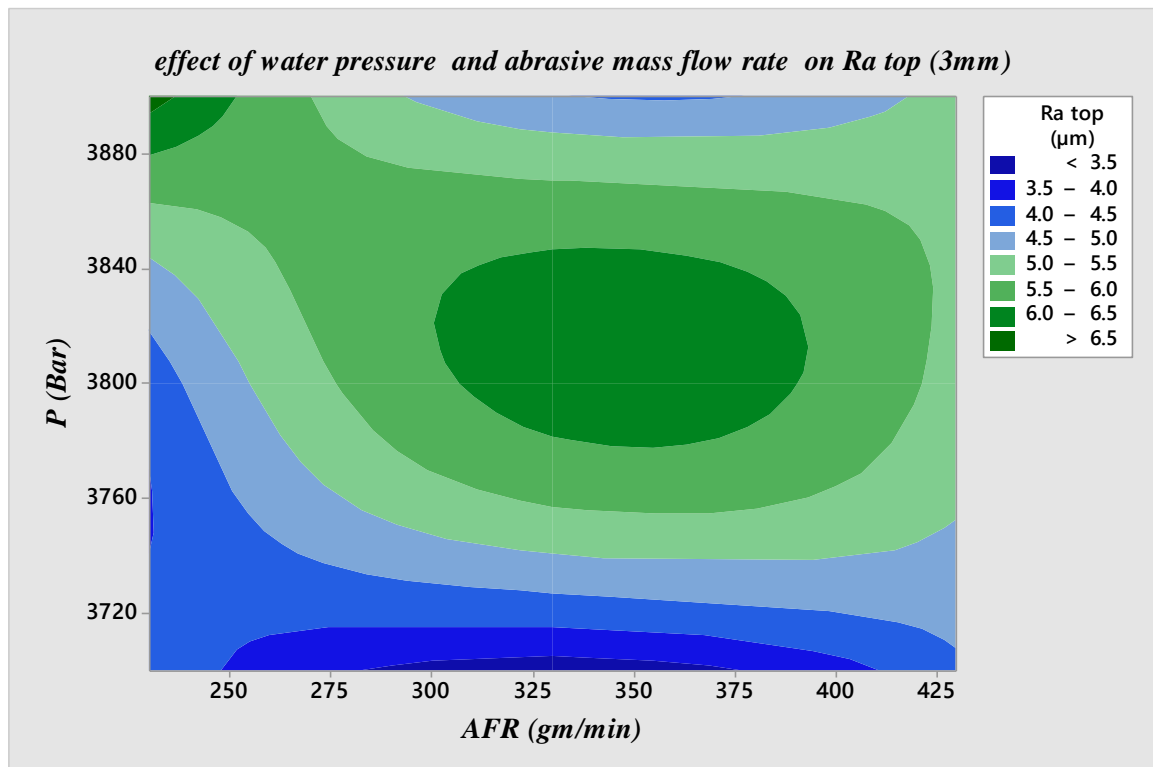


Figure 6.3 Effect of water pressure and abrasive mass flow rate on top roughness (3mm).

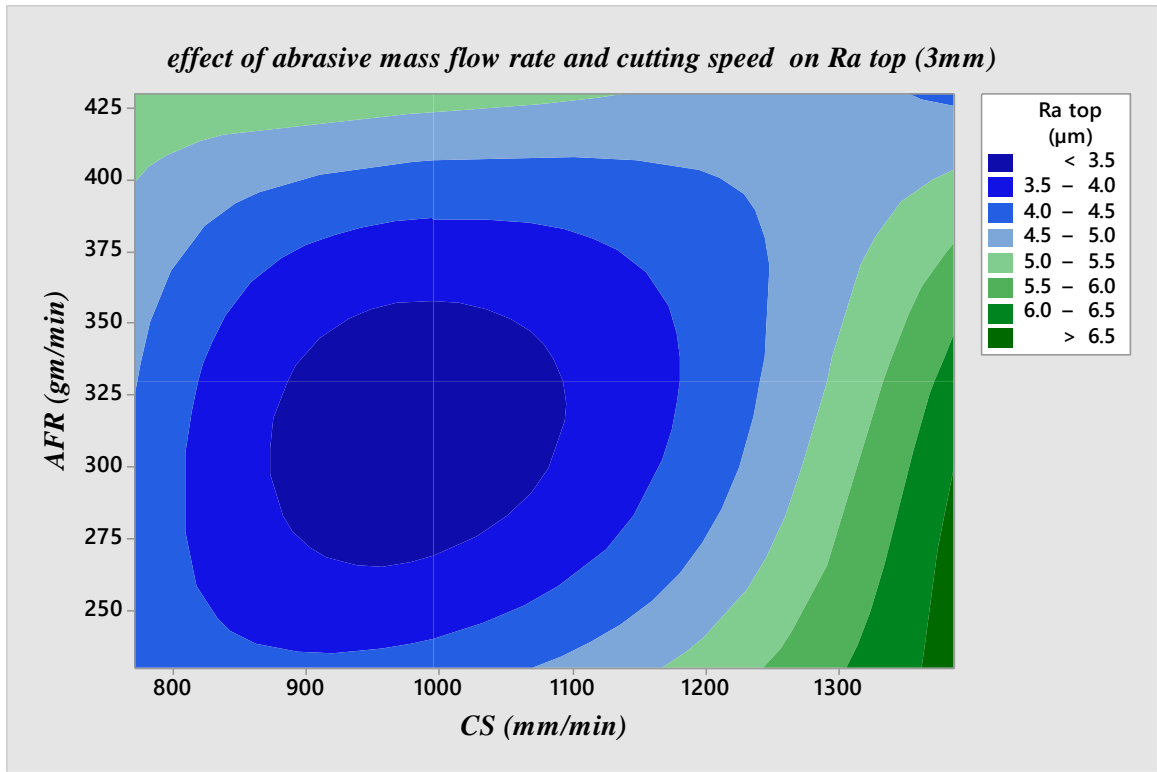


Figure 6.4 *effect of abrasive mass flow rate and cutting speed on top roughness (3mm)*

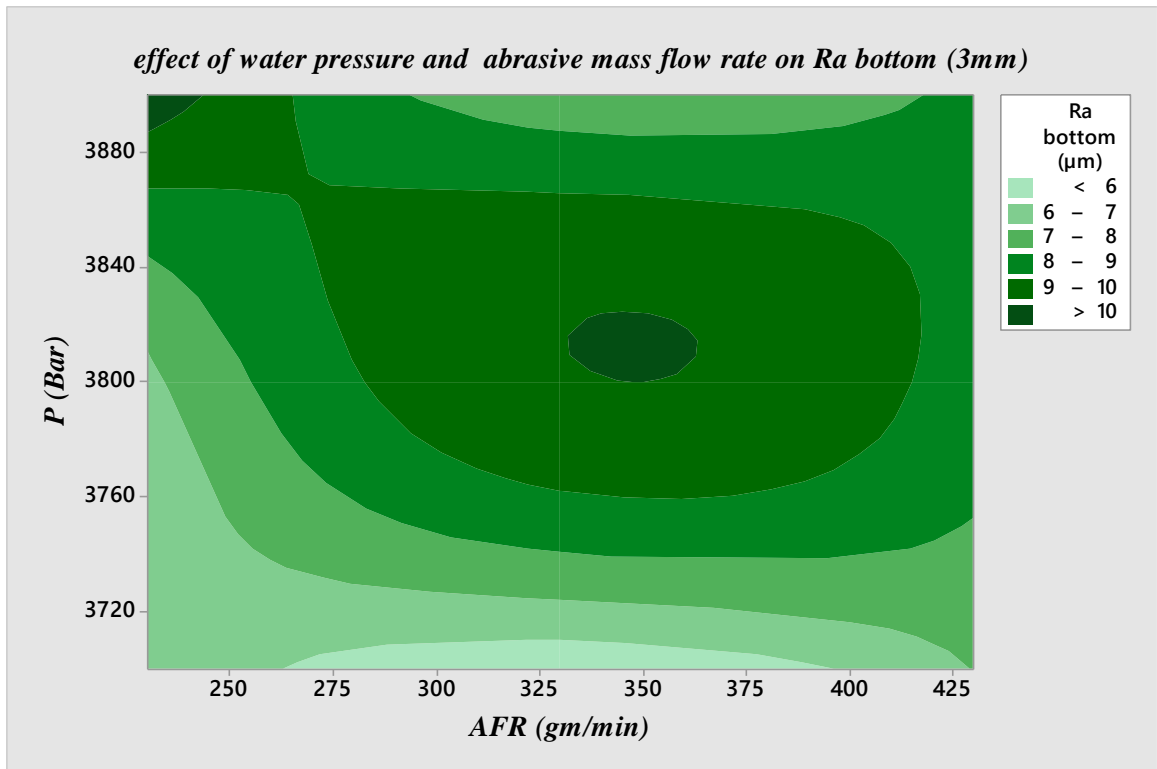


Figure 6.5 *Effect of water pressure and abrasive mass flow rate on bottom surface roughness.*

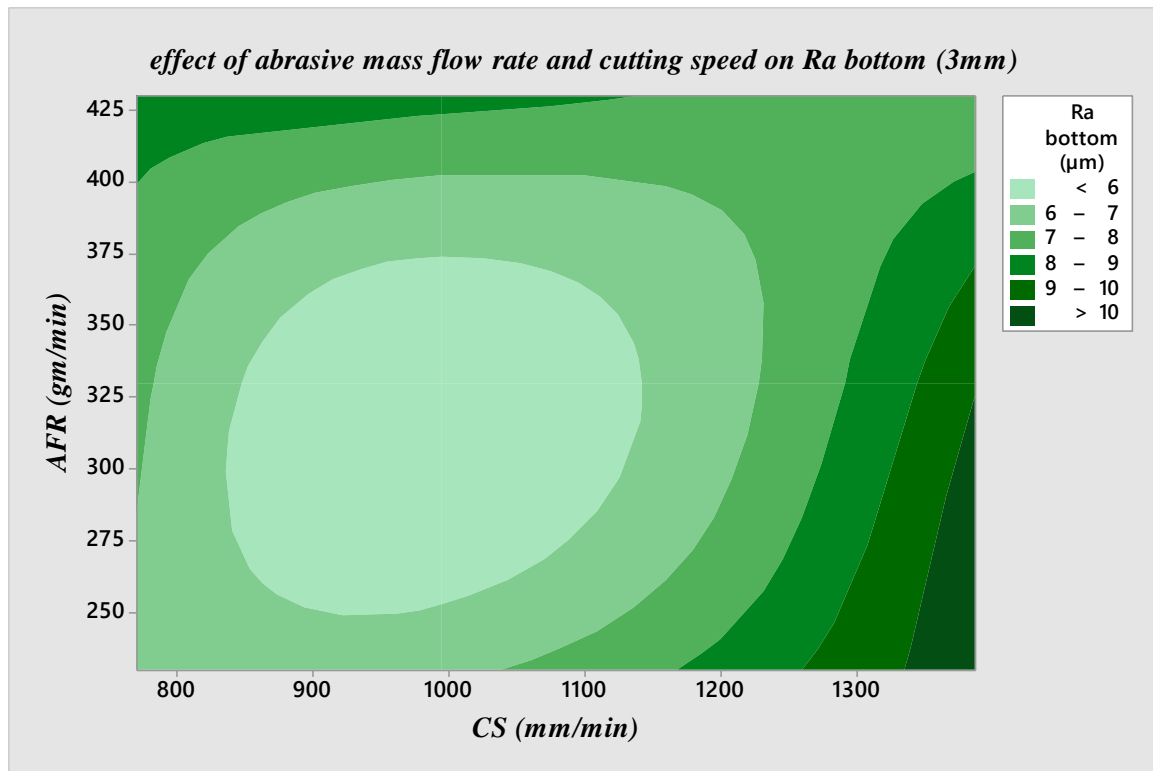


Figure 6.6 Effect of abrasive flow rate and cutting speed on bottom roughness

6.4. Analysis of Experimental Data (Parabolic Mixing Chamber)

All experimental data has been analyzed using Minitab 17.1.0 software. The analysis includes normality test of taper angle, 3mm from both top and bottom surface roughness values. Accordingly, these tests proof that the data set taken from the experiment fall inside the normal category. And these are the resulting findings with the help of contour plot.

6.5. Effect of selected input parametr on the taper angle (θ).

The three parameters studied and considered here are similar to those of the cylindrical type of the chamber. And these are water pressure, abrasive mass flow rate and cutting speed. All of these parameters play significant role in determining the shape and quality of the kerf characteristics such as kerf taper angle and roughness. The following contour plots show the relationship between two output variables; taper angle and surface roughness with those input parameters listed above.

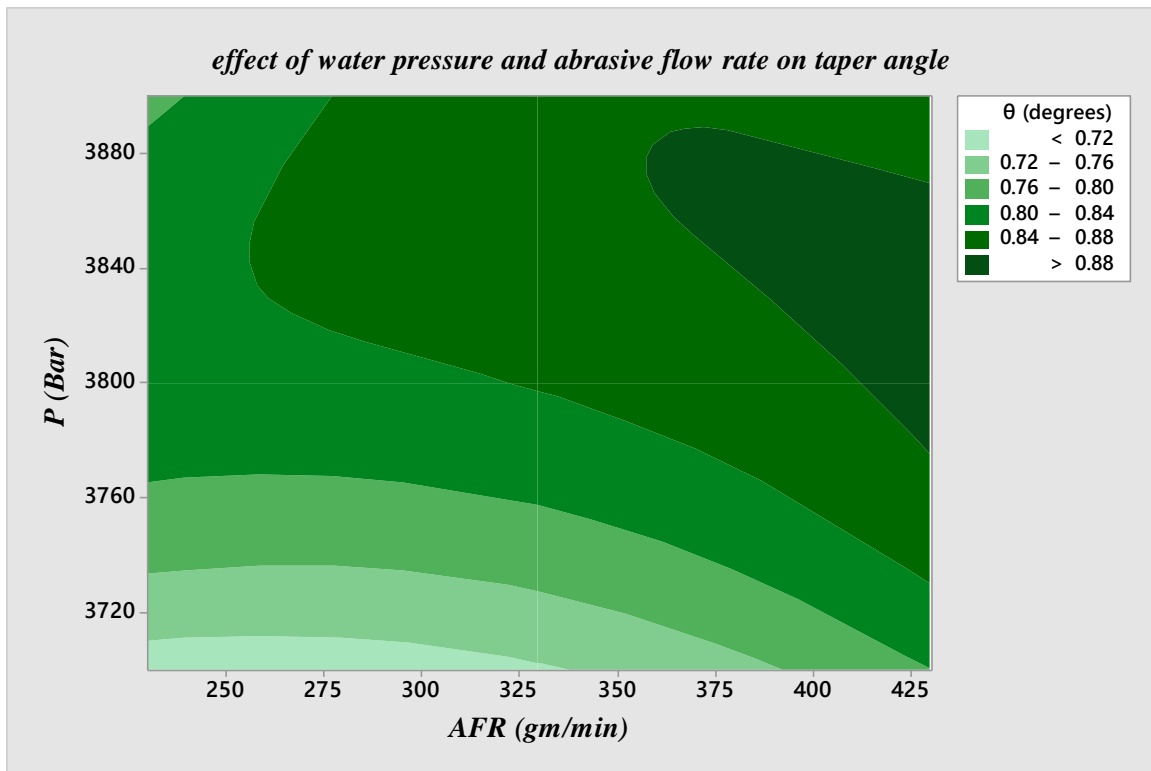


Figure 6.7 Effect of water pressure and abrasive mass flow rate on taper angle.

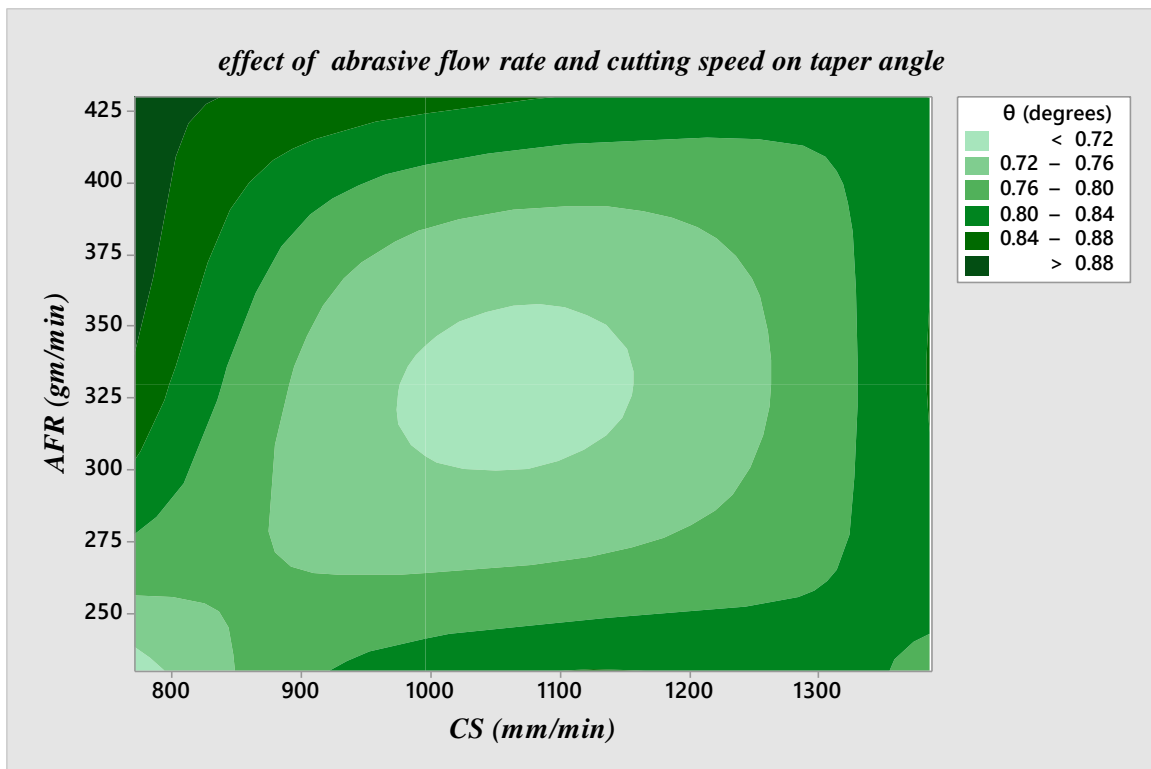


Figure 6.8 Effect of abrasive flow rate and cutting speed on taper angle.

6.6. Effect of selected input parametrs on surface roughness .

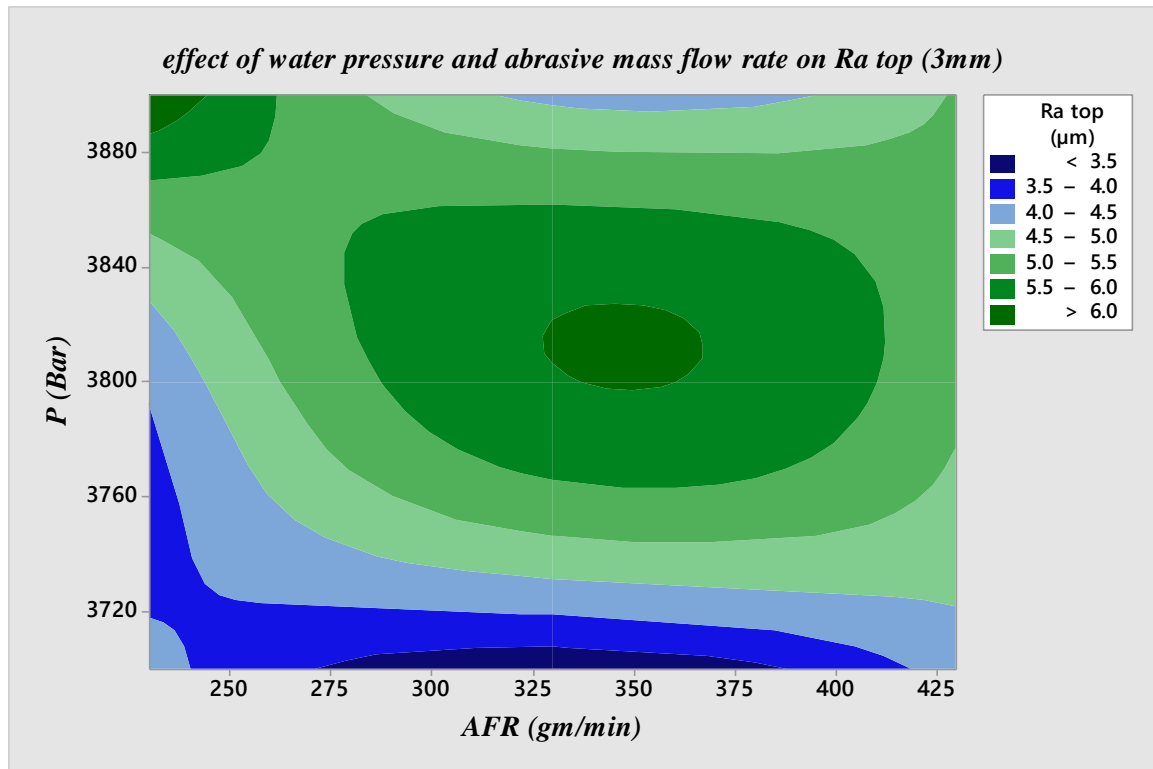


Figure 6.9 Effect of water pressure and abrasive mass flow rate on top surface roughness.

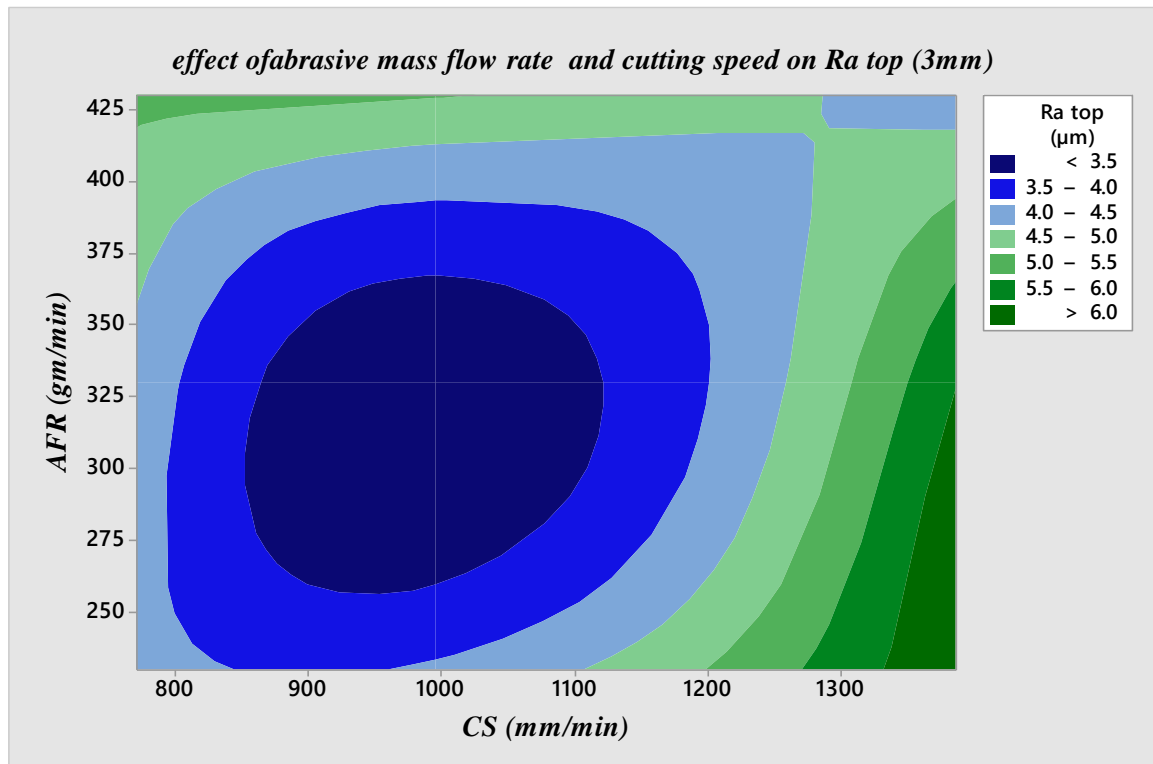


Figure 6.10 Effect of abrasive mass flow rate and cutting speed on top surface roughness.

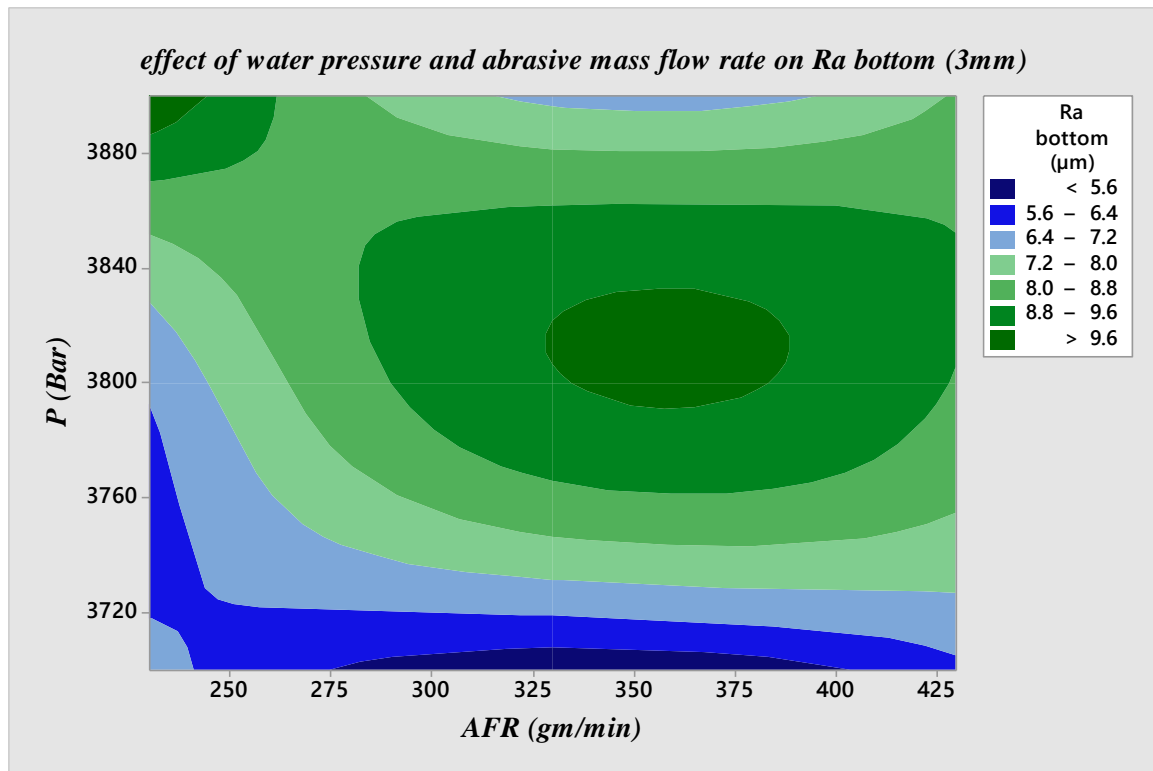


Figure 6.11 *Effect of water pressure and abrasive mass flow rate on bottom surface roughness.*

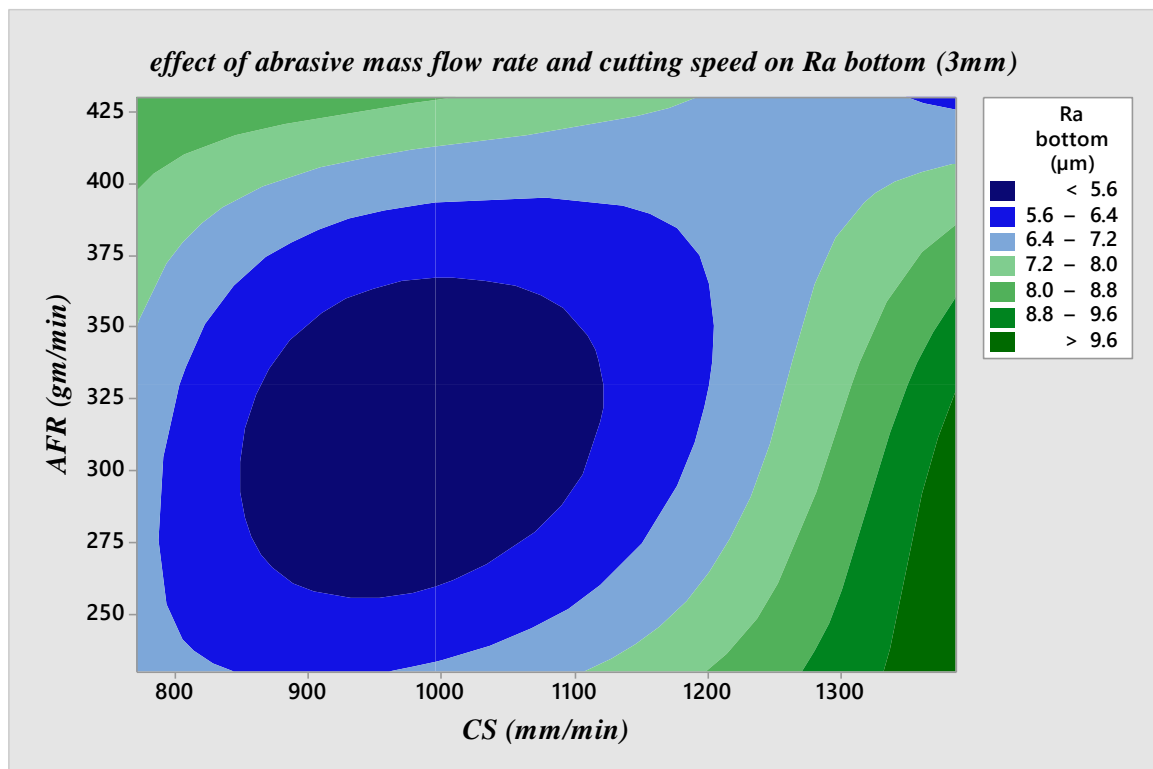


Figure 6.12 *Effect of abrasive mass flow rate and cutting speed on bottom surface roughness.*

6.7. Discussions

1. Impact of Mixing Chamber Geometry

The observed reduction in taper angle can be attributed to the optimized mixing of abrasive particles within the parabolic-shaped mixing chamber. The parabolic geometry facilitates efficient particle acceleration, leading to enhanced kinetic energy at the nozzle exit.

2. Surface Roughness Improvement

The reduced surface roughness with the modified mixing chamber suggests a more controlled abrasive flow. The parabolic shape minimizes turbulence and promotes a stable jet stream, resulting in a smoother machined surface.

3. Comparison with Previous Studies

Our findings align with the work of Smith et al. (2018), who also emphasized the significance of mixing chamber geometry in AWJ machining. However, this study uniquely focuses on the parabolic shape, demonstrating its superiority over conventional designs.

Chapter Seven

7. Conclusions and Recommendations

7.1. Conclusions

Process parameter selection plays a major role in the precise and effective usage of the AWJ for cutting a variety of technical materials. Either the available experimental data or a trustworthy mathematical model correlating all the relevant parameters could serve as the foundation for this wise decision.

Actual cost composition of an abrasive waterjet cutting operation could be fairly complicated. This study didn't attempt to cover every aspect of AWJ cutting cost. Cost factors such as depreciation, income tax, risk, and many more are not included. The focus of analysis is placed on the major cost factors. The approach used here is to determine the hourly cost for operating an abrasive waterjet system. Based on the parameter prediction as discussed in the previous section, cost for cutting a specific work piece can be evaluated.

The choice between both the laser and AWJ technique for profiling a component is not entirely based on the actual cutting cost. When choosing the method, it is very important to take in account subsequent manufacturing operations on the component. By a correct cutting choice further operation might be reduced or even excluded.

Although it's cost constraint the maximum thickness of material which can be cut is an order of magnitude or more than is possible by CO₂ laser. Steel cutting in thicknesses up to 100 mm is common. Most materials can be cut in sections of several tens of millimeters. This study examined a parabolic mixing chamber and uses modeling and experimentation to evaluate its cutting performance to that of a cylindrical mixing chamber. The following is a summary of the main findings:

- ❖ Water pressure and abrasive mass flow rate were shown to be the most important factors for taper angle based on an ANOVA analysis. Furthermore, water pressure and cutting speed are the most important variables for both top and bottom surface roughness.
 - ❖ Using a parabolic mixing chamber, the surface roughness from top 3mm was reduced from 4.9170 μm to 4.7351 μm ; surface roughness from bottom 3mm was reduced from 7.8673 μm to 7.5754 μm additionally the taper angle is lowered from 0.8998° to 0.8098°.
 - ❖ These values can be further used to calculate the percentage reduction of 3mm from top surface roughness to be about 3.70%, 3mm from bottom surface roughness to be 3.71% and taper angle to be about 11.11%.
-

- ❖ The data above indicates that there is less surface roughness on the top than the bottom, which is mostly because the two surfaces go through distinct machining processes. A work piece's top surface goes through turning or milling operations, which results in a smoother finish. However, there is harsh cutting or grinding done to the bottom surface, which increases surface roughness.
- ❖ It was shown that a mixing chamber with a parabolic form was more effective in combining abrasive, water, and air.

7.2. Recommendations for Further Study

To lower the overall cost of production or processing for the AWJM system, more research is required on the recycling and recharging of garnet material.

It is important to investigate the garnet's reusability, the recharged and recycled abrasive's cutting quality, and its cutting performance. Determining the ideal particle size is also necessary to achieve the best cutting performance for recycling and refilling Supreme garnet.

References

- [1] N. Srinath Reddy, D. Tirumala, R. Gajjela, and R. Das, “ANN and RSM approach for modelling and multi objective optimization of abrasive water jet machining process,” *Decis. Sci. Lett.*, vol. 7, no. 4, pp. 535–548, 2018, doi: 10.5267/j.dsl.2017.11.003.
 - [2] “Artificial Bee Colony in Optimizing Process Parameters of,” no. February, 2012.
 - [3] P. D. Unde, M. D. Gayakwad, N. G. Patil, R. S. Pawade, D. G. Thakur, and P. K. Brahmanekar, “Experimental Investigations into Abrasive Waterjet Machining of Carbon Fiber Reinforced Plastic,” *J. Compos.*, vol. 2015, pp. 1–9, 2015, doi: 10.1155/2015/971596.
 - [4] U. Tauseef, M. Shukla, and B. Pankaj, “Optimisation of surface finish in abrasive water jet cutting of Kevlar composites using hybrid Taguchi and response surface method,” *Int. J. Mach. Mach. Mater.*, vol. 3, no. 3–4, pp. 382–402, 2008, doi: 10.1504/IJMMM.2008.020970.
 - [5] V. Starčević, M. Horvat, M. Duspara, and I. Samardžić, “Optimization of abrasive waterjet machining process parameters,” *Teh. Glas.*, vol. 11, no. 4, pp. 143–149, 2017.
 - [6] Y. Ozcelik, M. Gursel, R. Ciccu, G. Costa, and A. Bortolussi, “Optimization of working parameters of water jet cutting in terms of depth and width of cut,” *Proc. Inst. Mech. Eng. Part E J. Process Mech. Eng.*, vol. 226, no. 1, pp. 64–78, 2012, doi: 10.1177/0954408911407706.
 - [7] M. El-hofy, M. O. Helmy, G. Escobar-palafox, K. Kerrigan, R. Scaife, and H. El-hofy, “Abrasive Water Jet Machining of Multidirectional CFRP Laminates,” *Procedia CIRP*, vol. 68, no. April, pp. 535–540, 2018, doi: 10.1016/j.procir.2017.12.109.
 - [8] D. Soni and P. R. Patel, “An Experimental Investigation and Parametric Study of Abrasive Water Jet Cutting Process,” *JETIR*, vol. 3, no. 6, pp. 155–162, 2016.
 - [9] H.-G. Abdel and A. El-Hofy, *Advanced machining processes, non traditional and hybrid machining processes*. 2005.
 - [10] M. P. Groover, *Fundamentals of Modern Manufacturing Materials, Processes, and Systems*. 1999.
 - [11] L. Kong, Y. Wang, X. Lei, C. Feng, and Z. Wang, “Integral modeling of abrasive waterjet micro-machining process,” *Wear*, vol. 482–483, no. June, p. 203987, 2021, doi: 10.1016/j.wear.2021.203987.
 - [12] L. FINNIE, “Erosion of Surfaces by Solid Particle,” vol. 3, pp. 87–103, 1960.
 - [13] H. R. Lee, Y. S. Cho, H. Y. Kim, and J. H. Ahn, “Effects of mixing chamber shape on
-

- cutting performance in abrasive water jet,” *Adv. Mater. Res.*, vol. 652–654, pp. 2134–2139, 2013, doi: 10.4028/www.scientific.net/AMR.652-654.2134.
- [14] H. Öktem, “An integrated study of surface roughness for modelling and optimization of cutting parameters during end milling operation,” *Int. J. Adv. Manuf. Technol.*, vol. 43, no. 9–10, pp. 852–861, 2009, doi: 10.1007/s00170-008-1763-3.
- [15] M. C. P. S. and D. N. M. Raju, “Influence of Abrasive Waterjet Cutting Conditions on Depth of Cut of Mild Steel,” *IJDMT*, vol. 3, no. 1, pp. 48–57, 2012.
- [16] V. Gupta, P. M. Pandey, M. Pal, R. Khanna, and N. K. Batra, “Minimization of kerf taper angle and kerf width using Taguchi ’ s method in abrasive water jet machining of marble,” *MSPRO*, vol. 6, no. 1, pp. 140–149, 2014, doi: 10.1016/j.mspro.2014.07.017.
- [17] E. Averin, “Universal Method for the Prediction of Abrasive Waterjet Performance in Mining,” *Engineering*, vol. 3, no. 6, pp. 888–891, 2017, doi: 10.1016/j.eng.2017.12.004.
- [18] M. S. Alsoufi, D. K. Suker, A. S. Alsabban, and S. Azam, “Experimental Study of Surface Roughness and Micro-Hardness Obtained by Cutting Carbon Steel with Abrasive WaterJet and Laser Beam Technologies,” vol. 4, no. 5, pp. 173–181, 2016, doi: 10.12691/ajme-4-5-2.
- [19] D. Doreswamy, “Machining of D2 Heat Treated Steel Using Abrasive Water Jet : The Effect of Standoff Distance and Feed Rate on Kerf Width and Machining of D2 Heat Treated Steel Using Abrasive Water Jet: The Effect of Standoff Distance and Feed Rate on Kerf Width and Surf,” no. August 2014, 2016, doi: 10.15623/ijret.2014.0308065.
- [20] A. Alberdi, A. Suárez, T. Artaza, and K. Ridgway, “Composite Cutting with Abrasive Water Jet Composite Cutting with Abrasive Water Jet,” *Procedia Eng.*, vol. 63, no. March 2015, pp. 421–429, 2013, doi: 10.1016/j.proeng.2013.08.217.
- [21] D. Julong, “Introduction to Grey System Theory,” 1988.
- [22] E. Williams, “Parameter Optimization of Advanced Machining Processes Using Cuckoo Optimization Algorithm and Hoopoe Heuristic,” no. July, 2014, doi: 10.1007/s10845-014-0925-4.
- [23] P. R. Kubade, A. Bidgar, A. Papti, and P. Potdar, “Parametric Optimization of Abrasive Water Jet Machining of Inconel- 718 material,” pp. 1236–1242, 2016.
- [24] M. Yunus and M. S. Alsoufi, “A Statistical Analysis of Joint Strength of dissimilar Aluminium Alloys Formed by Friction Stir Welding using Taguchi Design Approach , ANOVA for the Optimization of Process Paramet ...,” no. January, 2015.
- [25] H. Ganesan, “Optimization of Machining Parameters in Turning Process using Genetic Algorithm and Particle Swarm Optimization with Experimental Verification,” vol. 3, no. 2, pp. 1091–1102.
-

- [26] A. Mohd, H. Haron, and S. Sharif, "Optimization of process parameters in the abrasive waterjet machining using integrated SA – GA," *Appl. Soft Comput. J.*, vol. 11, no. 8, pp. 5350–5359, 2011, doi: 10.1016/j.asoc.2011.05.024.
- [27] M. A. M. Sibichakkravathi, P. Uthayakumar, K. Vignesh, "A Review on Optimization Techniques of Abrasive Waterjet Machining," *Int. Res. J. Eng. Technol.*, vol. 3, no. 10, pp. 423–429, 2016.
- [28] C. M. Parmar, P. K. Yogi, and T. D. Parmar, "Experimental Investigation on Abrasive Water Jet Machine Using Taguchi Techniques to Optimize Process Parameters of Various Materials - A Review," *Int. J. Technol. Res. Eng.*, vol. 1, no. 6, pp. 328–332, 2014.
- [29] K. S. Prasad, "A Review on Current Research Trends in Abrasive Water Jet Machining," *Int. Res. J. Eng. Technol.*, vol. 4, no. 6, pp. 2395–0072, 2017.
- [30] S. Gurusamy, R. Prakash, and L. Nagarajan, "Experimental study on abrasive water jet machining of AA5083 in a range of thicknesses Experimental study on abrasive water jet machining of AA5083 in a range of thicknesses Gurusamy Selvakumar * and Shanmuga Sundaram Ram Prakash Nagarajan Lenin," *Int. J. Abras. Technol.*, vol. x, no. y, pp. xxx–xxx, 2018, doi: 10.1504/IJAT.2018.10015291.
- [31] M. D. A. and P. J. J. K. S. Jai Aultrin, "Modelling the Cutting Process and Cutting Performance in Abrasive Waterjet Machining Using Genetic-Fuzzy Approach," *Int. Conf. Model. Optim. Comput.*, vol. 38, pp. 4013–4020, 2012, doi: 10.1016/j.proeng.2012.06.459.
- [32] T. U. Siddiqui, M. Shukla, and P. B. Tambe, "Comparative Investigation of Abrasive Waterjet Cut Kerf Quality Characteristics for Aramid, Glass and Carbon Fiber Reinforced Composites Used in Transport Aircraft Applications," *Am. WJTA Conf. Expo*, vol. 27, 2009.
- [33] N. Yuvaraj and M. P. Kumar, "Experimental Investigation of Abrasive Water Jet Cutting Performance on AISI D2 Steel by Influencing of Jet Impingement Angles and Abrasive Mesh Sizes," *Int. Conf. Precision, Meso, Micro Nano Eng.*, no. 9, 2015.
- [34] M. Sagar, "Experimental Investigation and Optimization of Process Parameters in Abrasive Water Jet Machine," *Int. Res. J. Eng. Technol.*, vol. 5, no. 3, pp. 2395–0072, 2018.
- [35] M. Todkar and J. Patkure, "Fuzzy Modelling and GA Optimization for Optimal Selection of Process Parameters to Maximize MRR in Abrasive Water Jet Machining," *Int. J. Theor. Appl. Res. Mech. Eng.*, vol. 3, no. 1, pp. 9–16, 2014.
- [36] J. K. P. and A. A. Abdulhafiz A Shaikh, Shaikh, "The Influence of Abrasive Water Jet Machining Parameters on Various Response — A Review," *Int. J. Mech. Eng. Rob. Res.*, vol. 4, no. 1, 2015.
- [37] D. Johnbasha, N. A. Nageswararao, K. N. Prasad, and S. Mahaboob, "Investigation of
-

- Machining Parameters in Abrasive Jet Machining on Ti-6Al-4V Using GRA and PCA,” *Int. Res. J. Eng. Technol.*, vol. 3, no. 12, pp. 1139–1144, 2016.
- [38] J. A. Ks and D. A. M, “Multi-Objective Optimization of Abrasive Water Jet Machining of Aluminium 6061 Alloy by Grey Relational Analysis,” *J. Chem. Pharm. Sci.*, vol. 9, no. 1, pp. 410–417, 2016.
- [39] C. Narayanan, R. Balz, D. A. Weiss, and K. C. Heiniger, “Author ’ s personal copy Modelling of abrasive particle energy in water jet machining,” *J. Mater. Process. Technol.*, 2013.
- [40] N. Yuvaraj and M. P. Kumar, “Optimisation of abrasive water jet cutting process parameters for AA5083-H32 aluminium alloy using fuzzy TOPSIS method,” *Int. J. Mach. Mach. Mater.*, vol. X, no. y, pp. xxx–xxx.
- [41] G. K. K. Kumar, M. Arunachalam, B. Abinash, and B. K. Kumar, “Optimization of Abrasive Water Jet Machining Process Parameters for Duplex Stainless Steel-2205 by Using Response Surface Methodology,” *Int. J. Sci. Res. Mech. Mater. Eng.*, vol. 2, no. 3, pp. 17–28, 2018.
- [42] K. K. G. K and bhavani sankar C, “Optimization of Abrasive Water Jet Machining Process Parameters for Inconel-825 By Using Grey Taguchi Method,” *Int. J. Sci. Res. Sci. Eng. Technol.*, Accessed: Jul. 12, 2019. [Online]. Available: https://www.academia.edu/37562945/Optimization_of_Abrasive_Water_Jet_Machining_Process_Parameters_for_Inconel-825_By_Using_Grey_Taguchi_Method
- [43] H. Orbanic and M. Junkar, “Simulation of abrasive water jet cutting process : Part 2 . Cellular automata approach,” *Model. Simul. Mater. Sci. Eng.*, vol. 1171, 2004, doi: 10.1088/0965-0393/12/6/011.
- [44] A. P. Markopoulos, W. Habrat, N. Galanis, and N. Karkalos, “Modelling and Optimization of Machining with the Use of Statistical Methods and Soft Computing Modelling and Optimization of Machining with the Use of Statistical Methods and Soft Computing,” no. January, 2016, doi: 10.1007/978-3-319-23838-8.
- [45] L. Nagdeve, “Parametric Optimization of Abrasive Water Jet Machining Using Taguchi Methodology,” *IJREAS*, vol. 2, no. 6, pp. 23–32, 2012.
- [46] J. Srinivas and A. L. Rao, “Response Surface Methodological for Prediction of Optimized Process Parameters in Abrasive Jet Machining of Haste Alloy,” *IJSRST*, vol. 3, no. 8, pp. 650–656, 2017.
- [47] K. S. K. Sasikumar, K. P. Arulshri, K. Ponappa, and M. Uthayakumar, “A study on kerf characteristics of hybrid aluminium 7075 metal matrix composites machined using abrasive

- water jet machining technology,” *Proc IMechE Part B J Eng. Manuf.*, 2016, doi: 10.1177/0954405416654085.
- [48] M. Uthayakumar and V. A. M. Kathiresan, “Experimental Investigation of the Process Parameters in Abrasive Water Jet Cutting of Redmud Reinforced Banana/ Polyester Hybrid Composites,” *5th Int. 26th All India Manuf. Technol. Des. Res. Conf.*, no. Aimtdr, pp. 12–15, 2014.
- [49] M. Singh, V. Kumar, and S. Kumar, “Methodology to predict the shape of the tool fabricated by AWJM process,” *Procedia CIRP*, vol. 41, pp. 898–901, 2016, doi: 10.1016/j.procir.2015.12.070.
- [50] S. Anwar, F. M. Abdullah, M. S. Alkahtani, S. Ahmad, and M. Alatefi, “Journal of King Saud University – Engineering Sciences Bibliometric analysis of abrasive water jet machining research,” *J. King Saud Univ. - Eng. Sci.*, vol. 31, no. 3, pp. 262–270, 2019, doi: 10.1016/j.jksues.2018.02.002.
- [51] J. Xu, B. You, and X. Kong, *Design and Experiment Research on Abrasive Water-jet Cutting Machine Based on Phased Intensifier*, vol. 41, no. 2. IFAC, 2008. doi: 10.3182/20080706-5-KR-1001.02513.
- [52] A. Parthiban, S. Sathish, and M. Chandrasekaran, “Optimization of Abrasive Water Jet Cutting Parameter for AISI 316L Stainless Steel Sheet,” *J. Appl. Fluid Mech. Pap. from Int. Conf. Newer Eng. Concepts Technol. ICONNECT2K17*, vol. 10, no. 1999, pp. 15–22, 2017.
- [53] D. Doreswamy, B. Shivamurthy, D. Anjaiah, and N. Y. Sharma, “An Investigation of Abrasive Water Jet Machining on Graphite / Glass / Epoxy Composite,” vol. 2015, 2015.
- [54] A. R. and S. Ajit Dhanawade, Ravi Upadhyaya and Kumar, “Experimental Study on Abrasive Water Jet Machining of PZT Ceramic,” *2nd Int. Conf. Meas. Instrum. Electron.*, vol. 1, no. 870, pp. 1742–6596, 2017.
- [55] C. Z. Huang, R. G. Hou, J. Wang, and Y. X. Feng, “The Effect of High Pressure Abrasive Water Jet Cutting Parameters on Cutting Performance of Granite,” *Key Eng. Mater. Tech Publ. Switz.*, vol. 305, pp. 560–564, 2006, doi: 10.4028/www.scientific.net/KEM.304-305.560.
- [56] I. Karakurt, G. Aydin, and K. Aydiner, “An investigation on the kerf width in abrasive waterjet cutting of granitic rocks,” *Arab J Geosci*, no. 1969, 2013, doi: 10.1007/s12517-013-0984-4.
- [57] D. K. Shanmugam and S. H. Masood, “An investigation on kerf characteristics in abrasive waterjet cutting of layered composites,” vol. 9, no. 1999, pp. 3887–3893, 2008, doi: 10.1016/j.jmatprotec.2008.09.001.
-

- [58] V. Gupta, P. M. Pandey, M. P. Garg, R. Khanna, and N. K. Batra, "Minimization of Kerf Taper Angle and Kerf Width Using Taguchi ' s Method in Abrasive Water Jet Machining of Marble Minimization of kerf taper angle and kerf width using Taguchi ' s method in abrasive water jet machining of marble," *Procedia Mater. Sci.*, vol. 6, no. January 2015, pp. 140–149, 2014, doi: 10.1016/j.mspro.2014.07.017.
- [59] A. A. A.-R. and A. K. A.-S. A. A. El-Domiaty, M. A. Shabara, "On the Modelling of Abrasive Waterjet Cutting," *Int J Adv Manuf Technol*, pp. 255–256, 1996.
- [60] M. C. P. Selvan and N. M. S. Raju, "Assesment of Process Parameters in Abrasive Waterjet Cutting of Stainless Steel," *Int. J. Adv. Eng. Technol.*, vol. 1, no. 3, pp. 34–40, 2011.
- [61] M. C. P. S. and D. N. M. Raju, "Influence of Abrasive Water Jet Cutting Conditions on Depth of Cut of Mild Steel," *Int. J. Des. Manuf. nternational J. Des. Manuf. Technol. (IJDMT)*, vol. 6995, pp. 48–57, 2012.
- [62] U. Aich, S. Banerjee, A. Bandyopadhyay, and P. Kumar, "Abrasive Water Jet Cutting of Borosilicate Glass," *MSPRO*, vol. 6, no. Icmpec, pp. 775–785, 2014, doi: 10.1016/j.mspro.2014.07.094.
- [63] K. S. J. Aultrin and M. D. Anand, "Optimization of Machining Parameters in AWJM Process for an Copper Iron Alloy Using RSM and Regression Analysis," vol. 2, no. 5, pp. 19–34, 2014.
- [64] M. Rajyalakshmi, "Abrasive Water Jet Machining - A Review on Current Development," *IJSTE - Int. J. Sci. Technol. Eng. /*, vol. 2, no. 12, pp. 428–434, 2016.
- [65] S. Arun, "Investigation of Metal Removal Rate and Surface Finish on Inconel 718 by Abrasive Water Jet Machining," *Int. J. Innov. Res. Adv. Eng.*, vol. 3, no. 11, pp. 43–47, 2016.
- [66] P. J. Pawar and R. V. Rao, "Erratum to : Parameter optimization of machining processes using teaching-learning-based optimization algorithm," p. 4961, 2013, doi: 10.1007/s00170-013-4961-6.
- [67] J. Kumar and G. S. Singh, "Optimization of Machining Parameters of Titanium Alloy Steel using : TOPSIS Optimization of Machining Parameters of Titanium Alloy Steel using : TOPSIS Method," no. June, 2018.
- [68] R. Khanna, R. D. Gupta, and V. Gupta, "Measuring Material Removal Rate of Marble by Using Abrasive Water Jet Machining," pp. 45–49, 2011.
- [69] S. K. Bhati, D. Gehlot, and K. Singh, "Parametric Optimization of Abrasive Jet Micromachining through Genetic Algorithm A Ctual Values of Process Parameters and Coded Levels," pp. 15127–15133, 2017, doi: 10.15680/IJIRSET.2017.0607342.

- [70] A. S. Bhumre, R. R. Gaikwad, A. V Shinde, A. V Thombare, A. K. Chandgude, and S. P. Kharat, "Optimization of Abrasive Water Jet Machine Parameters : A Review," no. May, pp. 5694–5699, 2019.
- [71] F. Kolahan and A. H. Khajavi, "Modeling and Optimization of Abrasive Waterjet Parameters using Regression Analysis," *World Acad. Sci. Eng. Technol.*, pp. 488–493, 2009.
- [72] S. M. Mullaikodi, "Synthesis, characterization and machinability studies on thin hybrid composites with SiC nano particles," *Mater. Res. Express*, 2019.
- [73] M.Hassen, "Micromanufacturing of Composite Materials: A Review," *Int. J. Extrem. Manuf.*, 2019.
- [74] Z. Zhang and J. Yan, "Manufacturing technologies toward extreme precision," *Int. J. Extrem. Manuf.*, 2019.
- [75] T.Nguyen, "A review on the erosion mechanisms in abrasive waterjet micromachining of brittle materials," *Int. J. Extrem. Manuf.*, 2019.
- [76] H. K. S. M. Chitrai Pon Selvan, N. Mohana Sundara Raju, "Effects of process parameters on surface roughness in abrasive waterjet cutting of aluminium," *Front. Mech. Eng.*, vol. 7, no. 4, pp. 439–444, 2012, doi: 10.1007/s11465-012-0337-0.
- [77] D. Begic-hajdarevic, A. Cekic, M. Mehmedovic, and A. Djelmic, "Experimental Study on Surface Roughness in Abrasive Water Jet," vol. 100, pp. 394–399, 2015, doi: 10.1016/j.proeng.2015.01.383.
- [78] D. R. S. Ashanira binti Mat Deris, Dr. Azlan Mohd Zain, "Hybrid GR-SVM approach to Surface Roughness Evaluation in Machining Process," *Fac. Comput. Sci. Inf. Syst.*.
- [79] G. S. Yadav and B. K. Singh, "Effect of Process Parameter in Abrasive Water Jet Cutting Using Response Surface Method," *Int. Res. J. Eng. Technol.*, vol. 3, no. 6, pp. 981–985, 2016.
- [80] N. Yuvaraj and M. P. Kumar, "Surface Integrity Studies on Abrasive Water Jet Cutting of AISI D2 Steel," *Mater. Manuf. Process.*, vol. 6914, no. August, 2016, doi: 10.1080/10426914.2016.1221093.
- [81] N. Tosun, I. Dagtekin, L. Ozler, and A. Deniz, "Abrasive Waterjet Cutting of Aluminum Alloys : Workpiece Surface Roughness," *Appl. Mech. Mater.*, vol. 404, pp. 3–9, 2013, doi: 10.4028/www.scientific.net/AMM.404.3.
- [82] C. P. Selvan and M. S. Raju, "Analysis of Surface Roughness in Abrasive Waterjet Cutting of Cast Iron," vol. 1, no. 3, pp. 174–182, 2012.
- [83] M. Yunus and M. S. Alsoufi, "Multi-output optimization of tribological characteristics control factors of thermally sprayed industrial ceramic coatings using hybrid Taguchi-grey
-

- relation analysis,” vol. 4, no. 3, pp. 208–216, 2016, doi: 10.1007/s40544-016-0118-6.
- [84] K. Monková *et al.*, “Factor Analysis of the Abrasive Waterjet Factors Affecting the Surface Roughness of Titanium,” no. 1, pp. 1–5.
- [85] T. Method, “Optimization MRR Of Stainless Steel 403 In Abrasive Water Jet Machining Optimization MRR Of Stainless Steel 403 In Abrasive Water Jet Machining Using Anova And Taguchi Method * Ramprasad , ** Gaurav Upadhyay , *** Kamal Hassan,” no. April 2015, 2016.
- [86] P. Shanmughasundaram, “Influence of Abrasive Water Jet Machining Parameters on the Surface Roughness of Eutectic Al-Si Alloy – Graphite Composites,” vol. 19, pp. 1–8, 2014.
- [87] R. V. Rao and V. D. Kalyankar, “Engineering Applications of Artificial Intelligence Parameter optimization of modern machining processes using teaching – learning-based optimization algorithm,” *Eng. Appl. Artif. Intell.*, vol. 26, no. 1, pp. 524–531, 2013, doi: 10.1016/j.engappai.2012.06.007.
- [88] “Parametric Optimization of Abrasive Waterjet Machining for Mild Steel : Taguchi Approach,” *Int. J. Curr. Eng. Technol.*, no. 2, pp. 28–30, 2014.
- [89] D. Kinik, B. Gánovská, S. Hloch, P. Monka, K. Monková, and Z. Hutyrová, “On-Line Monitoring of Technological Process of Material Abrasive Water Jet Cutting,” vol. 3651, pp. 351–357, 2015, doi: 10.17559/TV-20130904111939.
- [90] M. M. Korat and G. D. Acharya, “A Review on Current Research and Development in Abrasive Waterjet Machining,” *Int. J. Eng. Res. Appl.*, vol. 4, no. 1, pp. 423–432, 2014.
- [91] R. Varun and T. S. Nanjundeswaraswamy, “A Literature Review on Parameters Influencing Abrasive Jet Machining and Abrasive Water Jet Machining,” *J. Eng. Res. Appl.*, vol. 9, no. 1, pp. 24–29, 2019, doi: 10.9790/9622-.
- [92] S. Chakraborty and A. Mitra, “Parametric optimization of abrasive water-jet machining processes using grey wolf optimizer,” *Mater. Manuf. Process.*, vol. 0, no. 0, pp. 1–12, 2018, doi: 10.1080/10426914.2018.1453158.
- [93] M. Dittrich, M. Dix, M. Kuhl, B. Palumbo, and F. Tagliaferri, “Process Analysis of Water Abrasive Fine Jet Structuring of Ceramic Surfaces via Design of Experiment,” *6th CIRP Int. Conf. High Perform. Cutting*, vol. 14, pp. 442–447, 2014, doi: 10.1016/j.procir.2014.03.030.
- [94] P. Milano, A. Suarez, A. Alberdi, and R. Tecnalía, “Fine abrasive water jet machining of piezoelectric ceramics : cutting parameters optimization”.
- [95] M. A. Abdullah, J. F. Jamil, and M. A. Salim, “Performance Analysis of Abrasive Waterjet Machining Process at Low Pressure Performance Analysis of Abrasive Waterjet Machining Process at Low Pressure,” *IOP Conf. Ser. Mater. Sci. Eng.*, 2018, doi: 10.1088/1757-
-

899X/319/1/012051.

- [96] S. R. Lohar and P. R. Kubade, "Current Research and Development in Abrasive Water Jet Machining (AWJM): A Review," *Int. J. Sci. Res.*, vol. 5, no. 1, pp. 2014–2017, 2016.
- [97] D. Patel and P. Tandon, "Experimental investigations of gelatin-enabled abrasive water slurry jet machining," *Int J Adv Manuf Technol.*, pp. 1193–1194, doi: 10.1007/s00170-016-9154-7.
- [98] A. Momber, "Quantification of energy absorption capability in abrasive water jet machining," *Proc Instn Mech Engrs*, vol. 209, 1995, doi: 10.1243/PIME.
- [99] M. K. Babu and O. V. K. Chetty, "Studies on Recharging of Abrasives in Abrasive Water Jet Machining," *Int J Adv Manuf Technol.*, pp. 697–703, 2002.
- [100] V. Sharma and S. Chattopadhyaya, "Multi response optimization of process parameters based on Taguchi — Fuzzy model for coal cutting by water jet technology," *Int J Adv Manuf Technol.*, pp. 1019–1025, 2011, doi: 10.1007/s00170-011-3258-x.
- [101] M. Radovanovic, P. Dasic, and M. Stefanek, "Some Possibilities for Determining Abrasive," *13th Int. Sci. Conf. CO-MAT-TECH*, no. October, pp. 20–21, 2005.
- [102] P. R. Vundavilli, M. B. Parappagoudar, S. P. Kodali, and S. Benguluri, "Knowledge-Based Systems Fuzzy logic-based expert system for prediction of depth of cut in abrasive water jet machining process," *Knowledge-Based Syst.*, vol. 27, pp. 456–464, 2012, doi: 10.1016/j.knosys.2011.10.002.
- [103] P. Taylor, J. Wang, T. Kuriyagawa, and C. Z. Huang, "Machining Science and Technology : An International An Experimental Study to Enhance the Cutting Performance in Abrasive Waterjet Machining An Experimental Study to Enhance the Cutting," *Mach. Sci. Technol. An Int. J.*, pp. 37–41, 2007, doi: 10.1081/MST-120022777.
- [104] M. Yunus, M. S. Alsoufi, and S. M. Munshi, "Taguchi-Grey relation analysis for assessing the optimal set of control factors of thermal barrier coatings for high-temperature applications," *Mech. Adv. Mater. Mod. Process.*, 2016, doi: 10.1186/s40759-016-0011-z.
- [105] G. D. Sonawane and R. M. Bachhav, "Abrasive Water Jet Machining- A Review," *IOSR J. Mech. Civ. Eng.*, vol. 12, no. 4, pp. 44–52, 2015, doi: 10.9790/1684-12424452.
- [106] T. Oh, G. Joo, Y. Cha, and G. Cho, "Effect of Garnet Characteristics on Abrasive Waterjet Cutting of Hard Granite Rock," *Adv. Civ. Eng.*, vol. 2019, 2019.
- [107] V. N. Pi, "Recycling and Recharging of Supreme Garnet in Abrasive Abrasive Waterjet Waterjet Machining Machining," in *Abrasive Technology - Characteristics and Applications*. doi: 10.5772/intechopen.75180.
- [108] M. A. Raval and C. P. Patel, "Parametric Optimization of Magnetic Abrasive Water Jet
-

- Machining Of AISI 52100 Steel Using Grey Relational Analysis,” vol. 3, no. 4, pp. 527–530, 2013.
- [109] S. K. and D. G. P, “A Review on Abrasive Water Jet,” *Int. J. Recent Adv. Mech. Eng.*, vol. 3, no. 3, pp. 153–158, 2014.
- [110] A. Rowe *et al.*, “Effects of Abrasive Waterjet Machining on the Quality of the Surface Generated on a Carbon Fibre Reinforced Polymer Composite,” *Machines*, vol. 11, no. 7, 2023, doi: 10.3390/machines11070749.
- [111] J. G. A. Bitter, “A Study of Erosion Phenomena Part I,” vol. 6, 1963.
- [112] B. S. Chahar and A. K. Pun, “Erosion Wear of Ductile Materials : A Review,” *ELK Asia Pacific Journals*, 2018.
- [113] X. Li, H. Ding, Z. Huang, M. Fang, and B. Liu, “Solid particle erosion-wear behavior of SiC – Si₃N₄ composite ceramic at elevated temperature,” *Ceram. Int.*, pp. 1–7, 2014, doi: 10.1016/j.ceramint.2014.07.055.
- [114] F. Maisuriya, N. Chaudhari, M. Gandhi, and C. Chaudhari, “Parametric Optimization of Abrasive Jet Machine for Glass-a Review Parametric Optimization of Abrasive Jet Machine for Glass- a Review,” 2018.
- [115] A. I. Hassan and J. Kosmol, “Dynamic elastic plastic analysis of 3D deformation in abrasive waterjet machining,” vol. 113, pp. 337–341, 2001.
- [116] R. Kovacevict and M. E. I. Fang, “Modeling of the Influence of The Abrasive Waterjet Cutting Parameters on The Depth of Cut Based on Fuzzy Rules,” vol. 34, no. 1, pp. 55–72, 1992.
- [117] T. J. Labus, “Proceedings of the 8th American Water Jet Conference.”
- [118] C. A. V. L. I and H. J. J. Kals, “Modelling of high velocity, loose abrasive machining processes,” no. 2, pp. 2–5.
- [119] M. Hashish, R. Mohan, and T. J. Kim, “State of the Art of Research and Development in Abrasive Waterjet Machining,” vol. 119, no. November 1997, 2014.
- [120] M. Hashish, “A Model for Abrasive-Waterjet (AWJ) Machining,” vol. 111, 2016.
- [121] M. Hashish, “Pressure Effects in Abrasive-,” vol. 1, no. July 1989, 2013.
- [122] J. F. Dh. H. L. Oberg Eric, “Machinery_s Handbook. Tom 2,” pp. 112–192.
- [123] M. Hashish, “A Modeling Study of Metal Cutting With Abrasiwe Waterjets,” vol. 106, no. January 1984, 2016.

Appendices

**Table A-1. Important specifications of Scanning Electron Microscope (SU3800/
SU3900)**

Items	Product Features	
	SU3800	SU3900
Secondary Electron Resolution	3.0 nm (accelerating voltage 30 kV, WD = 5 mm, high vacuum mode)	
	15.0 nm (accelerating voltage 1 kV, WD = 5 mm, high vacuum mode)	
Backscattered Electron Resolution	4.0 nm (accelerating voltage 30 kV, WD = 5 mm, low vacuum mode)	
Magnification	×5 to ×300,000 (magnification of image*1)	
	×7 to ×800,000 (magnification of actual display*2)	
Accelerating Voltage	0.3 kV to 30 kV	
Low Vacuum Mode Setting	6 to 650 Pa	
Image Shift	± 75 μm (WD = 10 mm)	
Maximum Specimen Size	Φ 200 mm	Φ 300 mm
Specimen Stage	0 to 100 mm	0 to 150 mm
	0 to 50 mm	0 to 150 mm
	5 to 65 mm	5 to 85 mm
	360° in continuous mode	
	-20 to +90°	
	Φ 130 mm (in combination with R)	Φ 200 mm (in combination with R)
	80 mm (WD = 10 mm)	130 mm (WD = 10 mm)
	5-axis motor drive	
	Electron Optics	Pre-centered cartridge type tungsten hairpin filament
4-hole movable aperture		
Secondary electron detector, sensitive semiconductor backscattered electron detector		
WD = 10 mm (T.O.A = 35°)		
Image Display	Beam control: auto (AFS → ABA → AFC → ABCC)	
	Optical axis adjustment: auto (current alignment)	
	Beam brightness: auto	
	Auto brightness and contrast control (ABCC)	
	Auto focus control (AFC)	
	Auto stigmatism and focus (ASF)	
Auto filament saturation (AFS)		

	Auto beam alignment (ABA)
	Auto start (HV-ON→ABCC→AFC)
Operation Auxiliary Function	Raster rotation, dynamic focus, image improvement function, Data input (point-to-point measurement, angle measurement, texts), preset magnification, Stage positioning navigation function (SEM MAP), beam marking function
Optional function	■Hardware: Track ball, Joystick, Operation panel, Compressor, Ultra-sensitive low vacuum detector (UVD), Chamber scope, Camera navigation system ■Software: SEM data manager, External communication interface, 3D-capture, Stage free mode, EDS integration
Options (for External Devices)	Energy dispersive X-ray spectrometry (EDS), Length dispersive X-ray spectrometry (WDS), Various external stages (heating stage, cooling stage, tensile stage)



Figure A-1. Photograph of scanning electron microscope (SU3800/ SU3900) Indian Institute of Technology Delhi laboratory.

Table B-1. Important specifications of Keyence Profilometer VHX-1000E

Model		VHX-1000E		
Camera	Image capture device		1/1.8-inch, 2.11 million-pixel CCD image sensor	
			Total pixels : 1688 (H) x 1248 (V)	
			Effective pixels : 1628 (H) x 1236 (V)	
			Virtual pixels : 1600 (H) x 1200 (V)	
	Scan method		Progressive	
	Frame rate		15 F/s, 28 F/s switchable	
	Resolution		2 million pixels	1600 (H) x 1200 (V) Approx 1000 TV lines
			6 million pixels	1600 (H) x 1200 (V) Approx 1200 TV lines
				2 million pixels x 3 CCD mode (Excellent colour reproducibility)*1
			8 million pixels	3200 (H) x 2400 (V) Approx 1600 TV lines*2
			18 million pixels	4800 (H) x 3600 (V) Approx 2000 TV lines*2
	54 million pixels	4800 (H) x 3600 (V) Approx 2000 TV lines		
		18 million pixels x 3 CCD mode (Excellent colour reproducibility)*3		
	High Dynamic Range		16-bit resolution through RGB data from each pixel	
Gain		AUTO, NORMAL, PRESET		
Electronic shutter		AUTO, MANU, OFF, 1/15, 1/30, 1/60, 1/120, 1/250, 1/500, 1/1000, 1/2000, 1/5000, 1/9000, 1/19000		
Supercharge shutter		0.2 sec. to 17 sec. Can be set in increments of 0.1 sec.		
White balance		Auto, Manual, One-push set, Preset (2700K, 3200K, 5600K, 9000K)		
Back-focus adjustment		Not required		
LCD monitor	Size		Colour LCD (TFT) 17"*4	
	Panel size		365.76 (H) x 228.6 (V) mm*4	
	Pixel pitch		0.1905 (H) x 0.1905 (V) mm*4	
	Number of pixels		1920 (H) x 1200 (V) (WUXGA)*4	
	Display Colour		Approx 16,770,000 colours *5*4	
	Brightness		270 cd/m2 (typical)*4	

	Contrast ratio		450 : 1 (typ)*4
	Viewing angle		±80° (typical, horizontal), ±70° (typical, vertical)*4
CD-R/CD-RW/DVD drive unit	Unit		DVD-ROM drive unit
CD-R/CD-RW/DVD drive unit	Speed		CD-R/CD-RW : 24x Write, 24x Re-write, 24x Read, DVD : 8x Read
CD-R/CD-RW/DVD drive unit	Used disk		CD-R/CD-RW/DVD
	Storage capacity		700 MB, Approx 3500 images (When a 2 million-pixel image is compressed) to Approx 117 images (When a 2 million-pixel image is not compressed)
Hard disk drive unit			160 GB (including 45 GB reservation area), Approx 575,000 images (When a 2 million-pixel image is compressed) to Approx 19,000 Images (When a 2 million-pixel image is not compressed)
	Image format		
Observable image size			10000 (H) pixels x 10000 (V) pixels (when stitched)
Light source	Lamp		12 V, 100 W, Halogen lamp
	Lamp life		1000 hours (average)
	Colour temperature		3100 K (at maximum light intensity)
Video output			DVI (1920 x 1200 pixels)
Video output	Scanning frequency	Special LCD monitor	75 kHz (H), 60 Hz (V)
		External monitor	
Input	Mouse input		Supports USB mouse
	Keyboard input		Supports USB keyboards
	External remote input		Pause/ Recording, Non-voltage input (Contact/Noncontact)
Interface	LAN		RJ-45 (10BASE-T/100BASE-TX/1000BASE-T)
	USB 2.0 Series A		8 types
Software	Moving image recording software		Functions for recording/reproducing moving images

	High-quality depth composition software	Functions for composing a single image from a plurality of images obtained by focusing on and capturing an image of each portion of the target that is of a different height
	Real-time depth composition software	Displays full-focused images in real-time at the turn of the focus adjustment dial.
	Image improvement software	Image processing functions for correcting images to make observation easier
	Comment input software	Function for inputting and displaying comments such as letters, marks, or the like in an observation image
	Area measurement software	Measures areas of 2D images.
	Screen splitting software	Function for splitting an image vertically, horizontally, or into four parts, and displaying the image
Dimensions		420 x 416 x 181 mm (when stored)
Rating	Power voltage	100 to 240 VAC, 50/60 Hz
	Power consumption	340VA
Environmental resistance	Ambient temperature	+5 to +40 °C
	Relative humidity	35 to 80 % RH (No condensation)
Weight	Controller	Approx 11.6 kg
	Camera unit	Approx 1.00 kg (VHX-1100), Approx 0.90 kg (VHX-1020)
	Console	Approx 0.30 kg



Figure B-1. Photograph of Keyence Profilometer VHX-1000E (Indian Institute of Technology Delhi laboratory)